Breakdown of Lüscher Formalism near Left Hand Cuts

Presented by : Md Habib E Islam (Digonto)
Email: misla004@odu.edu
With Sebastian M. Dawid (U Washington)
and
Raúl Briceño (UC Berkeley)

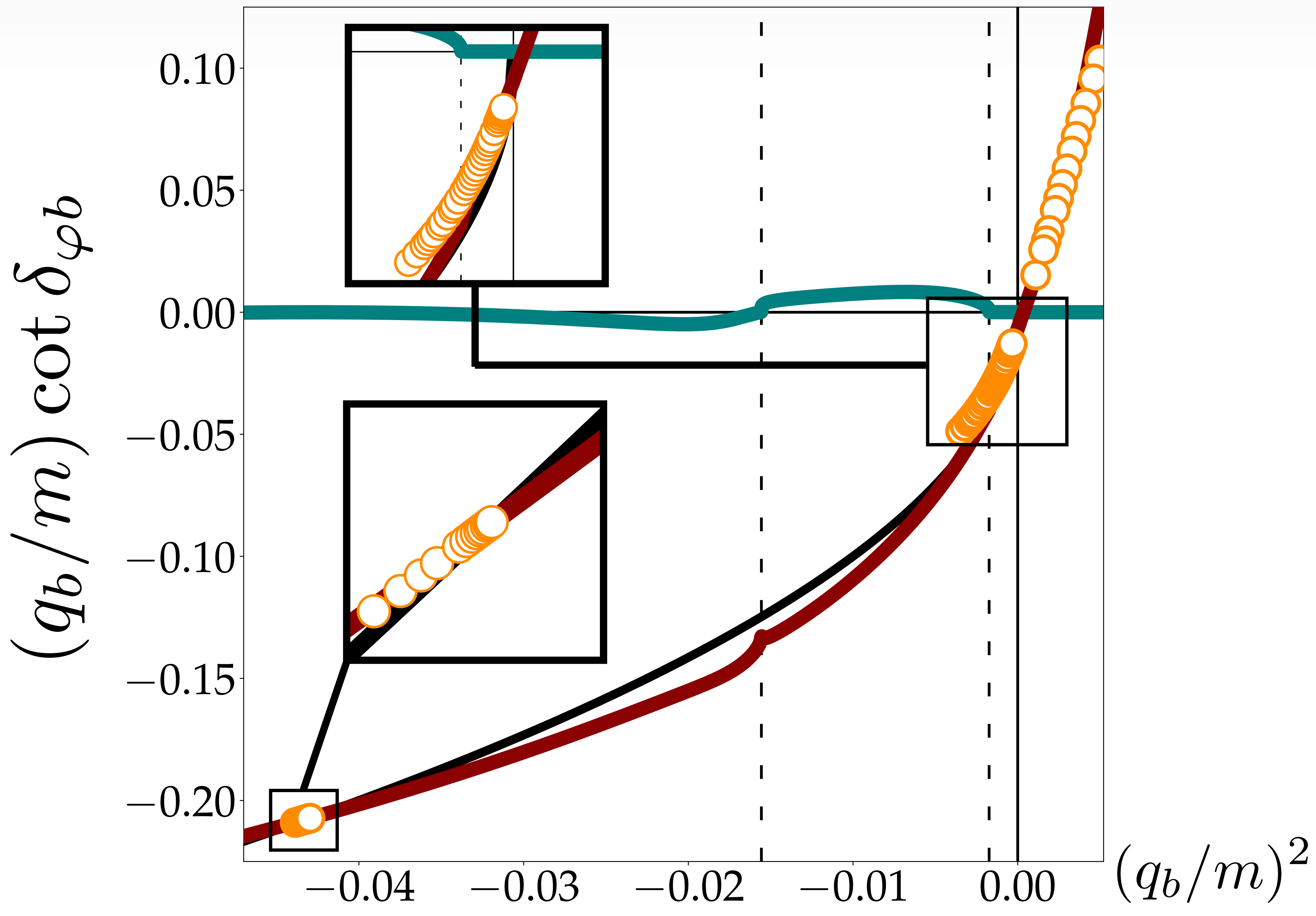

Outline

- Why three body physics is important?
- What toy model are we using?
- What is the left hand cut?
- How were the orange points derived from Lüscher formalism?
- How were the solid lines derived from solving Integral equations?

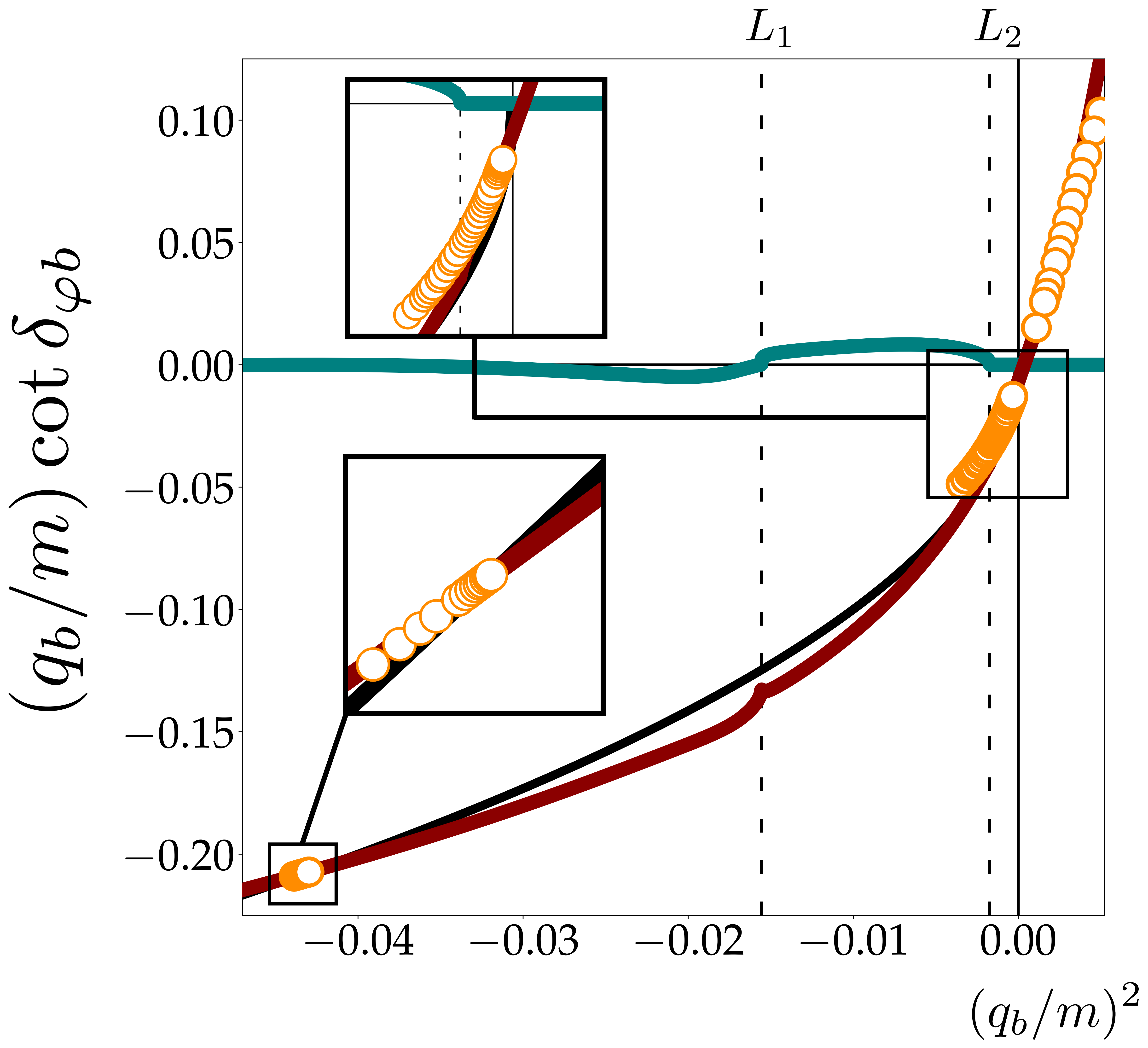

Why Three Body Physics?

Particle Data Group, 2022
LHCb collaboration, 2022
M. Padmanath, 2022
Meng-Lin Du, 2023

Interesting resonances decay to three particle final states under strong interactions

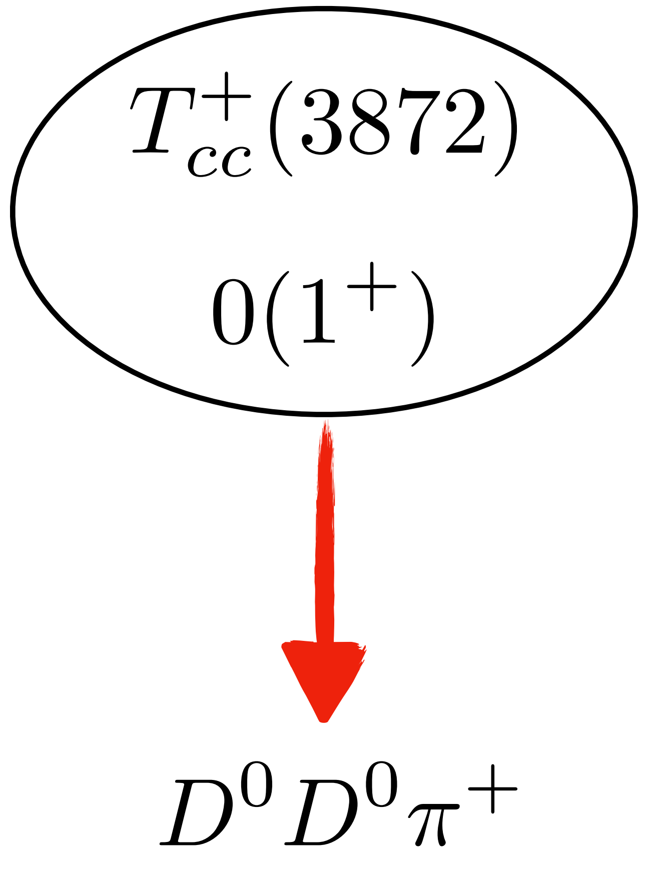

Experiment

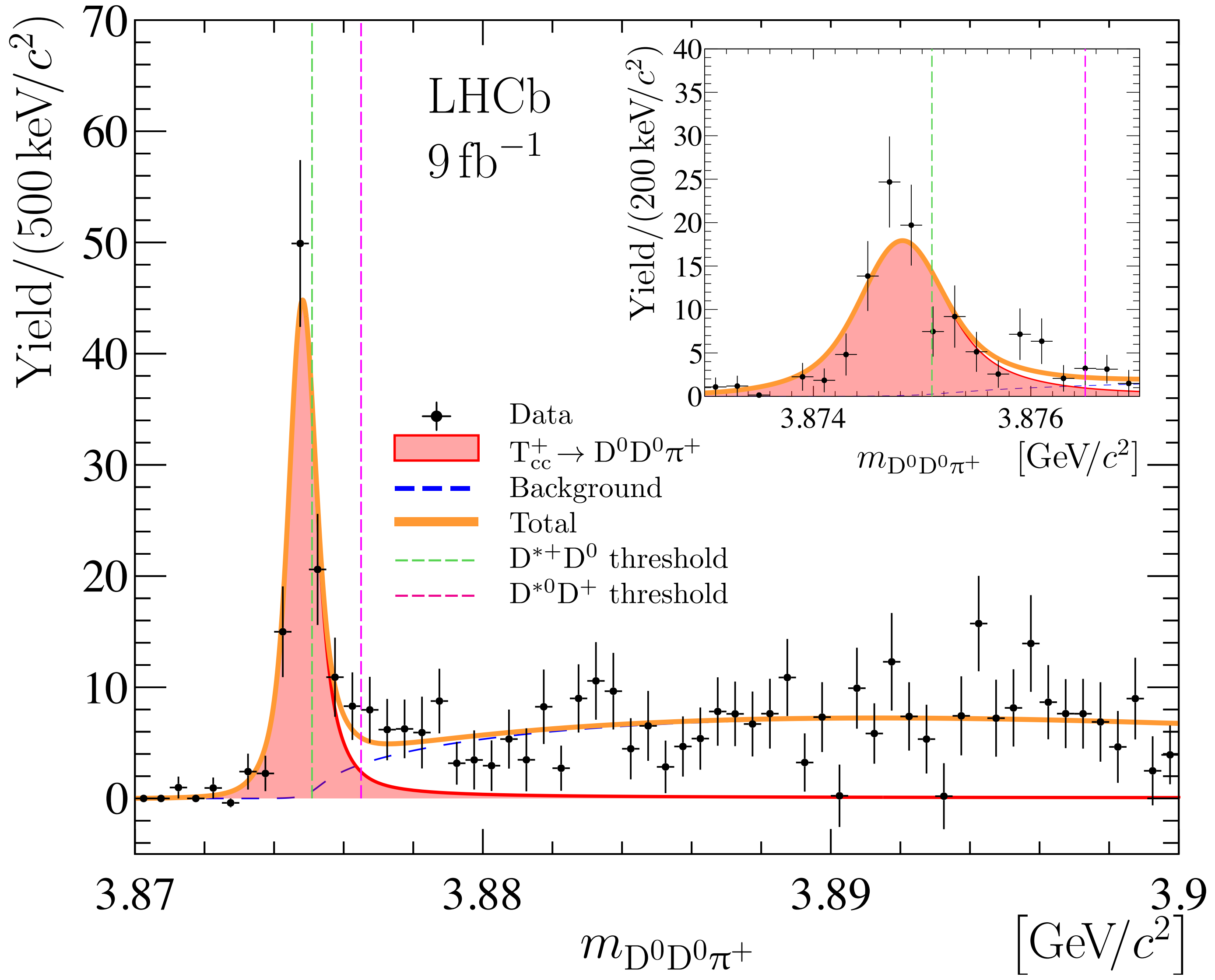

Lattice

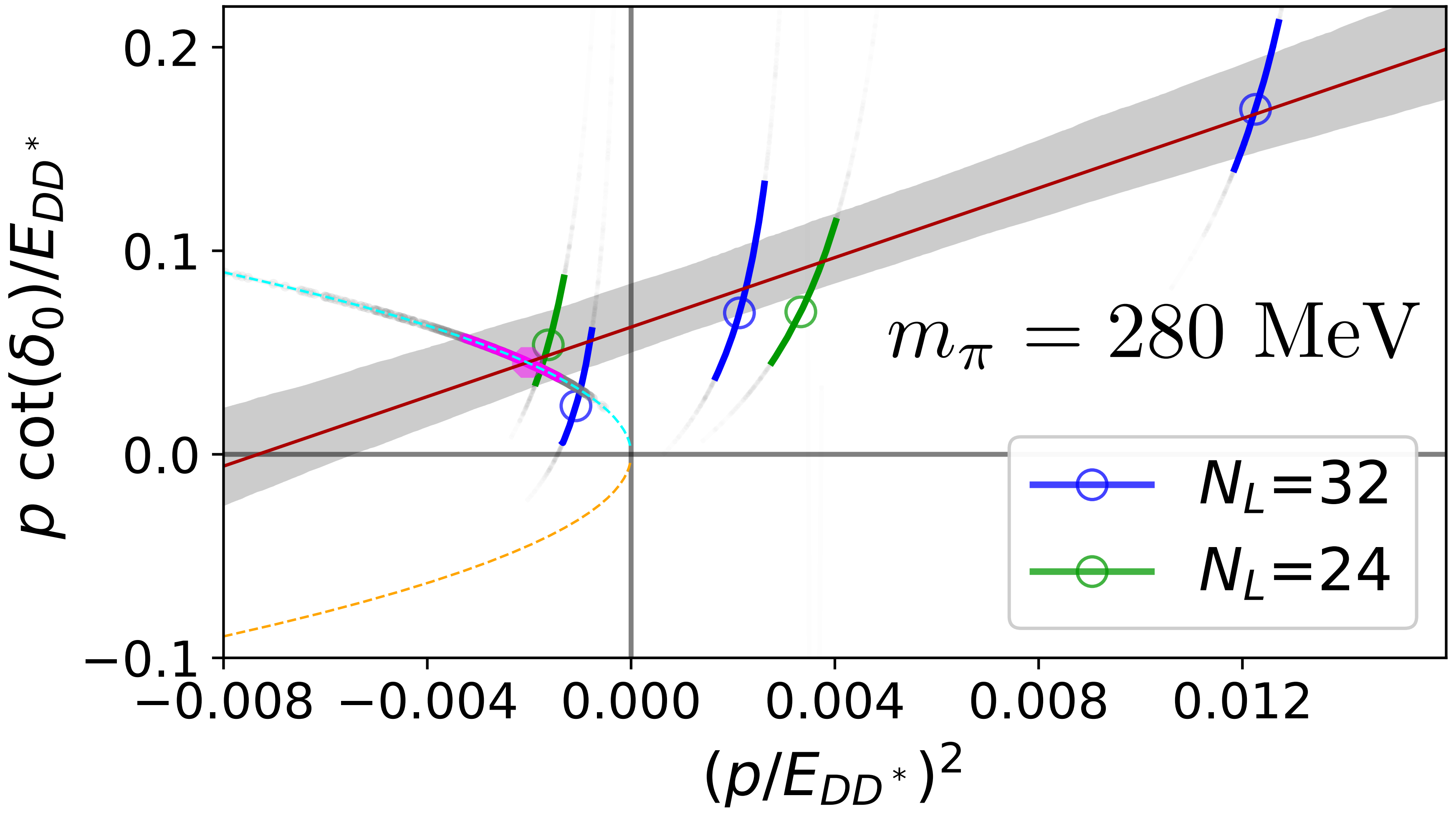

Phenomenology

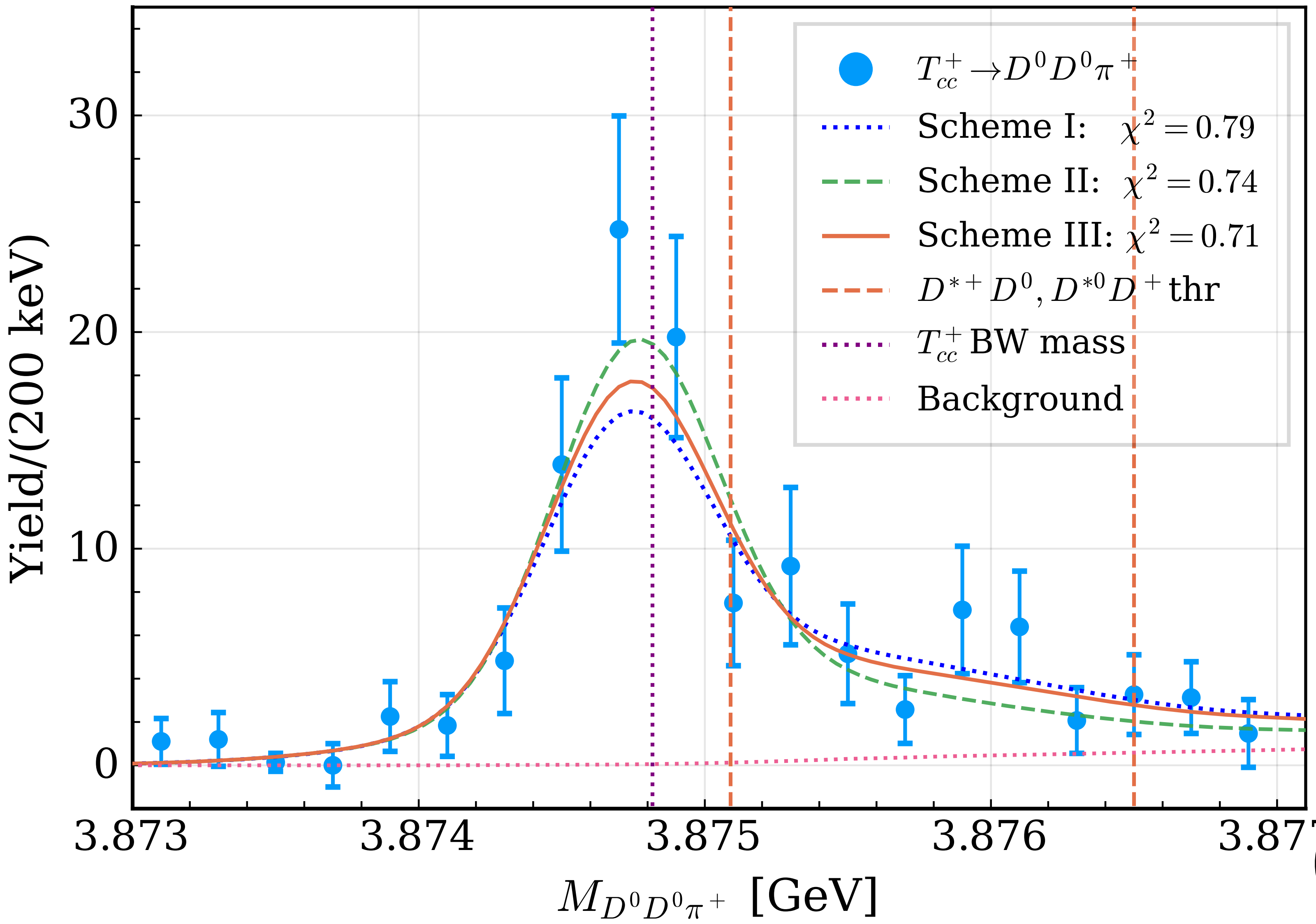

Physical Threshold

Threshold on the lattice

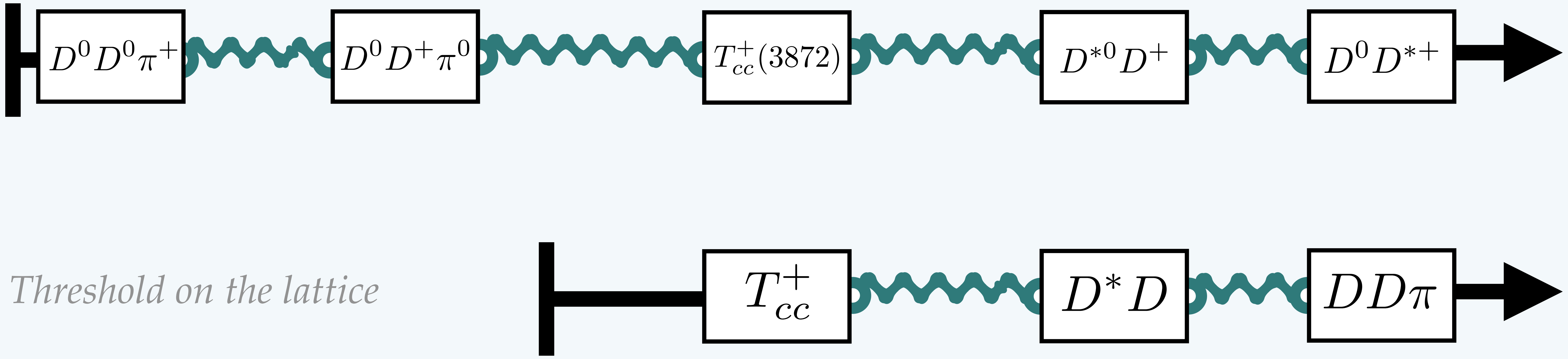

Why Three Body Physics?

Particle Data Group, 2022
LHCb collaboration, 2022
M. Padmanath, 2022
Meng-Lin Du, 2023

Interesting resonances decay to three particle final states under strong interactions

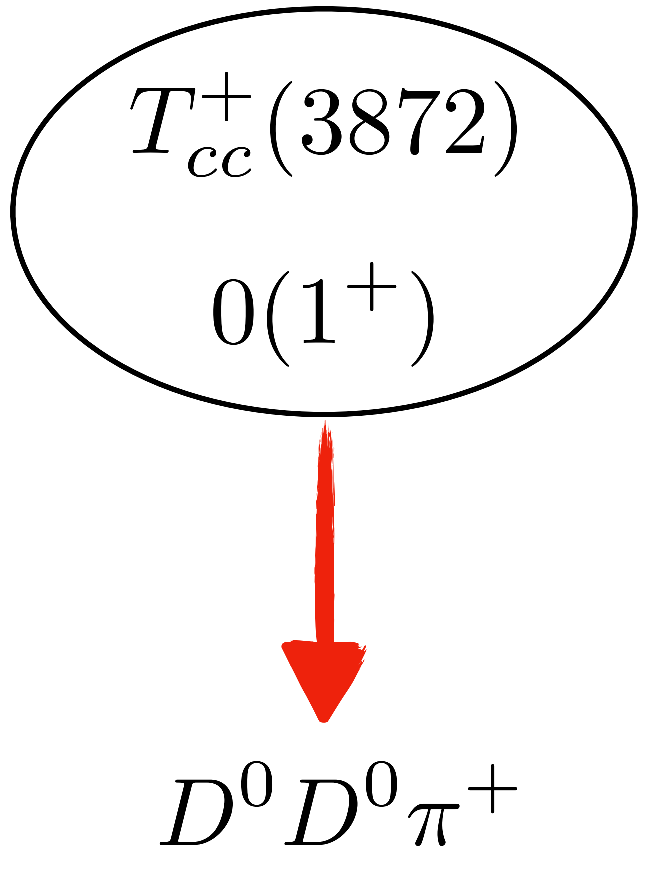

Experiment

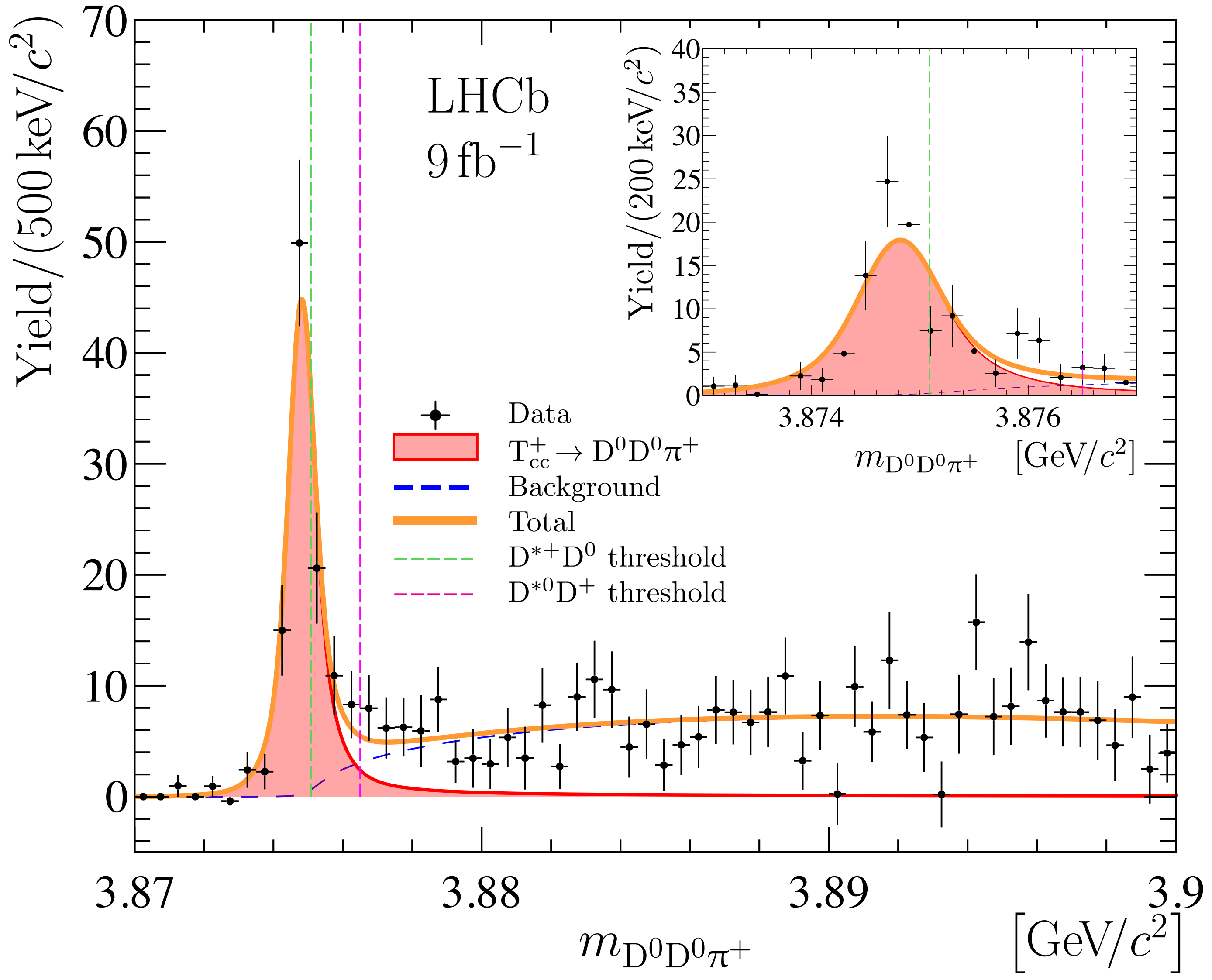

Lattice

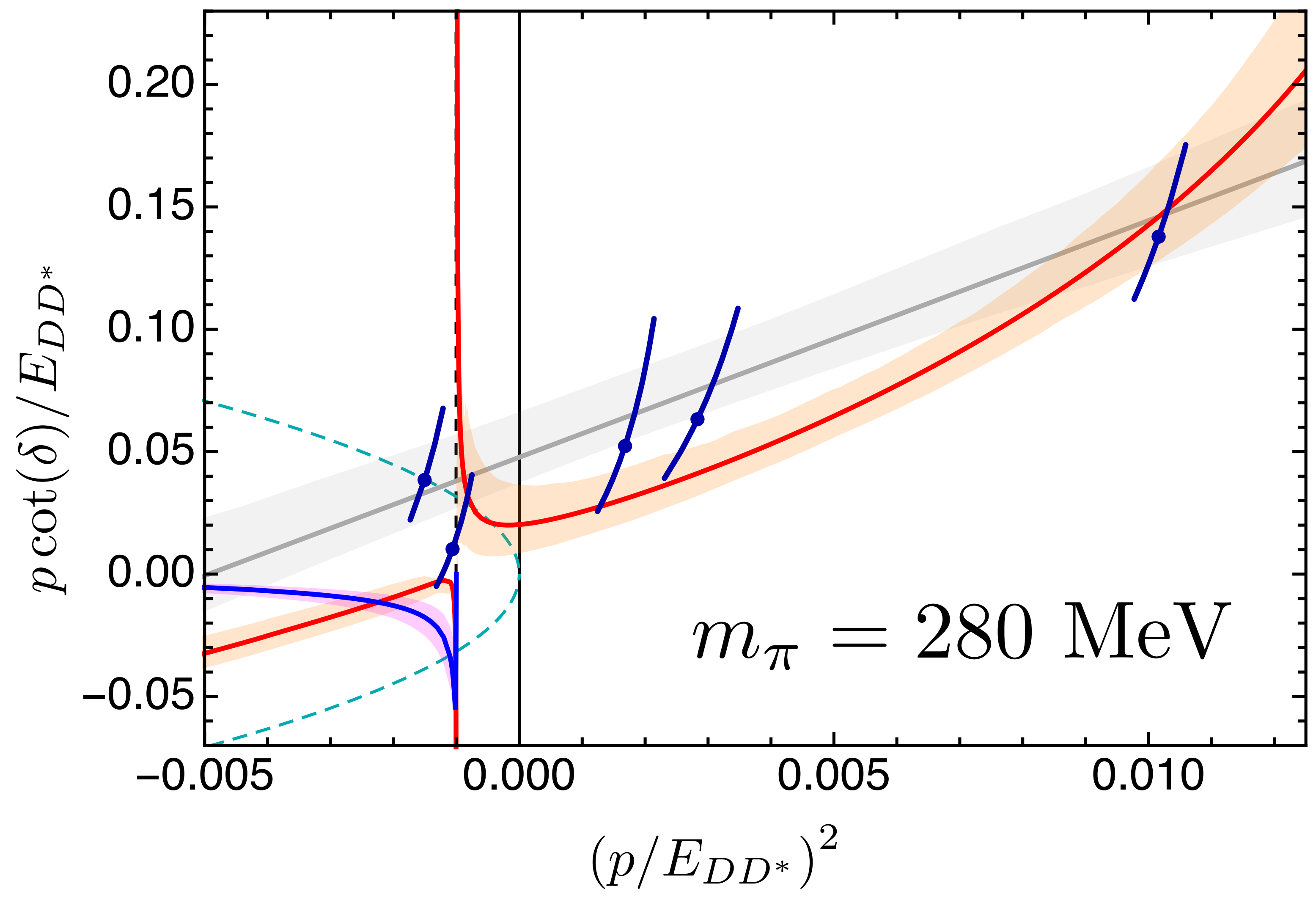

Phenomenology

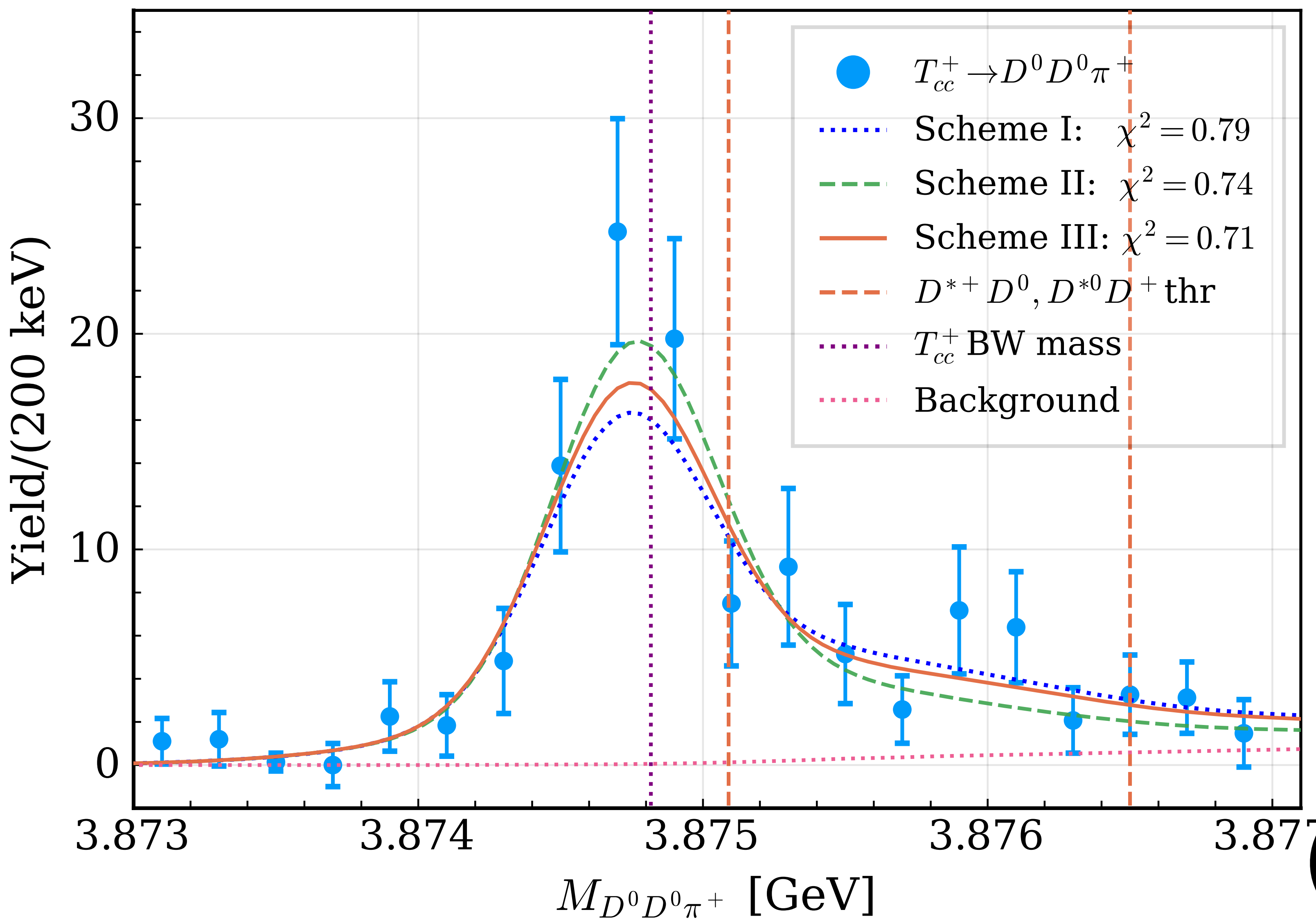

Physical Threshold

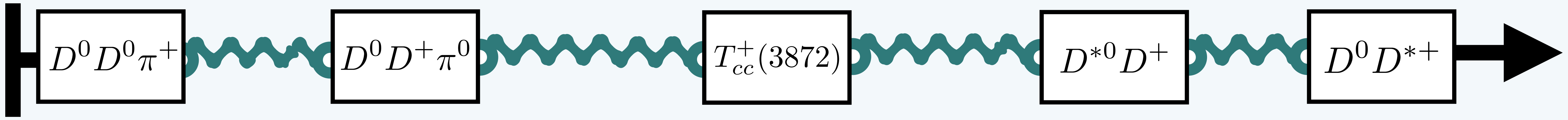

Threshold on the lattice

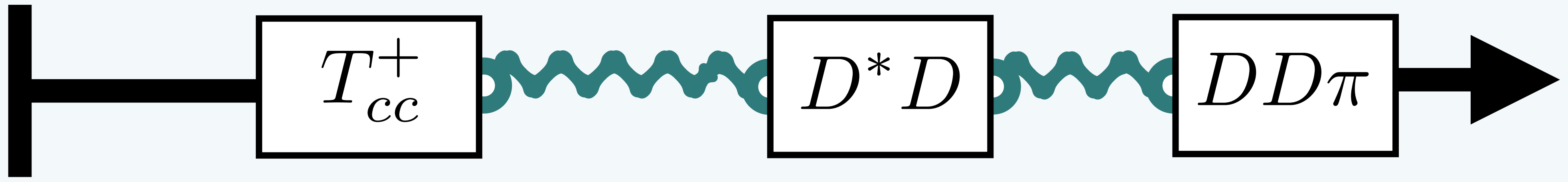

The Recipe

Finite volume spectroscopy

Infinite-volume three-body K-matrix

Infinite-volume scattering amplitude

Amplitude analysis, Bound-states and resonances

Hansen and Sharpe, 2014, 2015
Mai and Döring, 2017
Briceño, Hansen and Sharpe, 2018
Hansen, Romero-Lopéz and Sharpe, 2020
Blanton and Sharpe, 2020
Jackura, 2022

Toy Model

Assuming $\boxed{\mathcal{K}_3} = 0$ *, and all identical scalar particles*

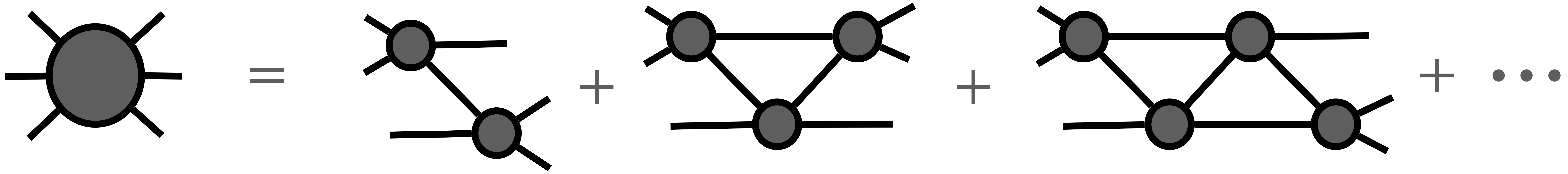

Infinite volume integral equation $\mathcal{D} = -\mathcal{M}_2 G \mathcal{M}_2 - \mathcal{M}_2 \int_q G\mathcal{D}$

Finite volume Quantization condition $\det[\cancelto{0}{\mathcal{K}_3} + F_3^{-1}] = 0$

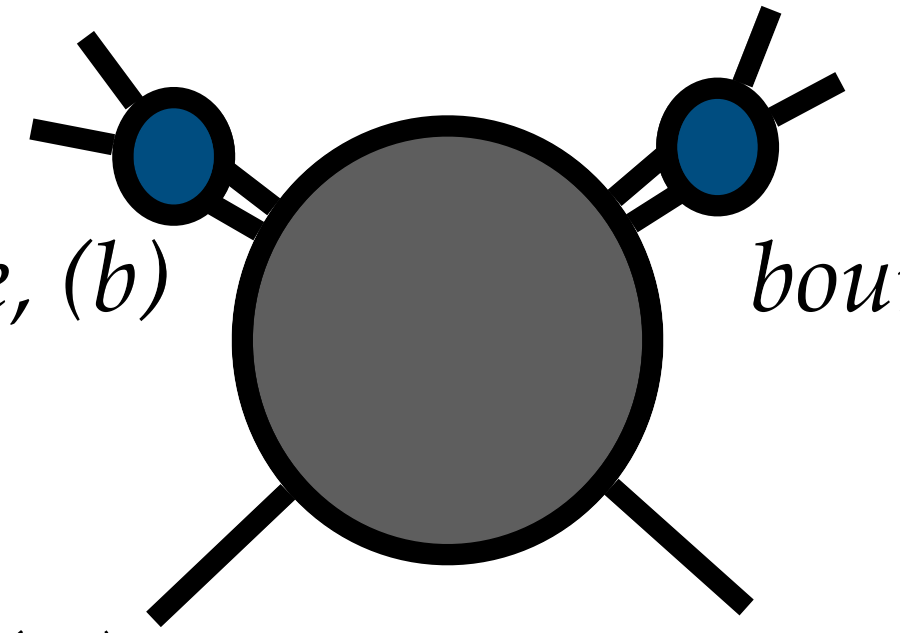

$$\mathcal{D} = \frac{-g}{\sigma_p - m_b^2} \mathcal{M}_{\varphi b} \frac{-g}{\sigma_k - m_b^2}$$

Two-body bound-state residue g^2

Two-body bound-state mass m_b

Solution Process

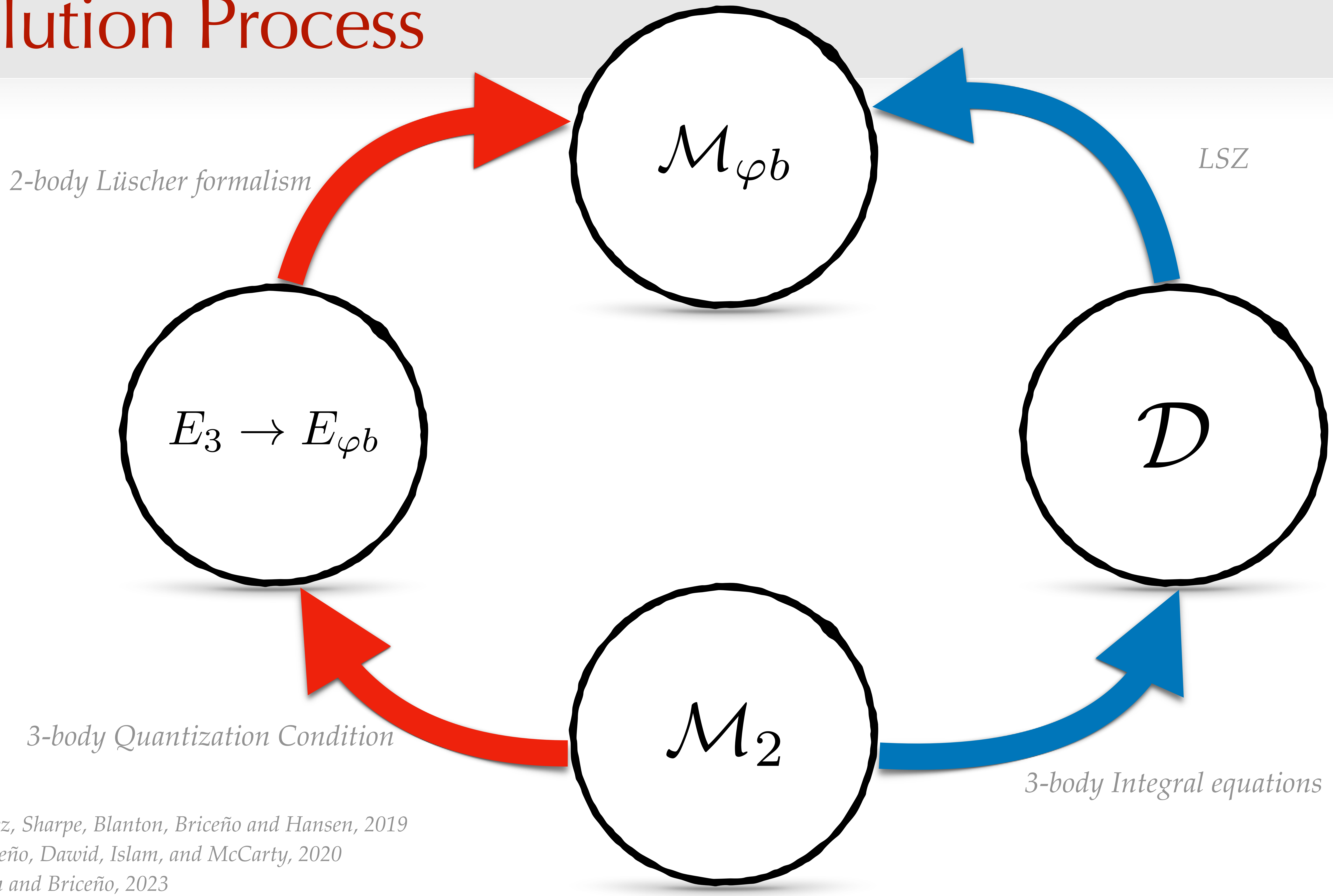

Romero-López, Sharpe, Blanton, Briceño and Hansen, 2019
Jackura, Briceño, Dawid, Islam, and McCarty, 2020
Dawid, Islam and Briceño, 2023

Outline

- ✓ Why the breakdown is important in three body physics?
- ✓ What toy model are we using?
- What is the left hand cut?
- How were the orange points derived from Lüscher formalism?
- How were the solid lines derived from solving Integral equations?

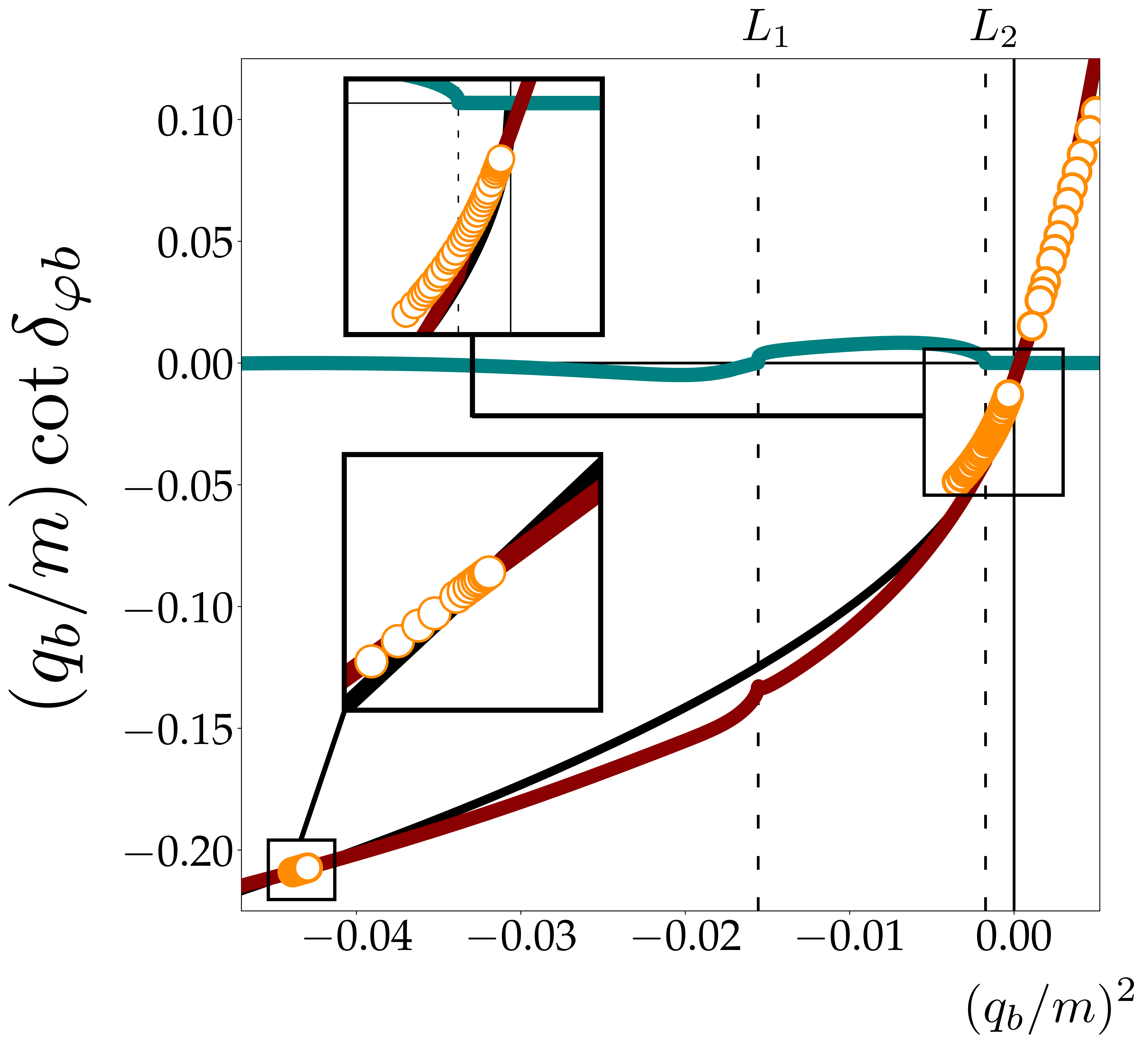

Left Hand Cut

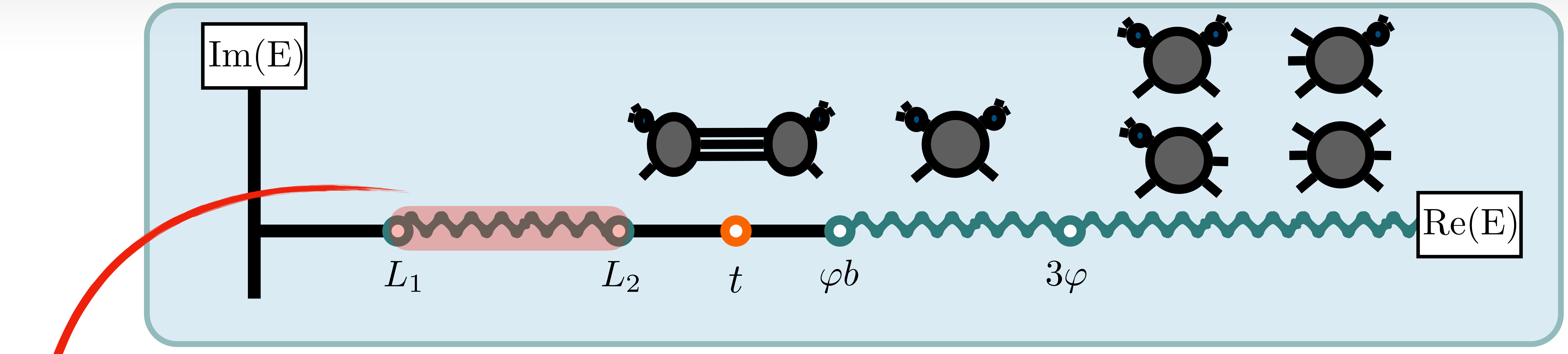

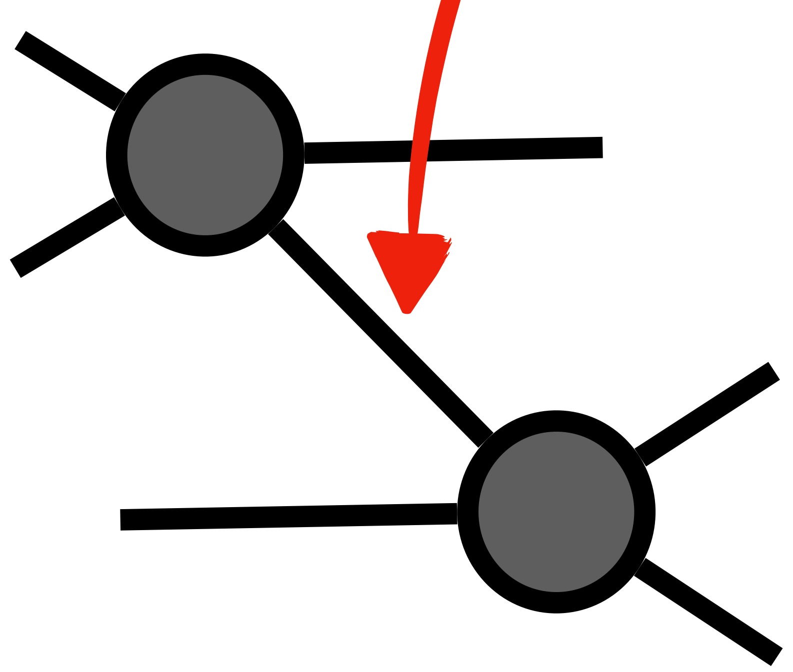

$$G \sim \log\left(\frac{Z-1}{Z+1}\right)$$

Branch points at $Z = \pm 1$

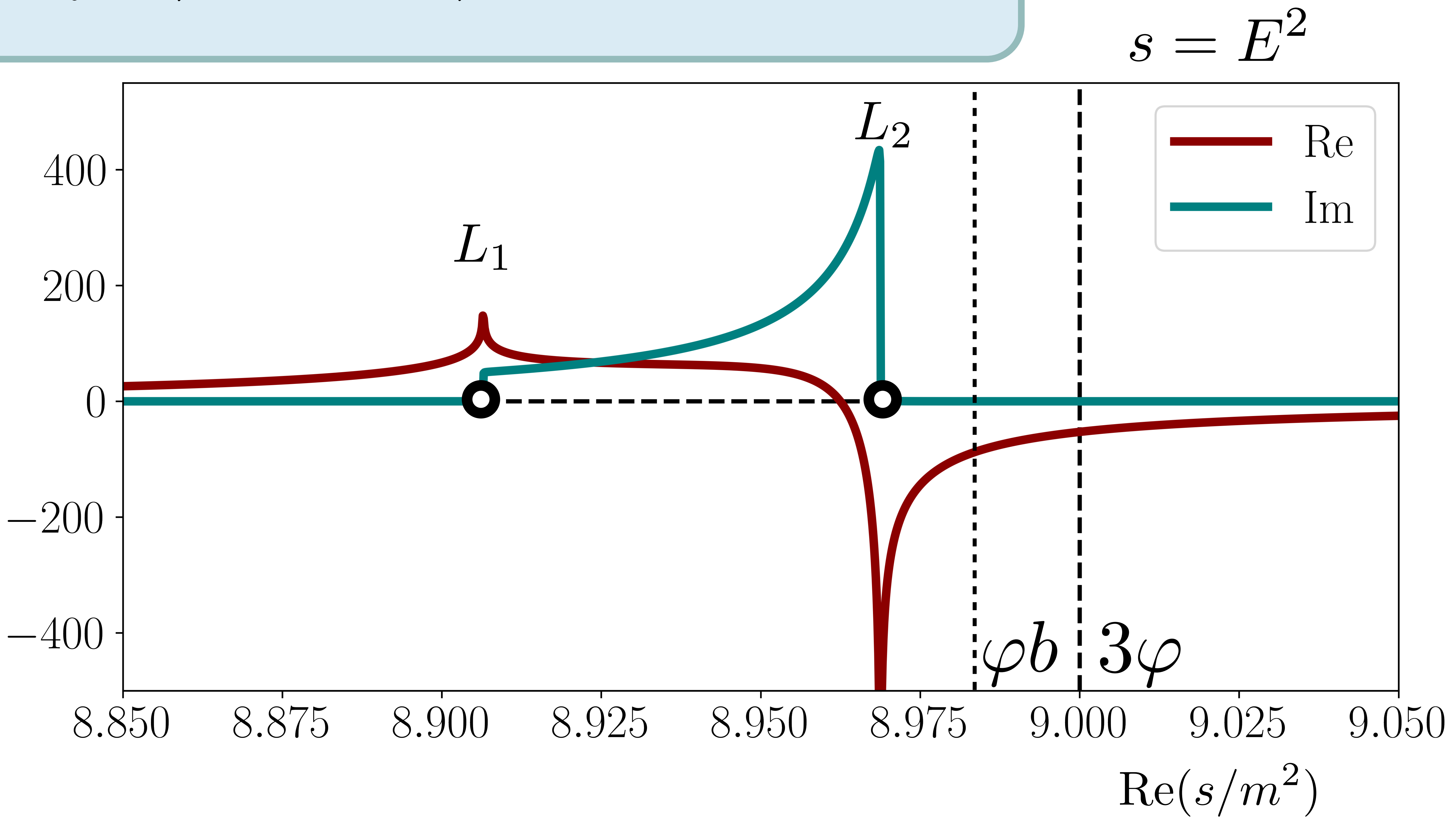

Outline

- ✓ Why the breakdown is important in three body physics?
- ✓ What toy model are we using?
- ✓ What is the left hand cut?
- How were the orange points derived from Lüscher formalism?
- How were the solid lines derived from solving Integral equations?

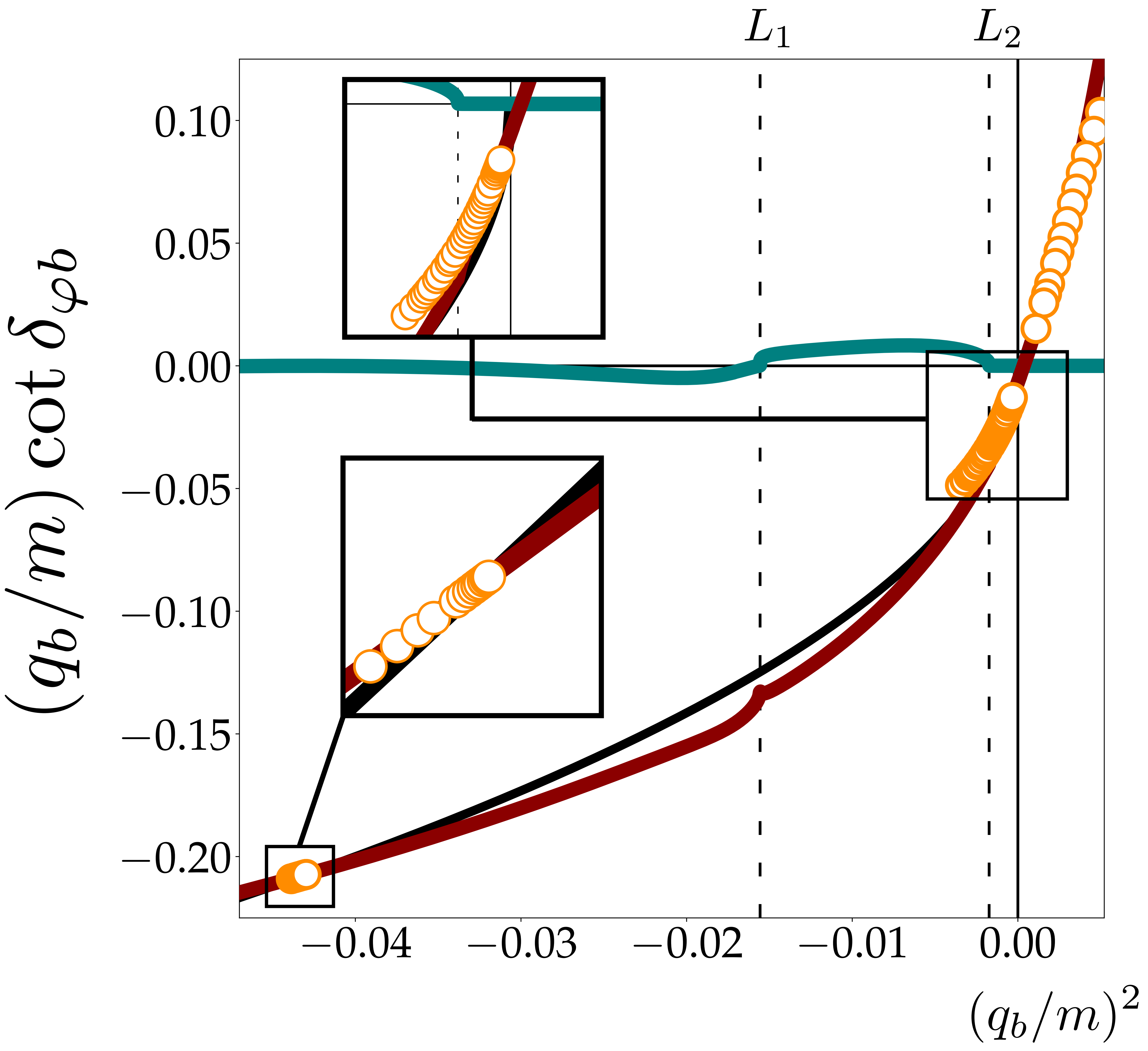

Phase Shifts from Lüscher formalism

$$\det[\cancel{\mathcal{K}_3}^{\,0} + F_3^{-1}] = 0$$

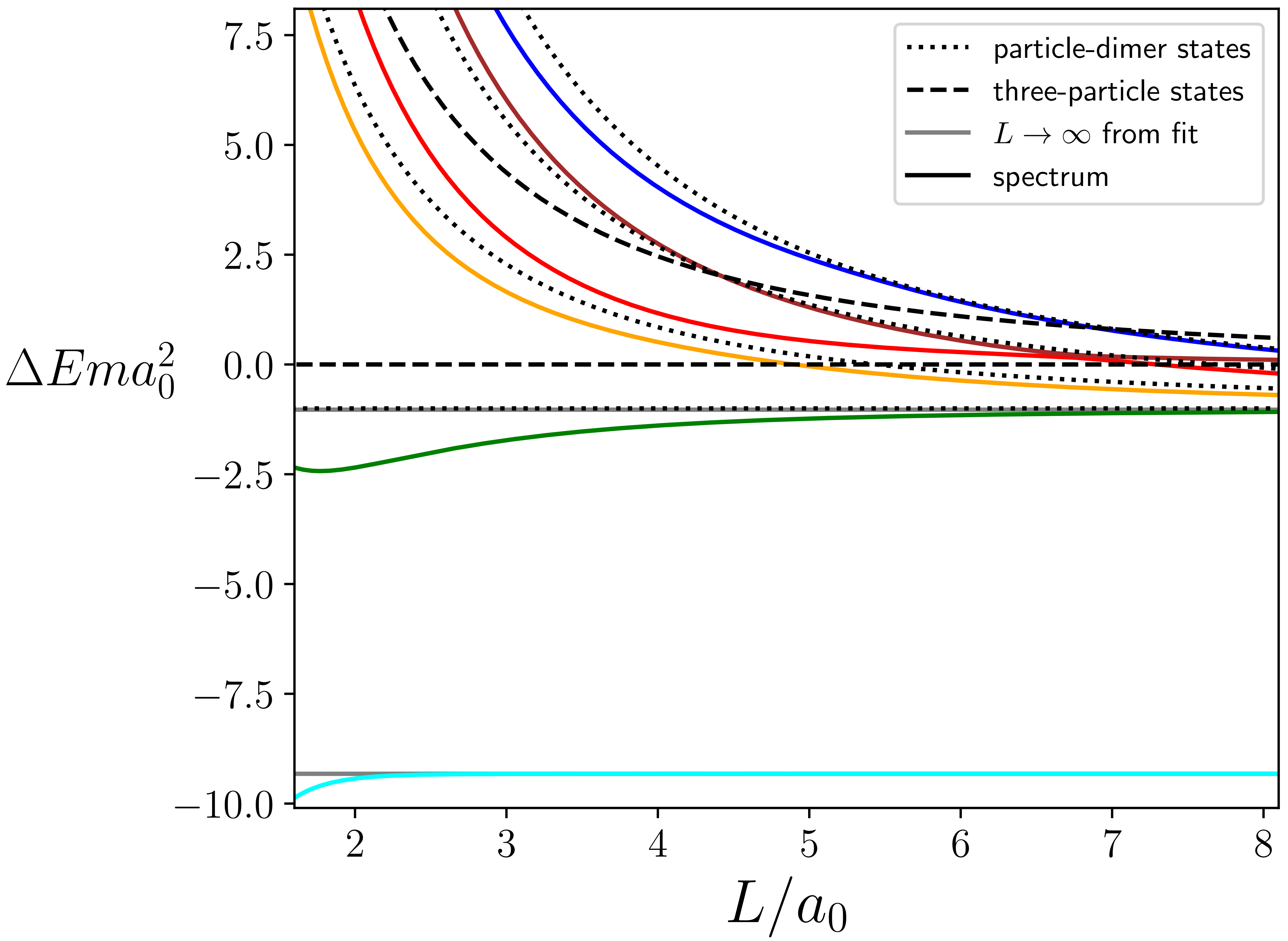

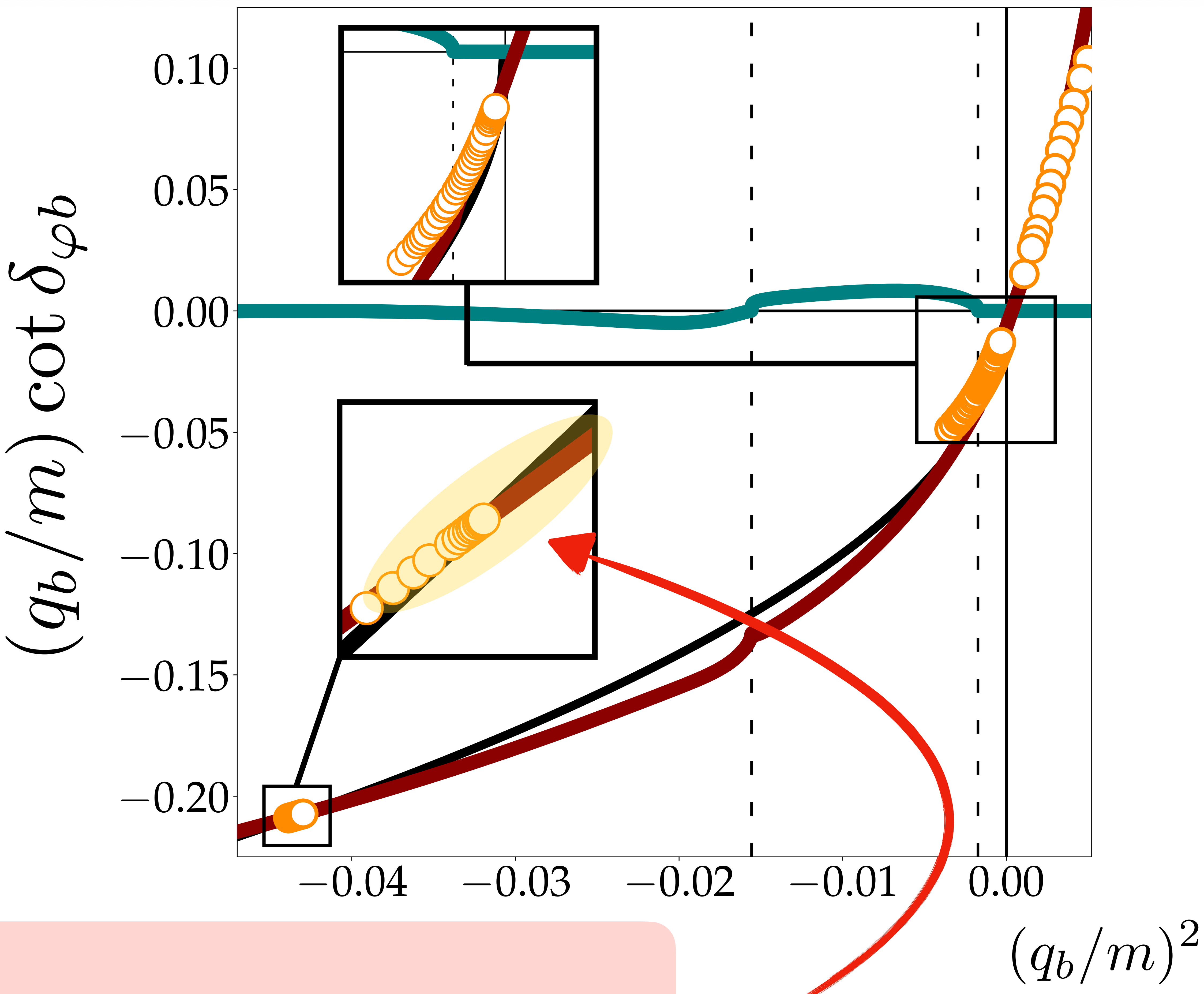

$$\det[\rho_{\varphi b}\cot\delta_{\varphi b} + F_2] = 0$$

Spectra obtained using 3-body Quantization condition
Phase shift calculated using 2-body Lüscher formalism

Romero-López, Sharpe, Blanton, Briceño and Hansen, 2019

Phase Shifts from Integral Equations

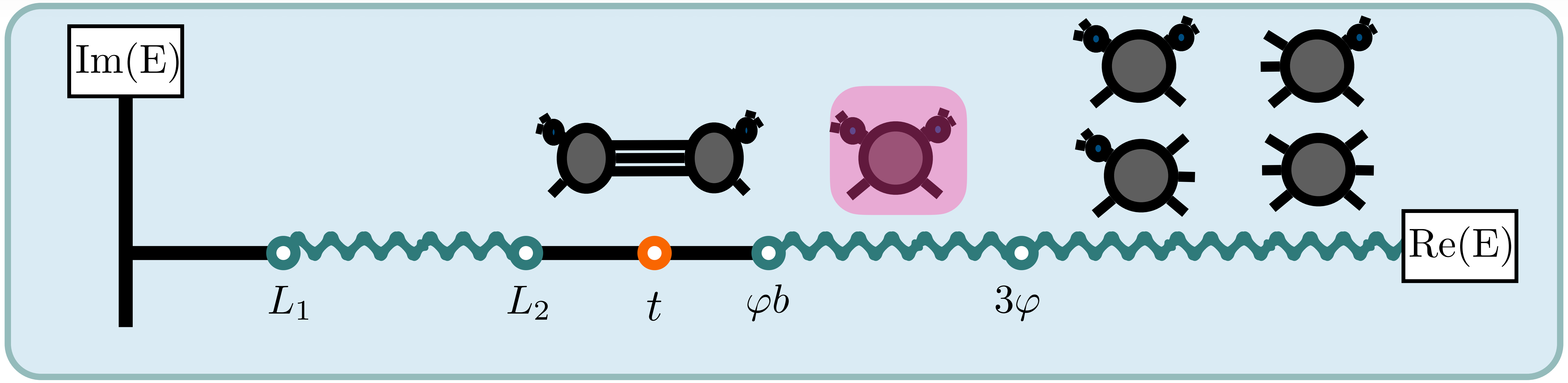

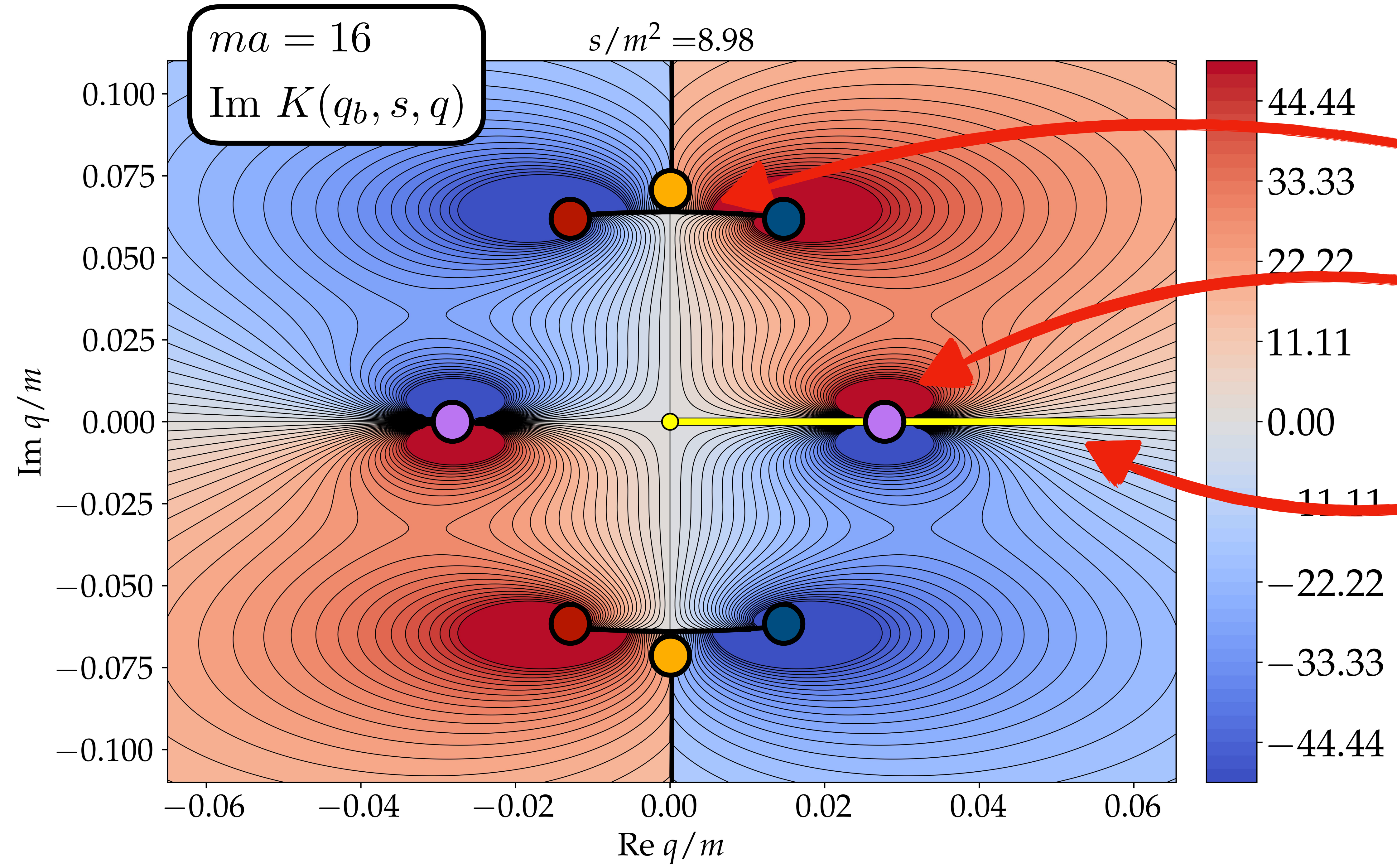

$$\mathcal{D} = -\mathcal{M}_2 G \mathcal{M}_2 - \mathcal{M}_2 \int_q G\mathcal{D}$$

Singularity cut from the one particle exchange function

Two body amplitude has a pole in the integration region

Momentum integration interval

$$K(p,s,q) = \frac{q^2}{(2\pi)^2 \omega_q} G_S(p,s,q) \mathcal{M}_2(q,s)$$

Jackura, Briceño, Dawid, Islam, and McCarty, 2020
Dawid, Islam and Briceño, 2023

Phase Shifts from Integral Equations

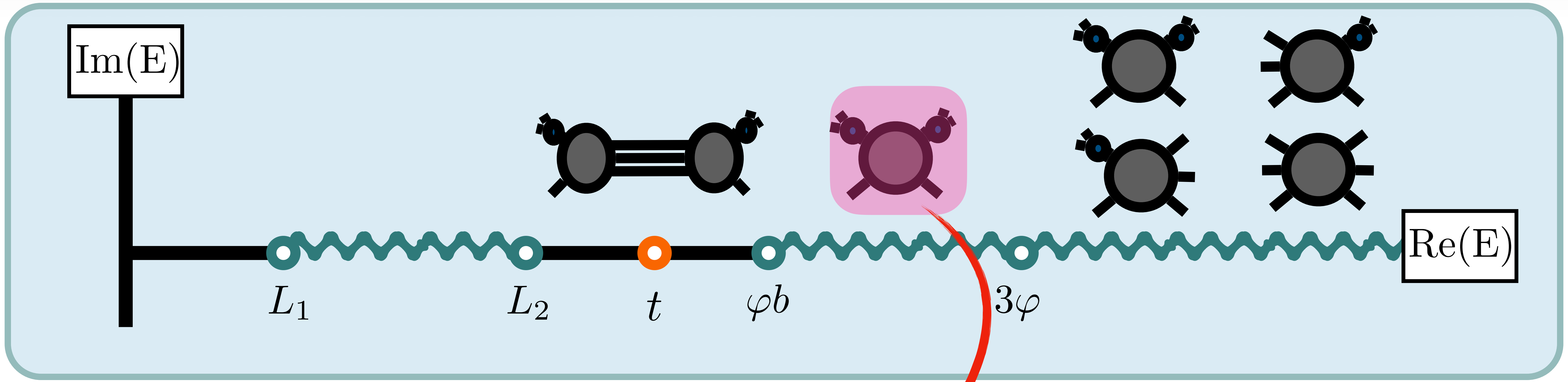

$$s = E^2$$

$$\mathcal{D} = -\mathcal{M}_2 G \mathcal{M}_2 - \mathcal{M}_2 \int_q G\mathcal{D}$$

Follows two-body unitarity condition:

$$|\rho_{\varphi b}\mathcal{M}_{\varphi b}| \leq 1$$

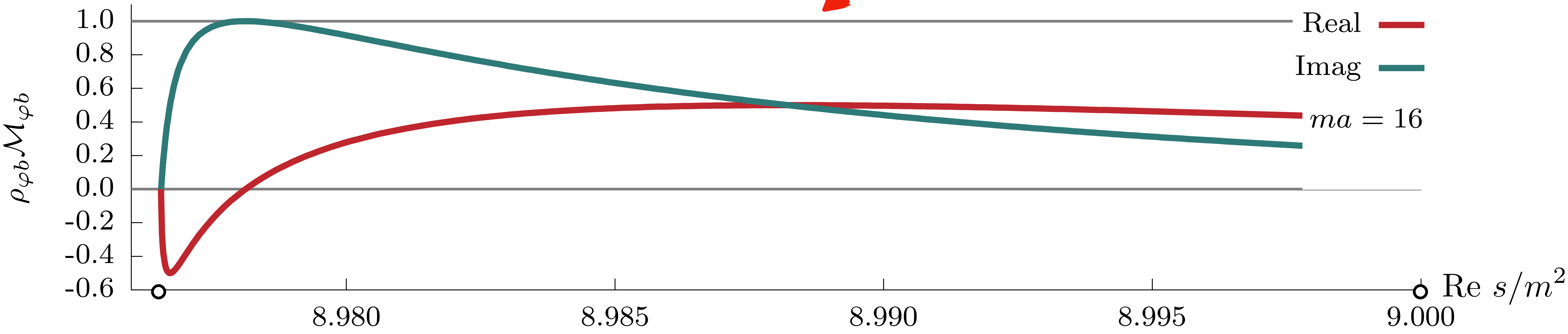

Jackura, Briceño, Dawid, Islam, and McCarty, 2020
Dawid, Islam and Briceño, 2023

Phase Shifts from Integral Equations

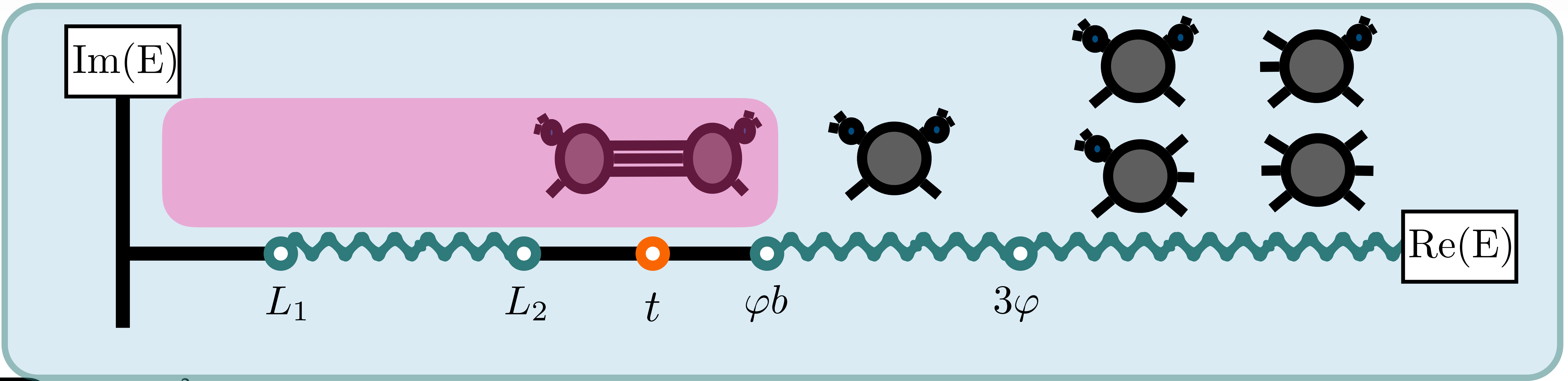

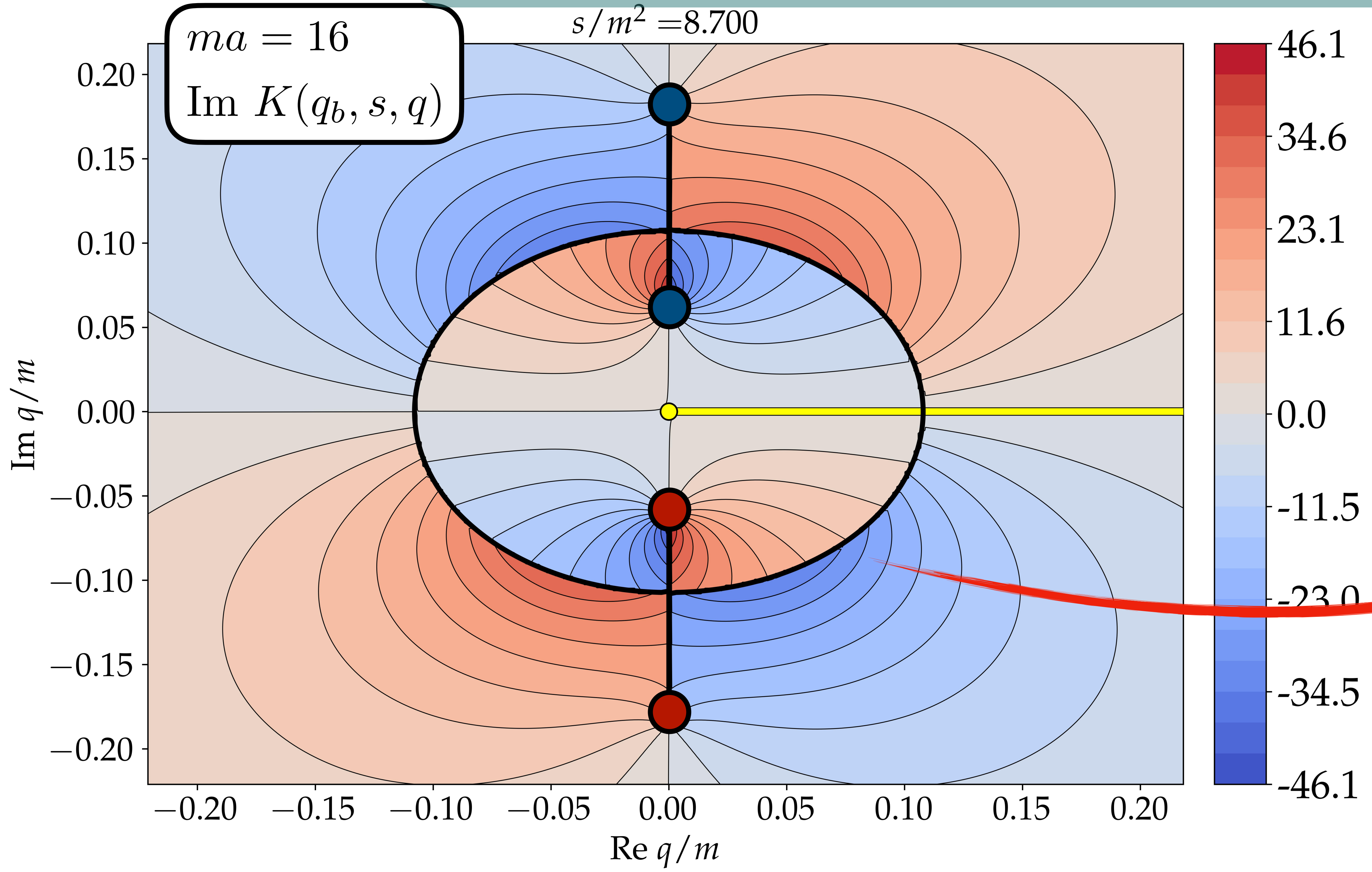

$$\mathcal{D} = -\mathcal{M}_2 G \mathcal{M}_2 - \mathcal{M}_2 \int_q G\mathcal{D}$$

Logarithmic cut forms a circle around the end point of integration

$$K(p,s,q) = \frac{q^2}{(2\pi)^2\omega_q} G_S(p,s,q)\mathcal{M}_2(q,s)$$

q_b is the spectator momenta corresponding to two-body bound-state energy, $\sigma_q = m_b^2$

Romero-López, Sharpe, Blanton, Briceño and Hansen, 2019
Jackura, Briceño, Dawid, Islam, and McCarty, 2020
Dawid, Islam and Briceño, 2023

Phase Shifts from Integral Equations

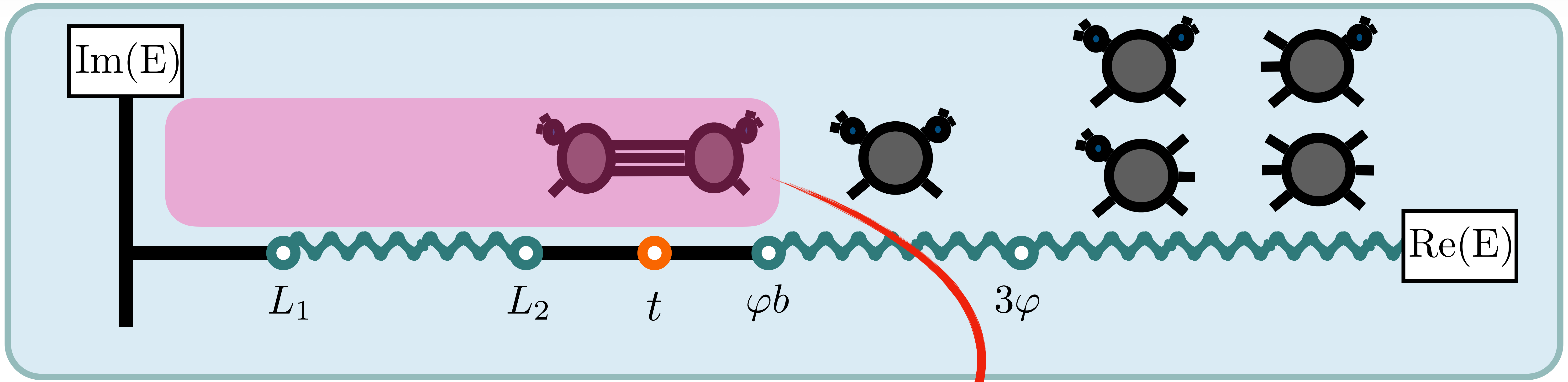

$s = E^2$

$$\mathcal{D} = -\mathcal{M}_2 G \mathcal{M}_2 - \mathcal{M}_2 \int_q G\mathcal{D}$$

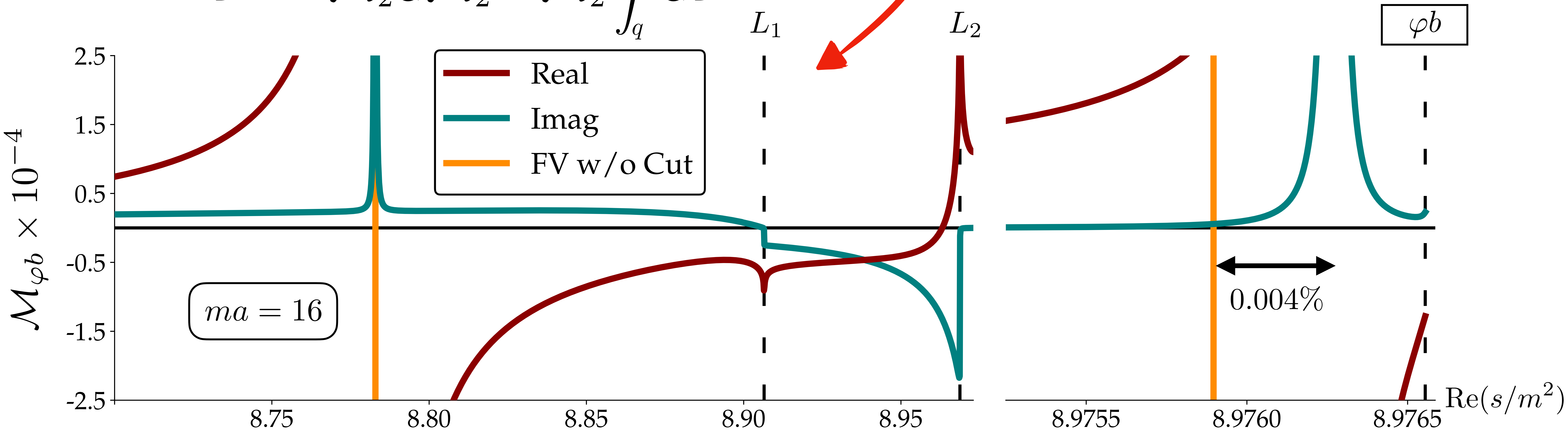

Romero-López, Sharpe, Blanton, Briceño and Hansen, 2019
Jackura, Briceño, Dawid, Islam, and McCarty, 2020
Dawid, Islam and Briceño, 2023

Breakdown near Left Hand Cut

Romero-López, Sharpe, Blanton, Briceño and Hansen, 2019
Jackura, Briceño, Dawid, Islam, and McCarty, 2020
Dawid, Islam and Briceño, 2023

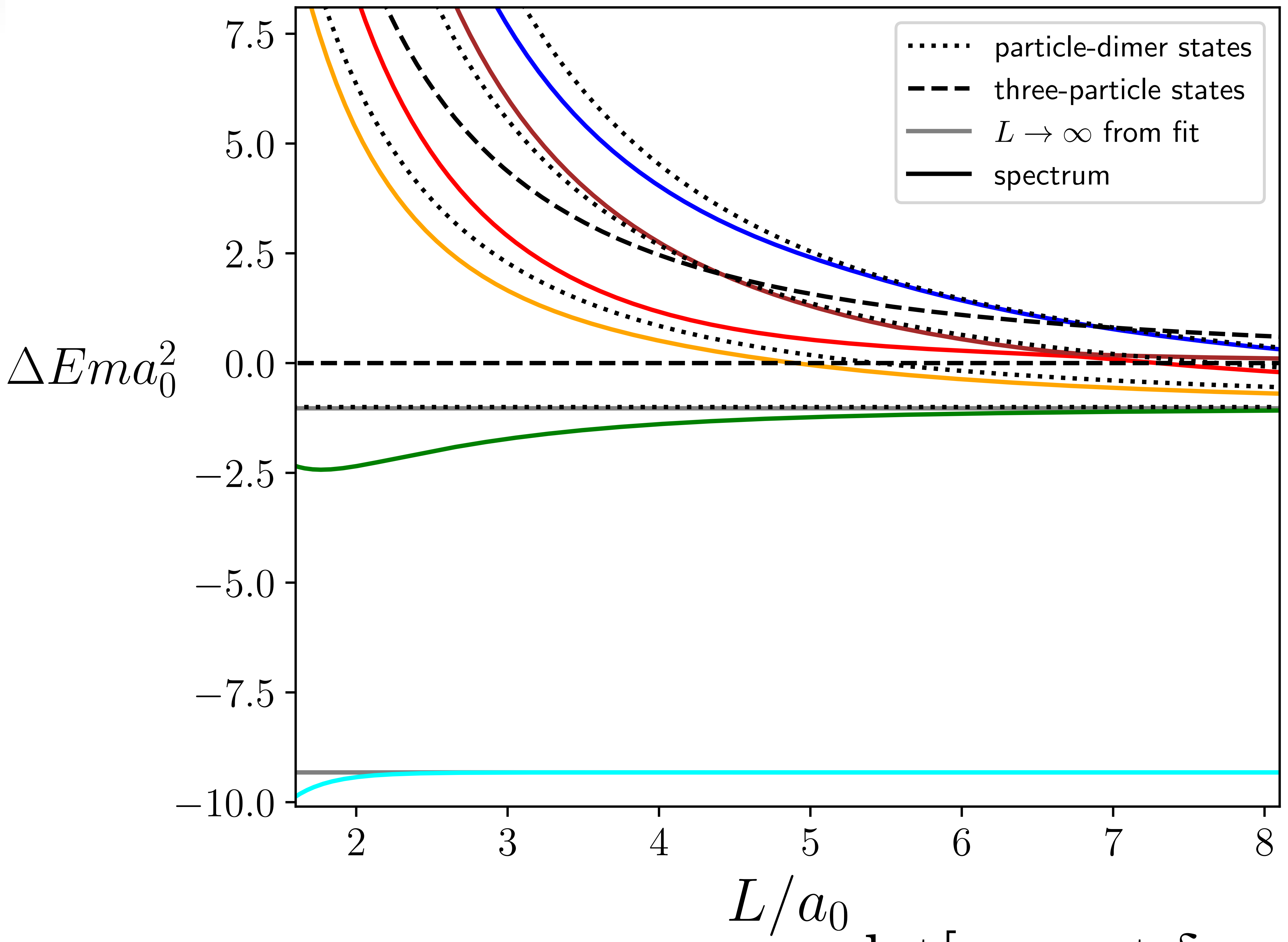

2-body Lüscher formalism

$$\det[\rho_{\varphi b} \cot \delta_{\varphi b} + F_2] = 0$$

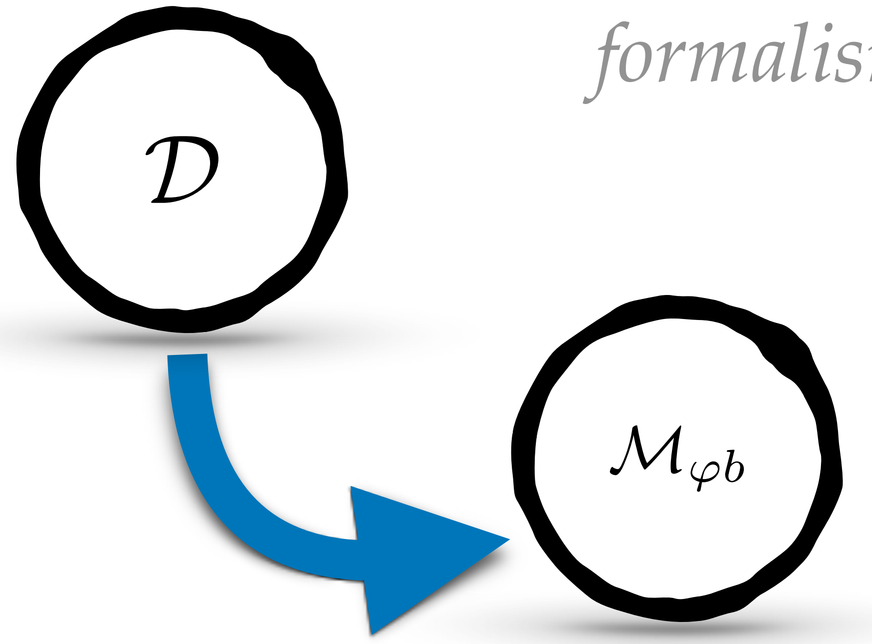

Solving Integral equations:

$$q_b \cot \delta_{\varphi b} = 8\pi\sqrt{s}\mathcal{M}_{\varphi b}^{-1} + i q_b$$

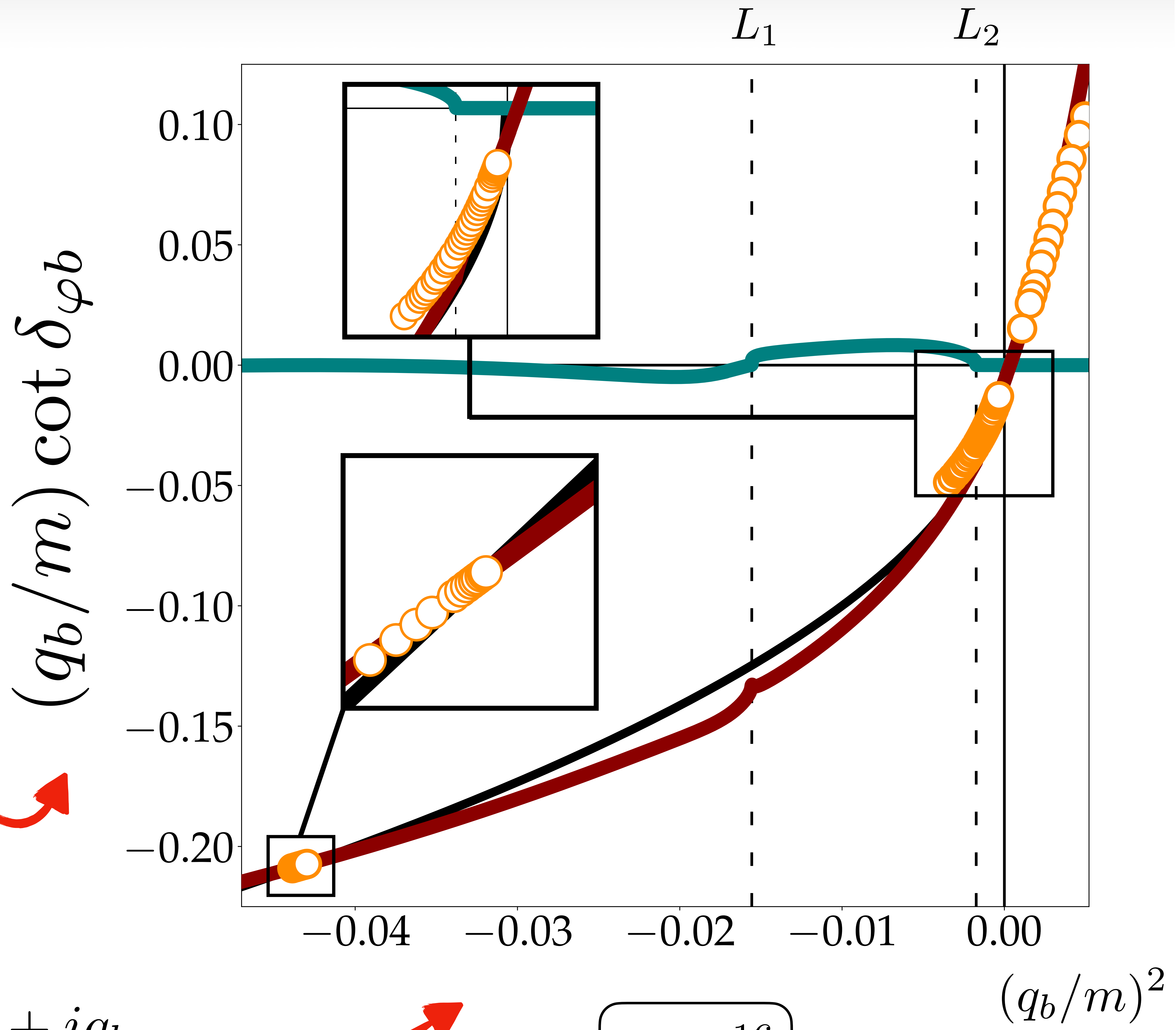

$ma = 16$

Summary

- We have shown breakdown of the Lüscher formalism in the vicinity of the left hand cuts
- We have addressed the complications in studying bound-state-spectator amplitude above and below threshold and shown possible solutions to them
- We have performed consistency checks with toy model that provides confidence for both finite-volume and infinite-volume formalisms

Thank you

Backup Slides

Three Body Scattering Amplitude

Assuming $\boxed{\mathcal{K}_3} = 0$ *, and all identical scalar particles*

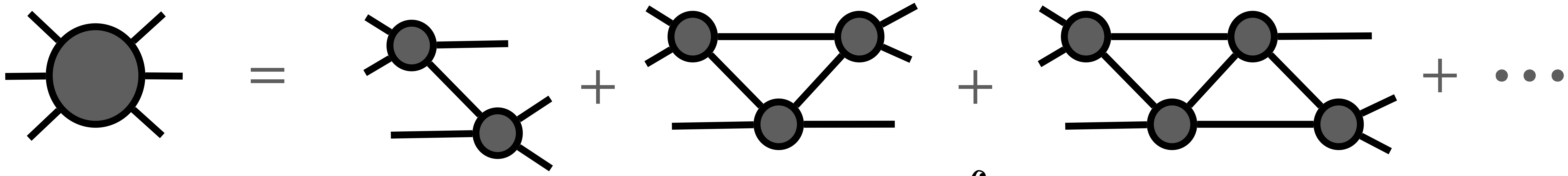

$$\mathcal{D} = -\mathcal{M}_2 G \mathcal{M}_2 - \mathcal{M}_2 \int_q G\mathcal{D}$$

Two-body scattering amplitude

$$\mathcal{M}_2 = \frac{1}{\mathcal{K}_2^{-1} - i\rho}$$

$$= \frac{1}{\rho \cot \delta_0 - i\rho}$$

Leading order effective range expansion

$$= \frac{16\pi\sqrt{\sigma_q}}{-\frac{1}{a} - i\sqrt{\frac{\sigma_q}{4} - m^2}}$$

If a>0, we have a bound-state in the two body system with mass, $m_b = 2\sqrt{m^2 - 1/a^2}$

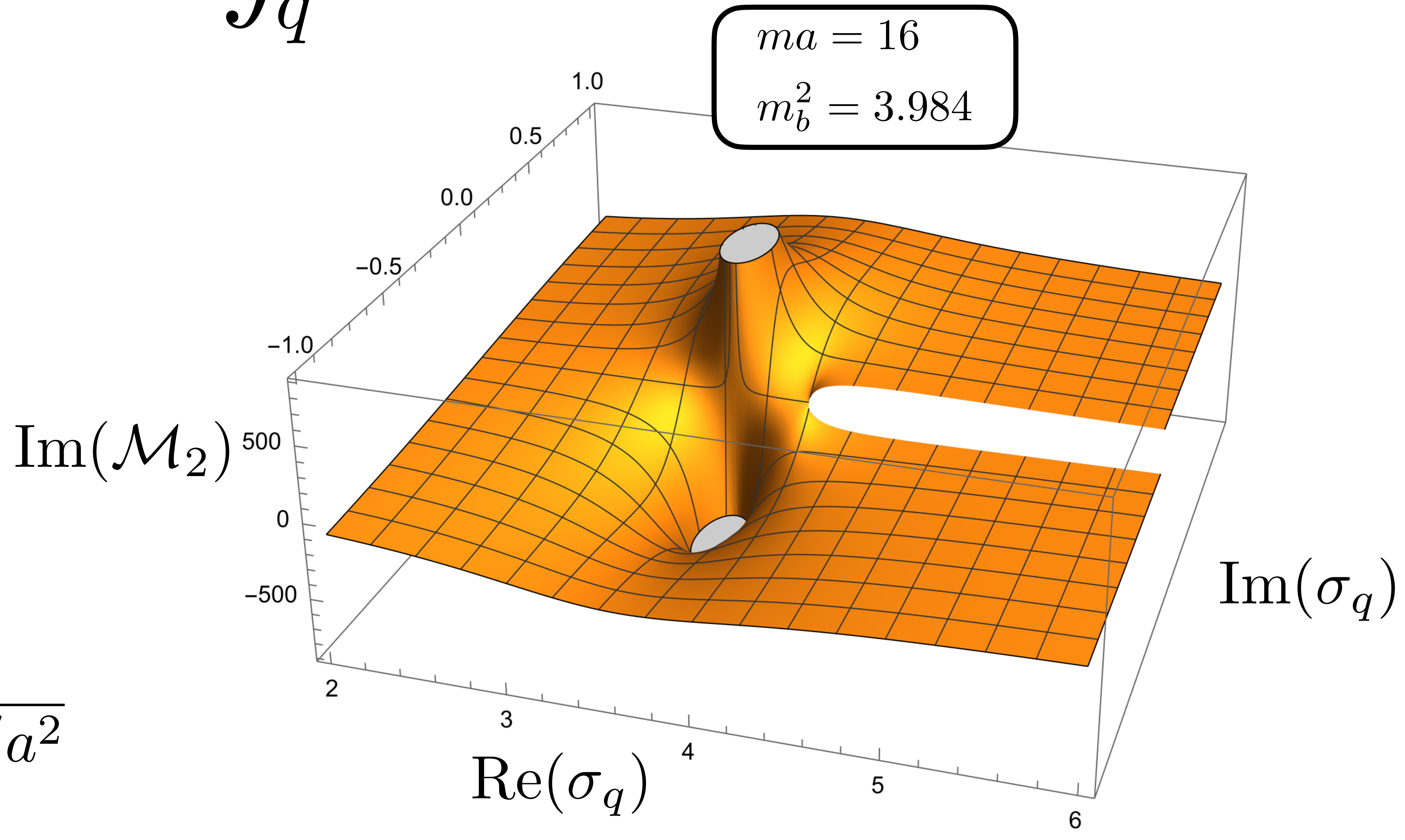

Solving Integral Equations:

1. Introduce $\mathcal{D} = \mathcal{M}_2 d \mathcal{M}_2$

2. Project onto partial wave, $\ell = 0$ sector

$$d_S(p,s,k) = -G_S(p,s,k) - \int_0^{q_{max}} dq \frac{q^2}{(2\pi)^2\omega_q} G_S(p,s,q)\mathcal{M}_2(q,s)d_S(q,s,k)$$

3. Soften singularities using non-zero epsilon, or isolate them

4. Write as matrix equation:

$$d(N,\epsilon) = -G(\epsilon) - P\cdot G(\epsilon)\cdot\mathcal{M}_2(\epsilon)\cdot d(N,\epsilon)$$

5. Recover the exact result by taking $N\to\infty$, $\epsilon\to 0$ limit

6. $\mathcal{M}_{\varphi b} = g^2 \lim_{\sigma_p,\sigma_k\to m_b^2} d_S$

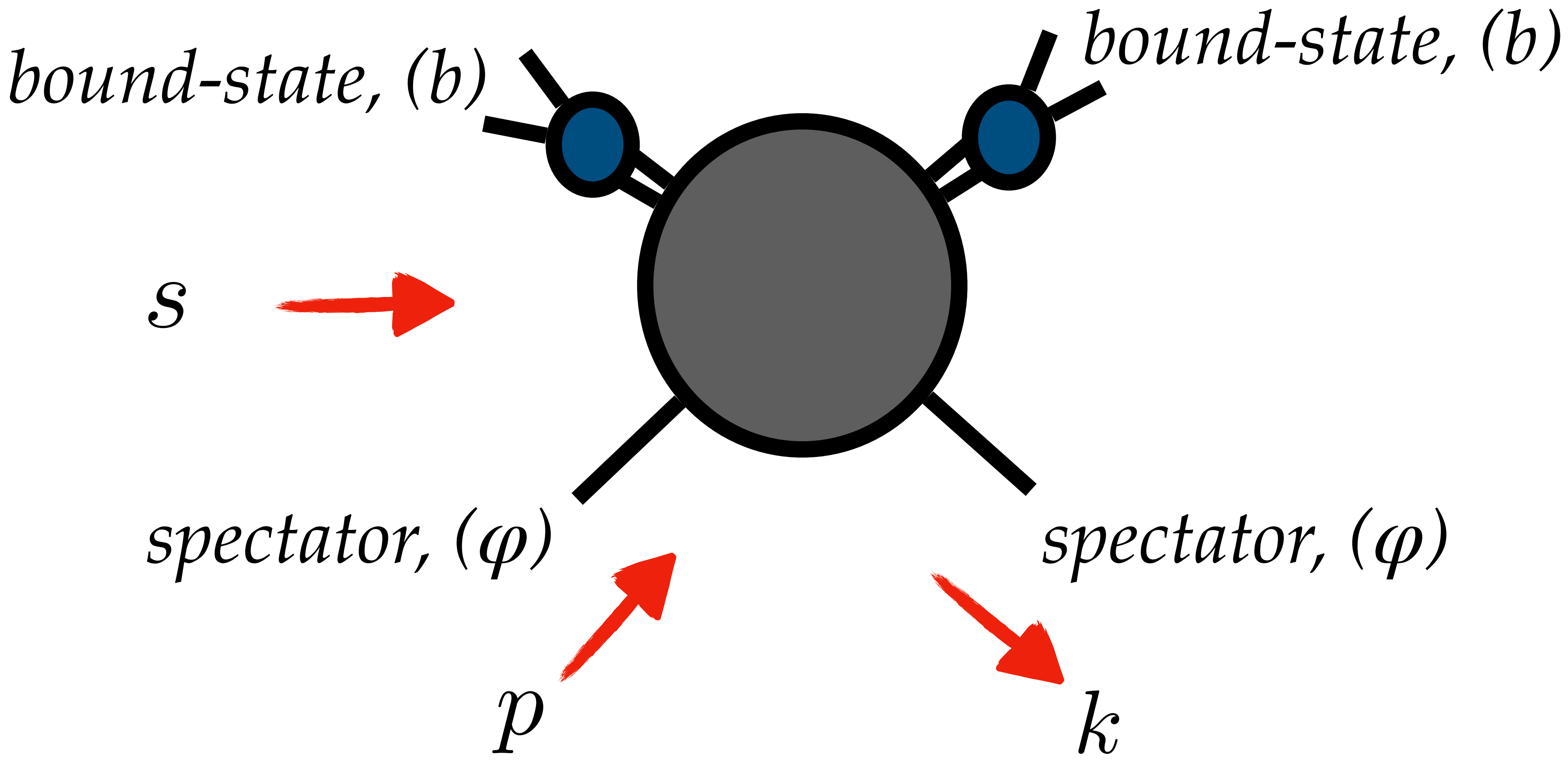

E1

Phase shifts:

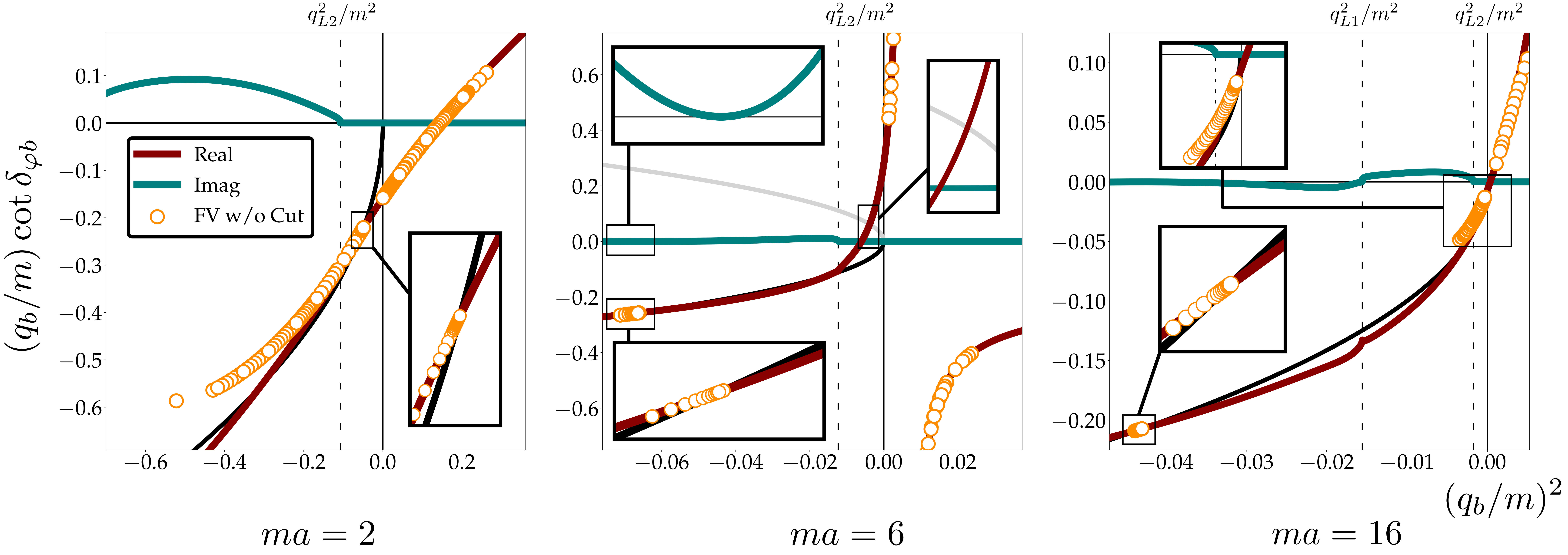

E2

Kinematic Region of Interest

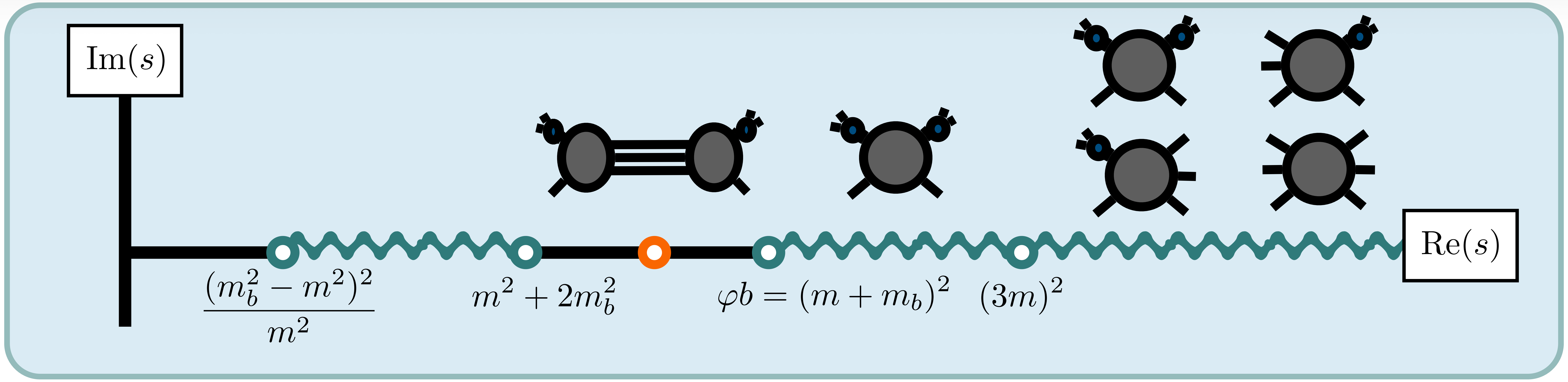

$$d_S(p,s,k) = -G_S(p,s,k) - \int_0^{q_{max}} dq \frac{q^2}{(2\pi)^2\omega_q} G_S(p,s,q)\mathcal{M}_2(q,s)d_S(q,s,k)$$

E3

φb Scattering Length, b_0

Romero-López, Sharpe, Blanton, Briceño and Hansen, 2019
Jackura, Briceño, Dawid, Islam, and McCarty, 2020
Bedaque, Hammer, van Kolck, 1999

Fit to leading order effective range expansion to get φb scattering length, b_0

$$\lim_{q\to 0} q \cot \delta_{\varphi b} = -\frac{1}{b_0}$$

$$\mathcal{M}_{\varphi b} = \frac{8\pi\sqrt{s}}{\underbrace{q \cot \delta_{\varphi b}}_{0} - iq}$$

Hints at possible trimers

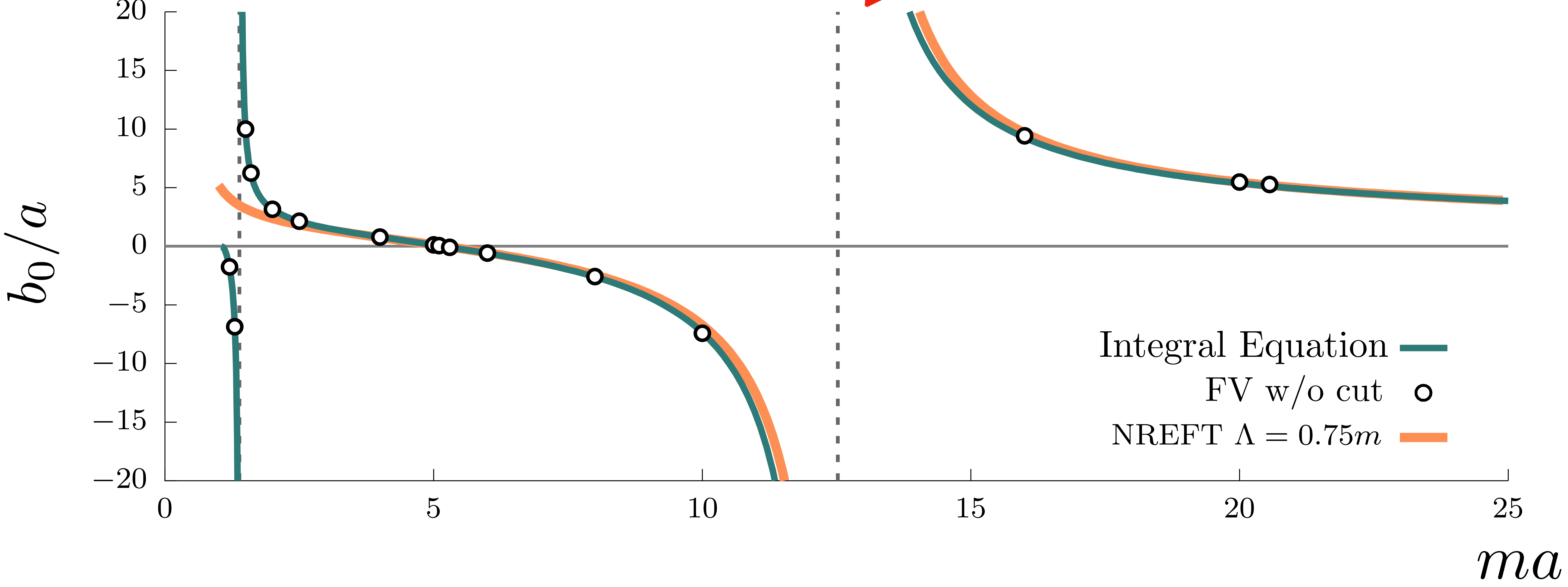

E4

Three body breakups

Romero-López, Sharpe, Blanton, Briceño and Hansen, 2019
Jackura, Briceño, Dawid, Islam, and McCarty, 2020

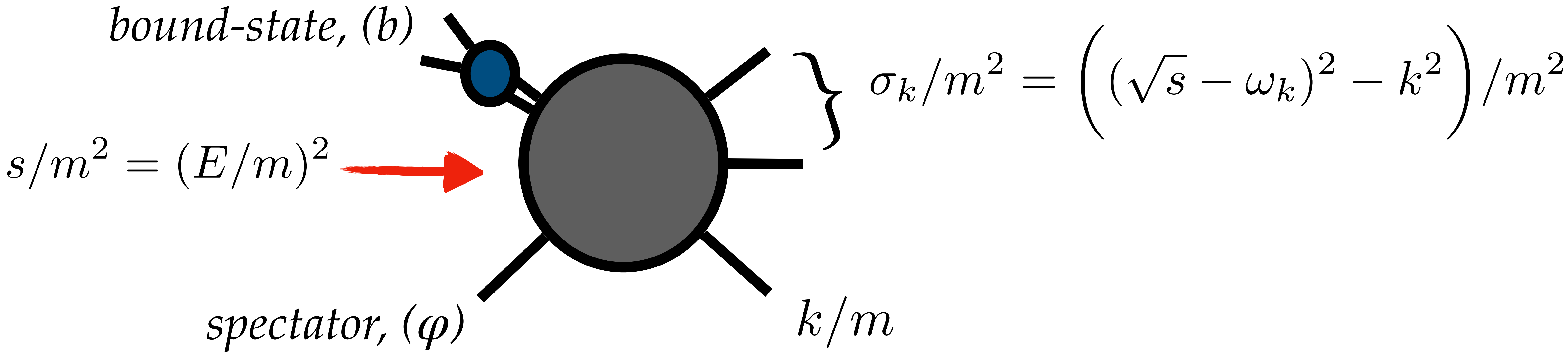

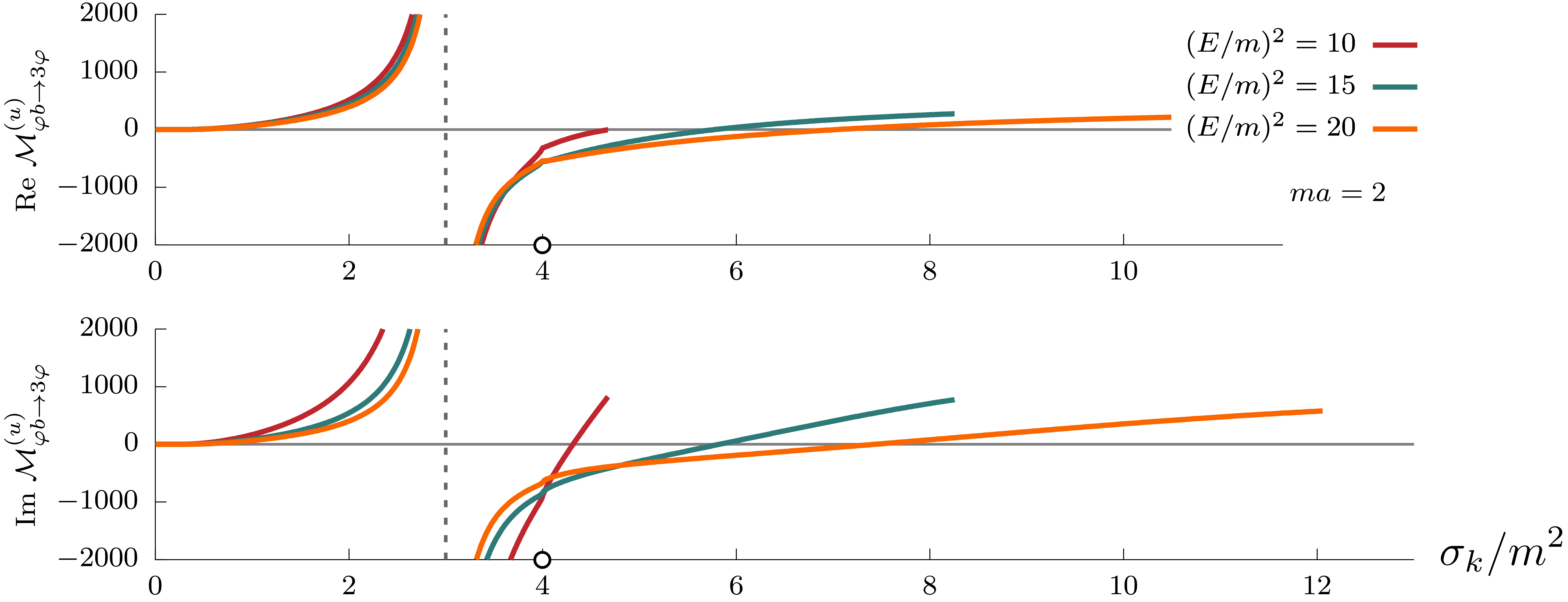

Three-Body Bound-states and Virtual States

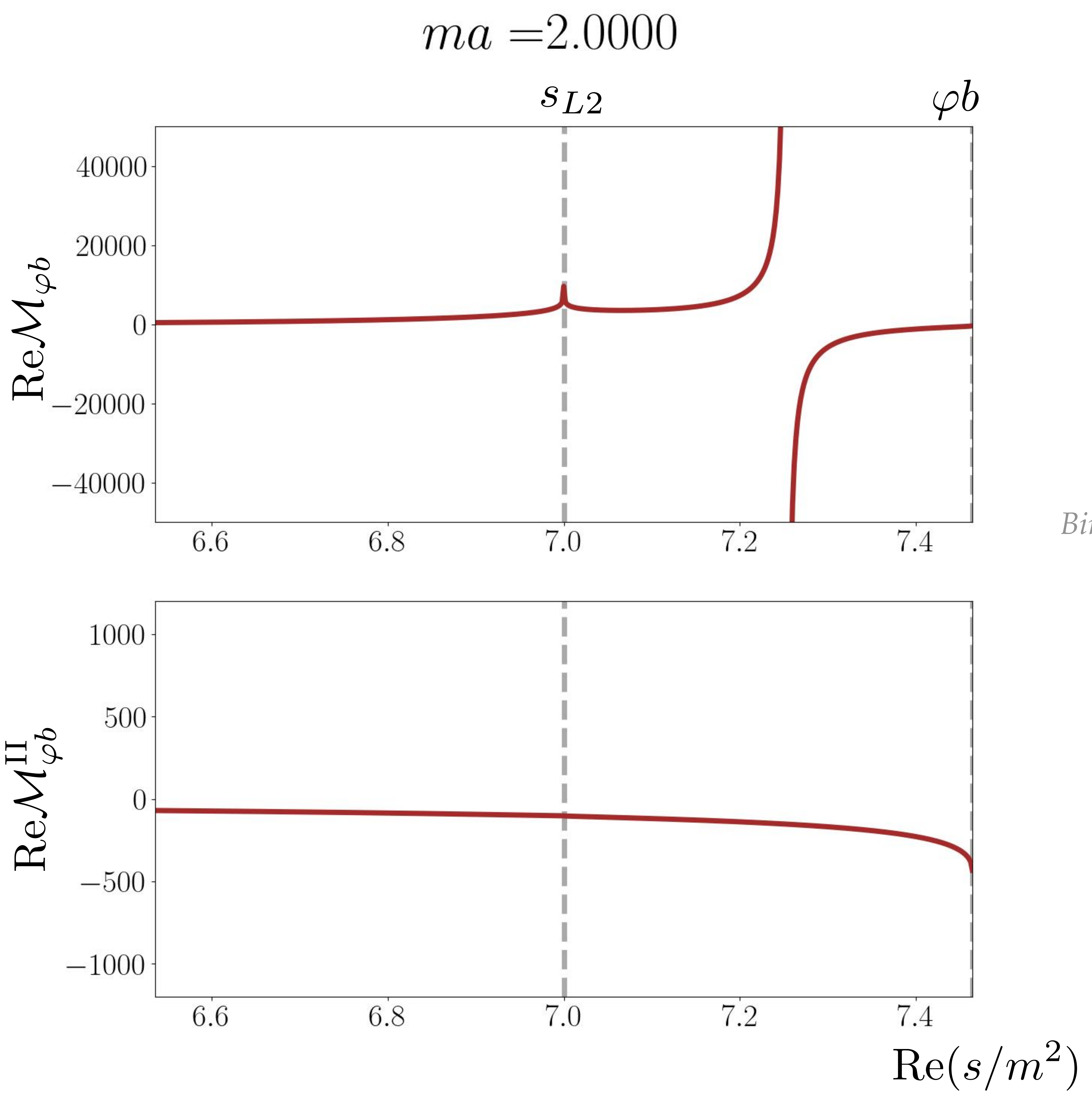

Amplitude on the Second Riemann Sheet

$$\mathcal{M}^{\mathrm{II}}_{\varphi b}(s) = \frac{\mathcal{M}_{\varphi b}(s)}{1 + 2i\rho_{\varphi b}(s)\mathcal{M}_{\varphi b}(s)}$$

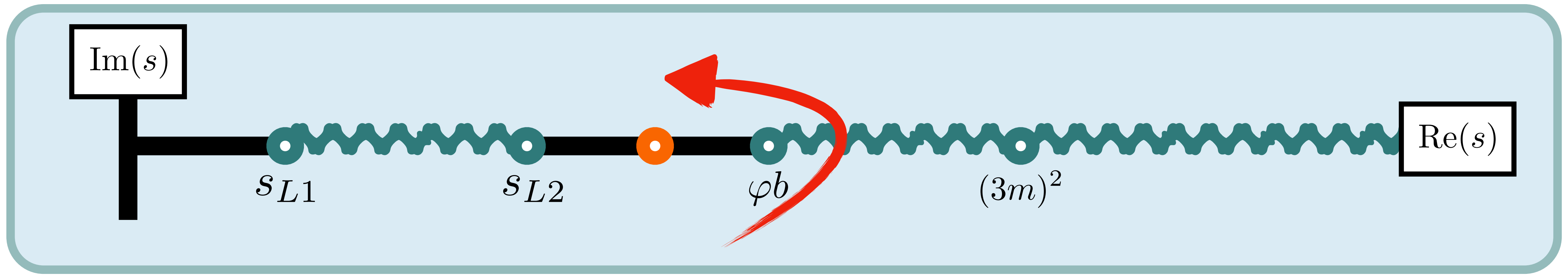

Binding energies E/m

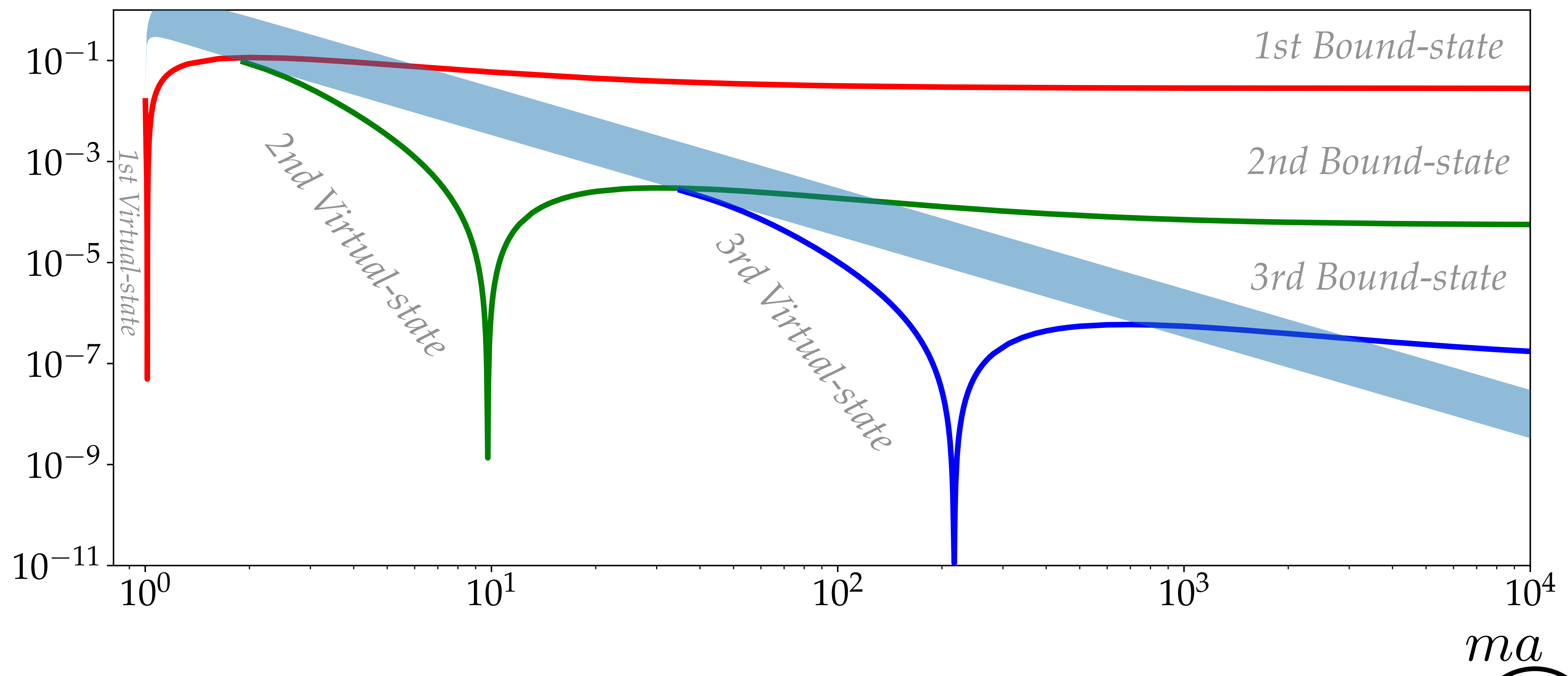

E6

Three-Body Bound-states and Virtual States

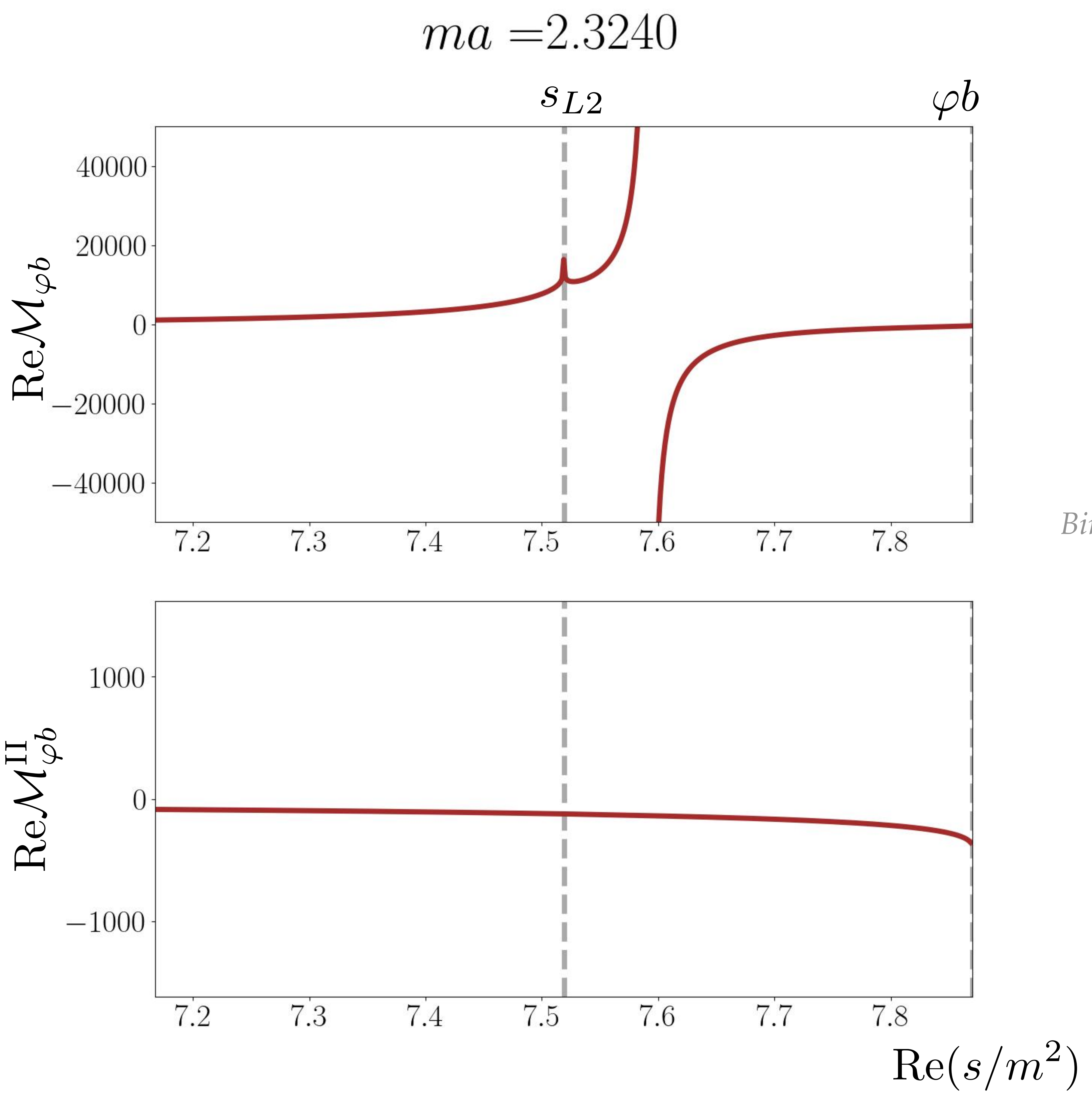

Amplitude on the Second Riemann Sheet

$$\mathcal{M}^{\mathrm{II}}_{\varphi b}(s) = \frac{\mathcal{M}_{\varphi b}(s)}{1 + 2i\rho_{\varphi b}(s)\mathcal{M}_{\varphi b}(s)}$$

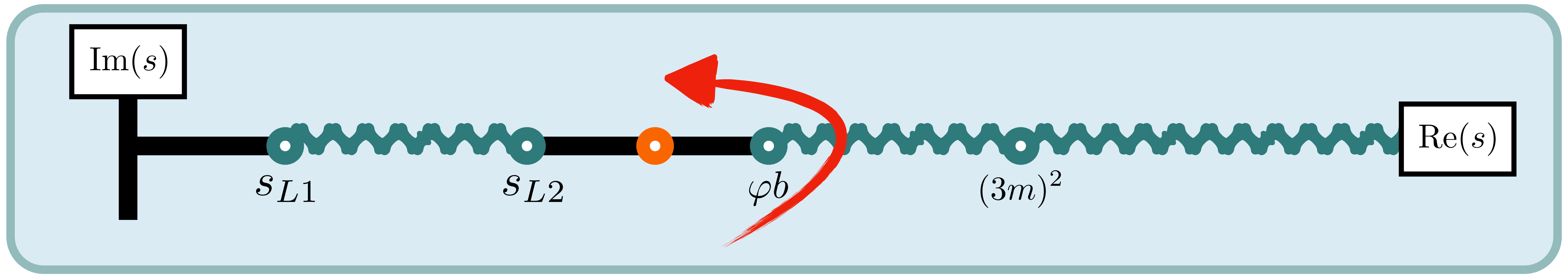

Binding energies E/m

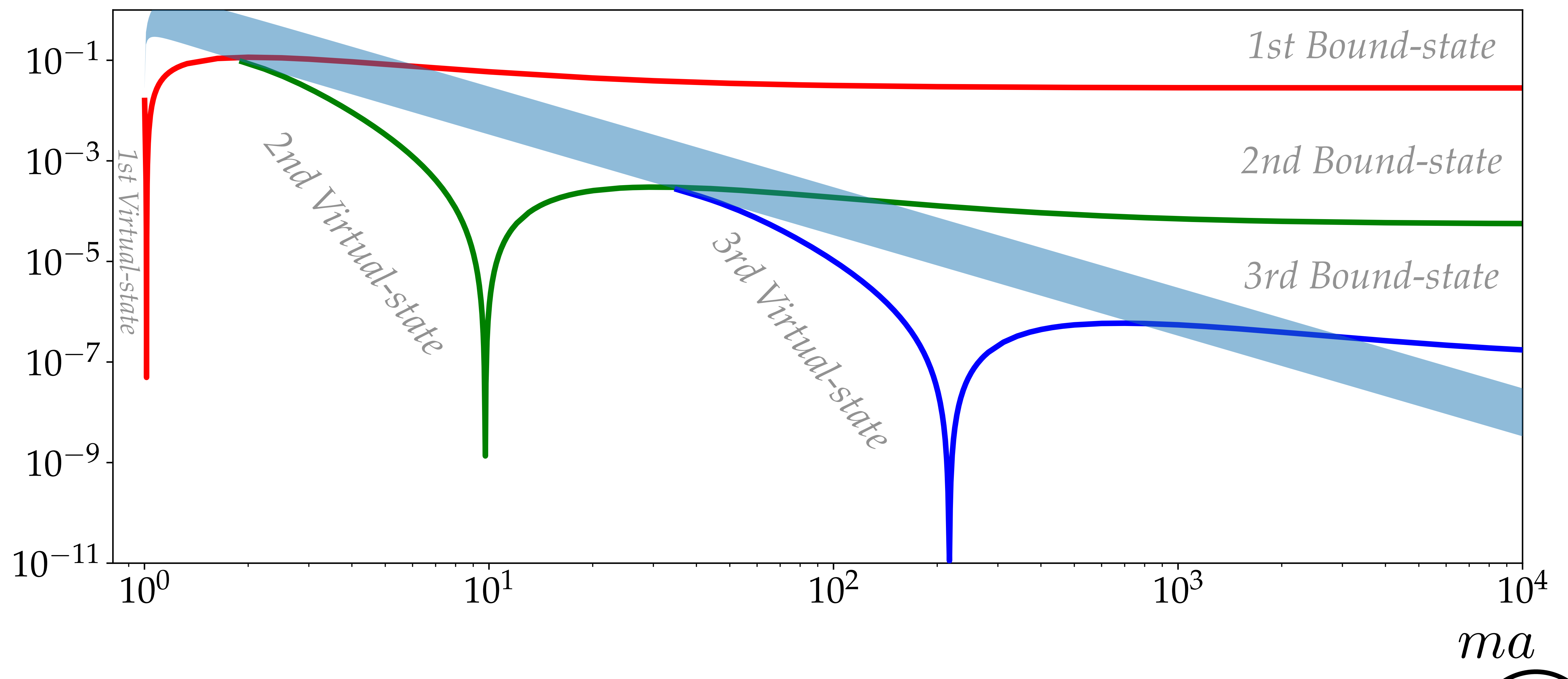

E7

Three-Body Bound-states and Virtual States

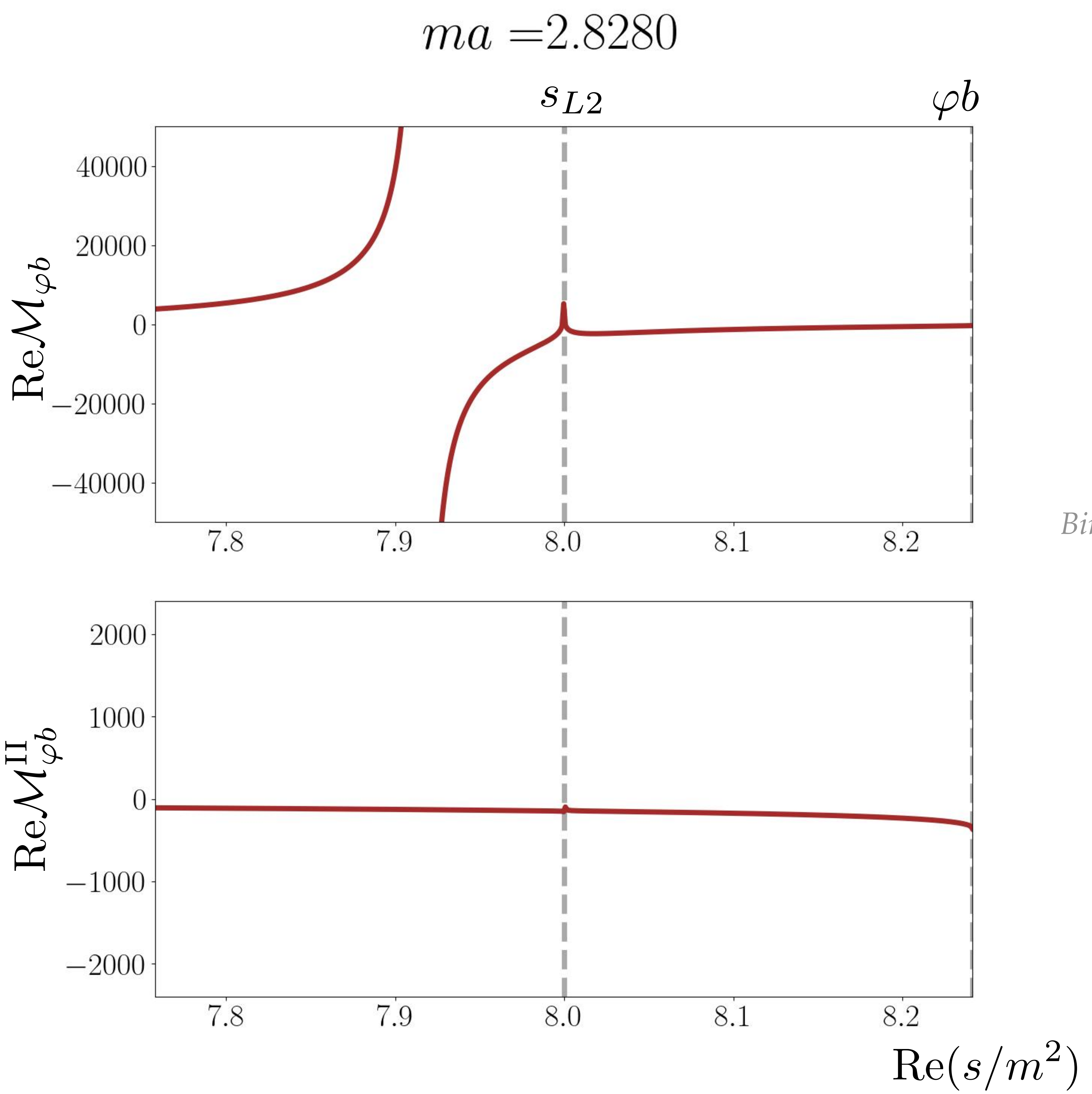

Amplitude on the Second Riemann Sheet

$$\mathcal{M}^{\mathrm{II}}_{\varphi b}(s) = \frac{\mathcal{M}_{\varphi b}(s)}{1 + 2i\rho_{\varphi b}(s)\mathcal{M}_{\varphi b}(s)}$$

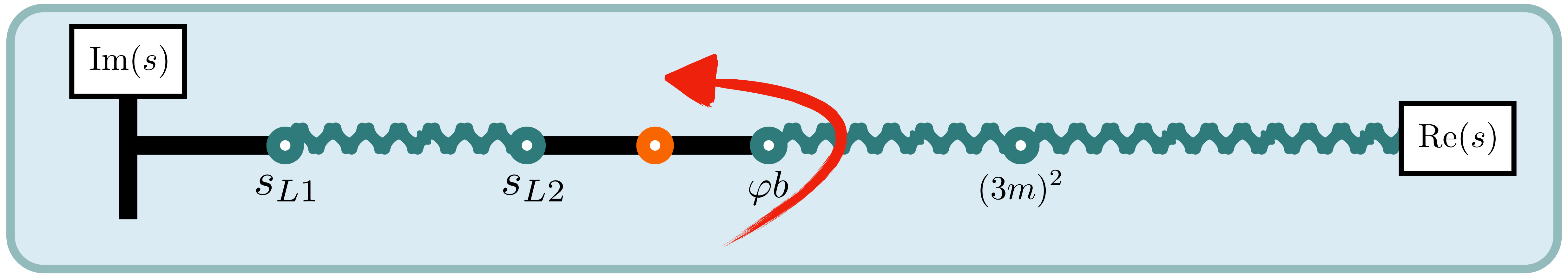

Binding energies E/m

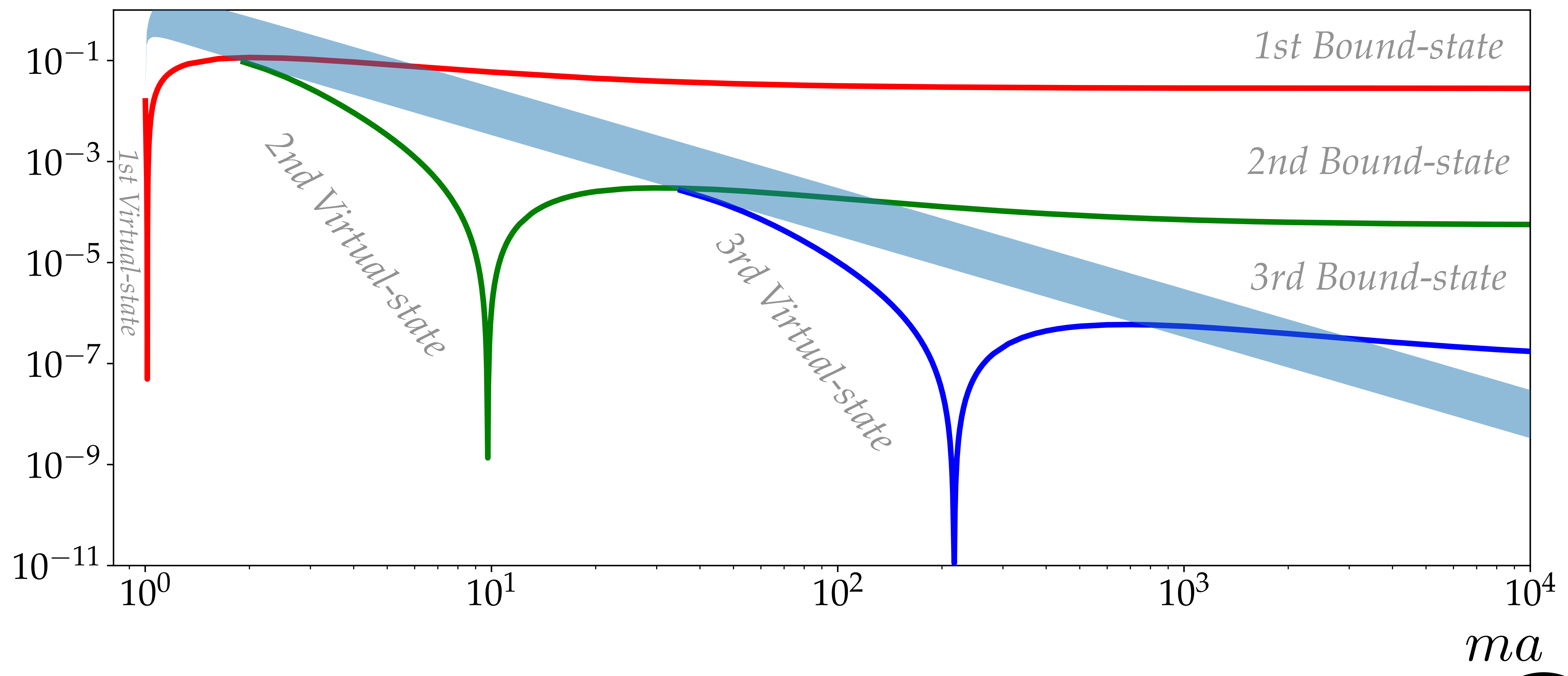

Three-Body Bound-states and Virtual States

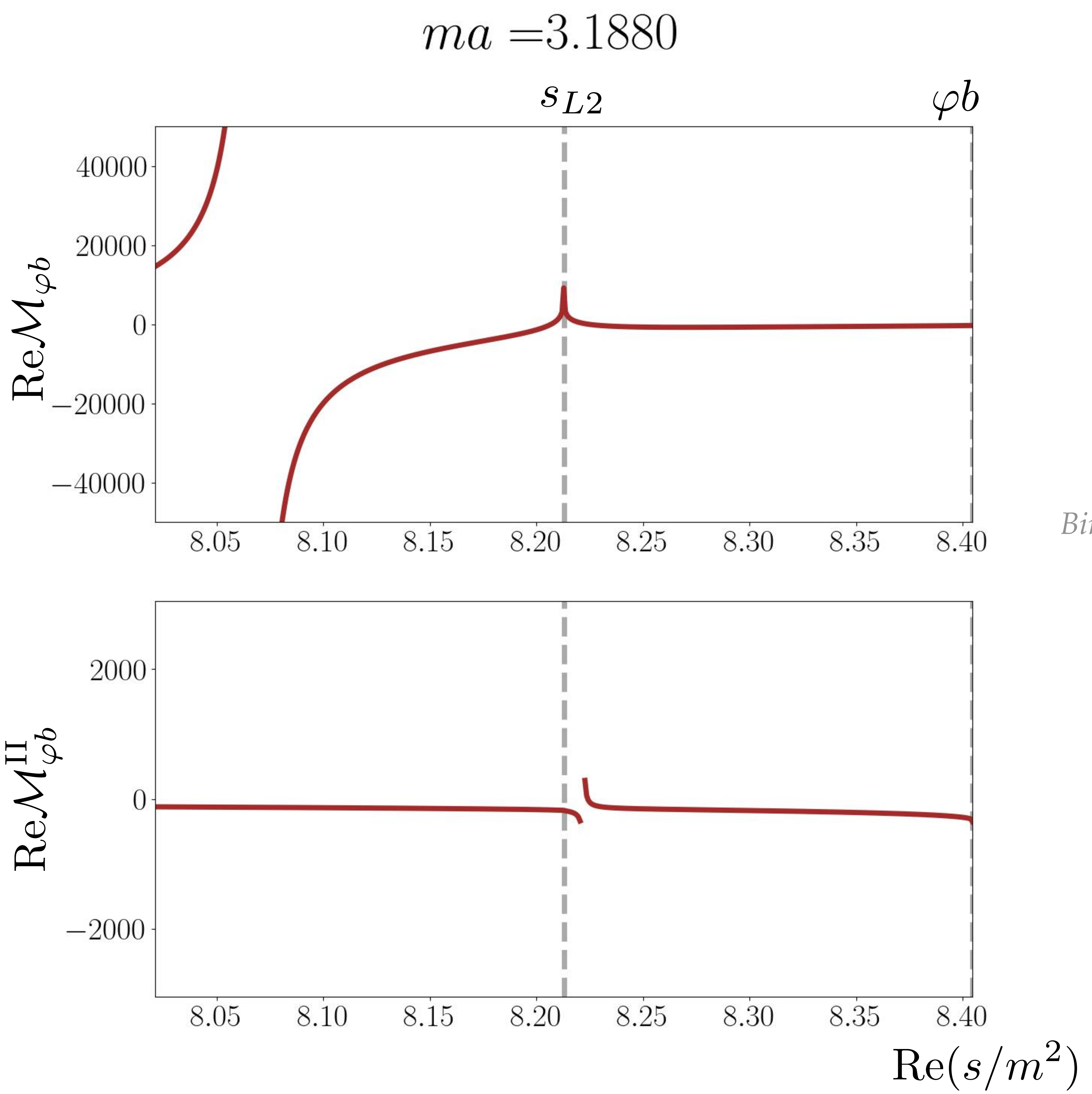

Amplitude on the Second Riemann Sheet

$$\mathcal{M}^{\mathrm{II}}_{\varphi b}(s) = \frac{\mathcal{M}_{\varphi b}(s)}{1 + 2i\rho_{\varphi b}(s)\mathcal{M}_{\varphi b}(s)}$$

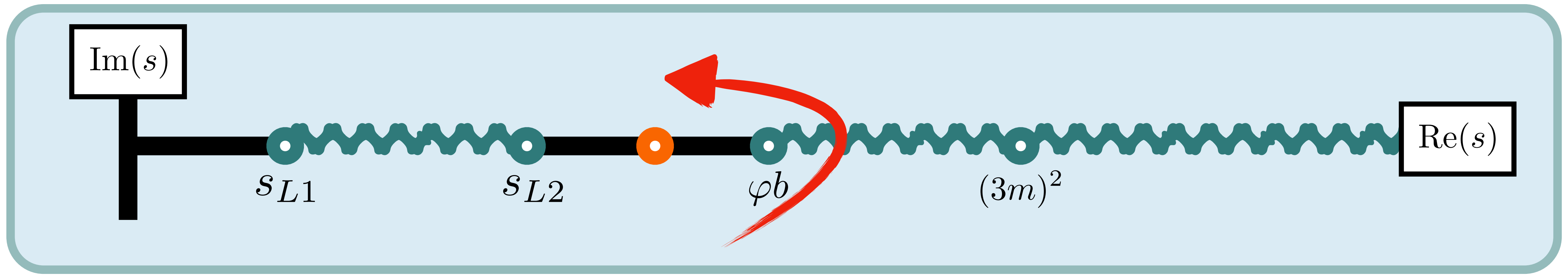

Binding energies E/m

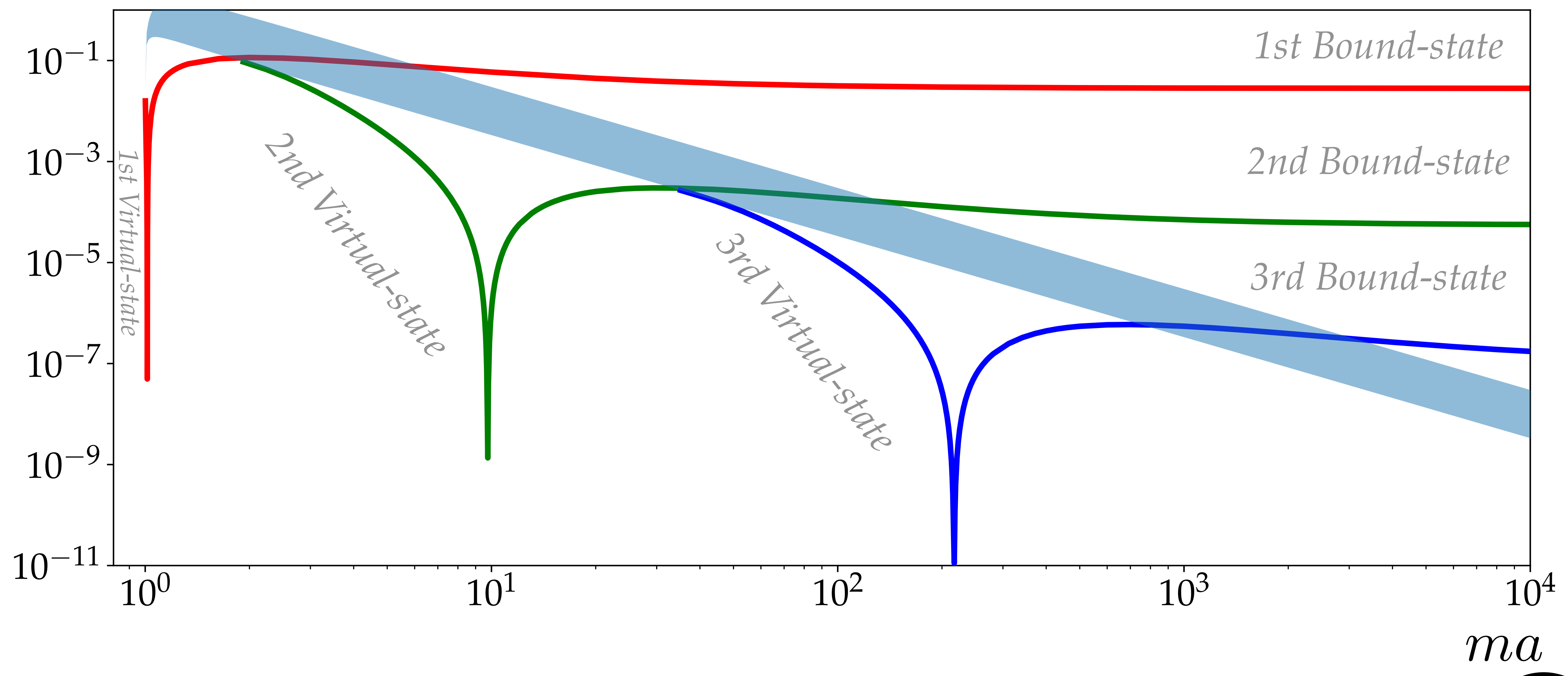

E9

Three-Body Bound-states and Virtual States

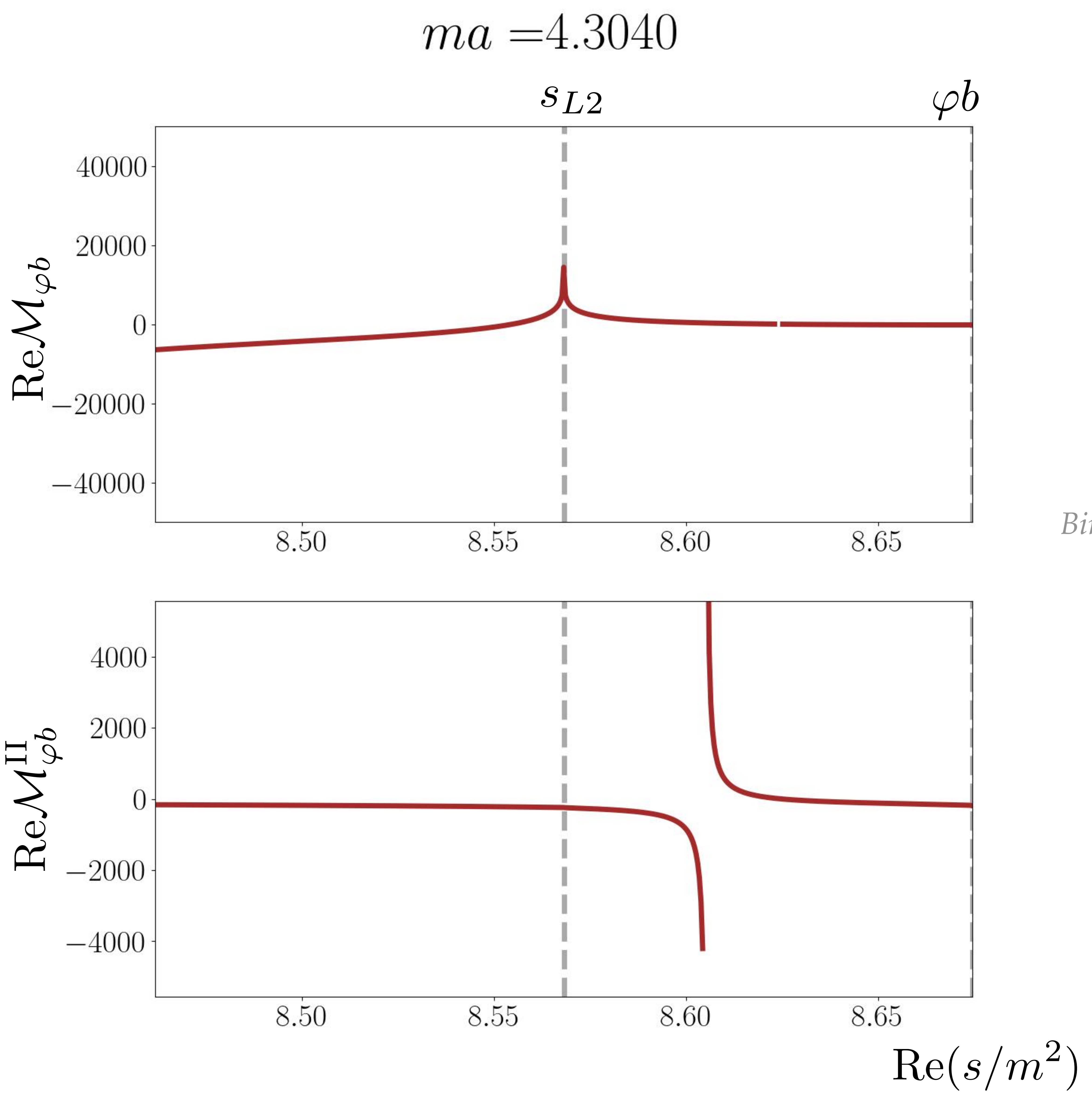

Amplitude on the Second Riemann Sheet

$$\mathcal{M}^{\mathrm{II}}_{\varphi b}(s) = \frac{\mathcal{M}_{\varphi b}(s)}{1 + 2i\rho_{\varphi b}(s)\mathcal{M}_{\varphi b}(s)}$$

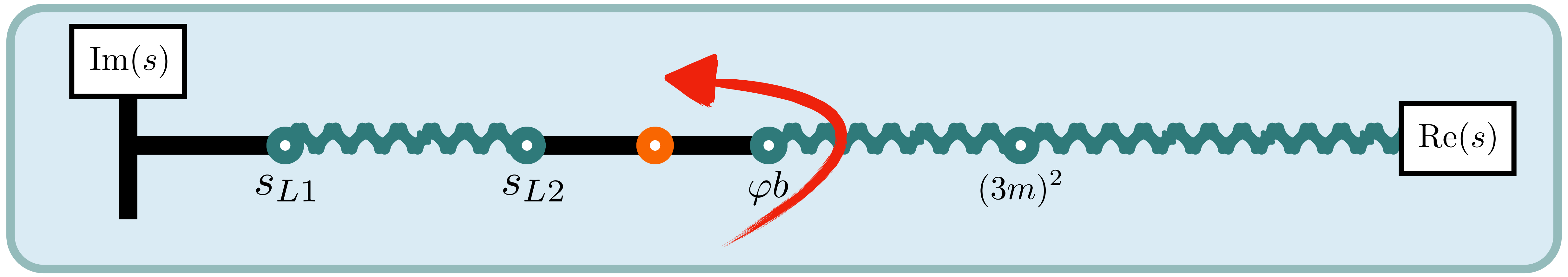

Binding energies E/m

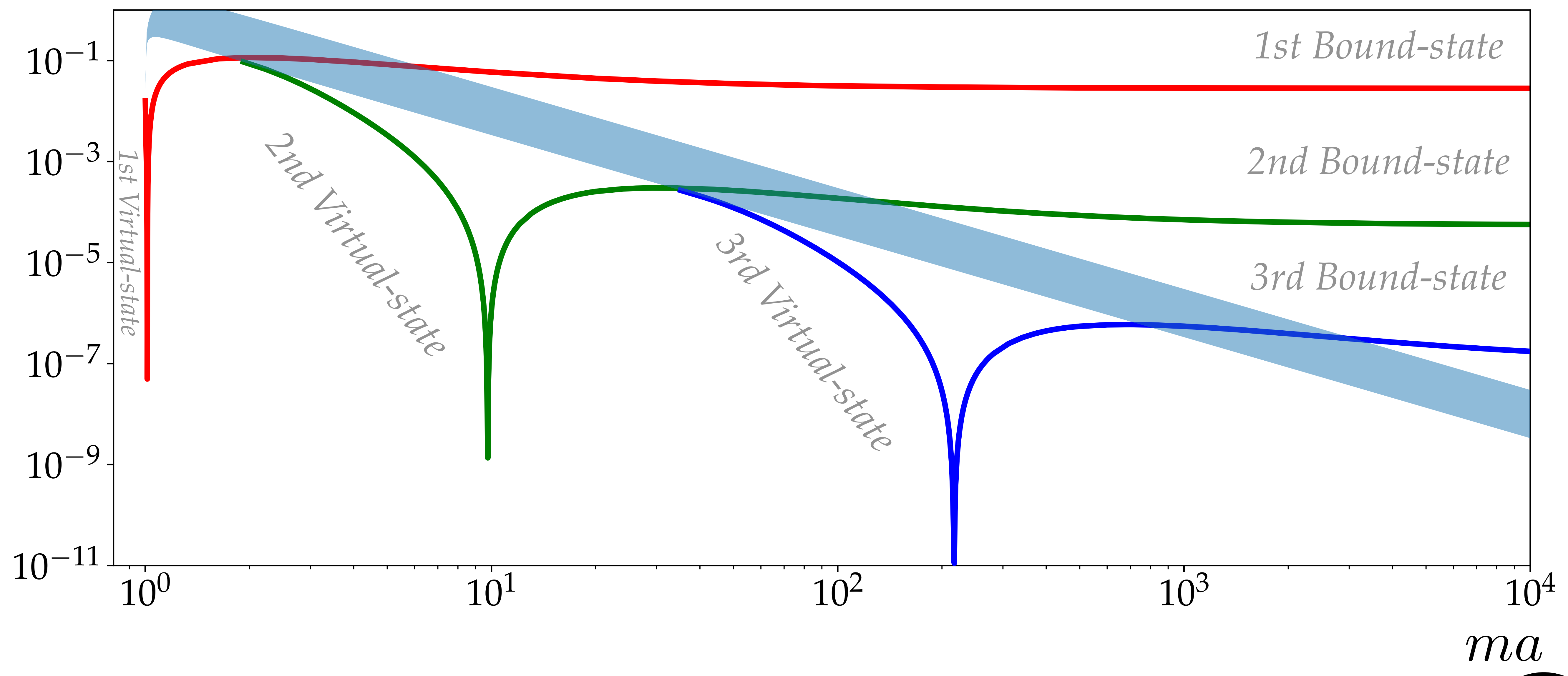

E10

Three-Body Bound-states and Virtual States

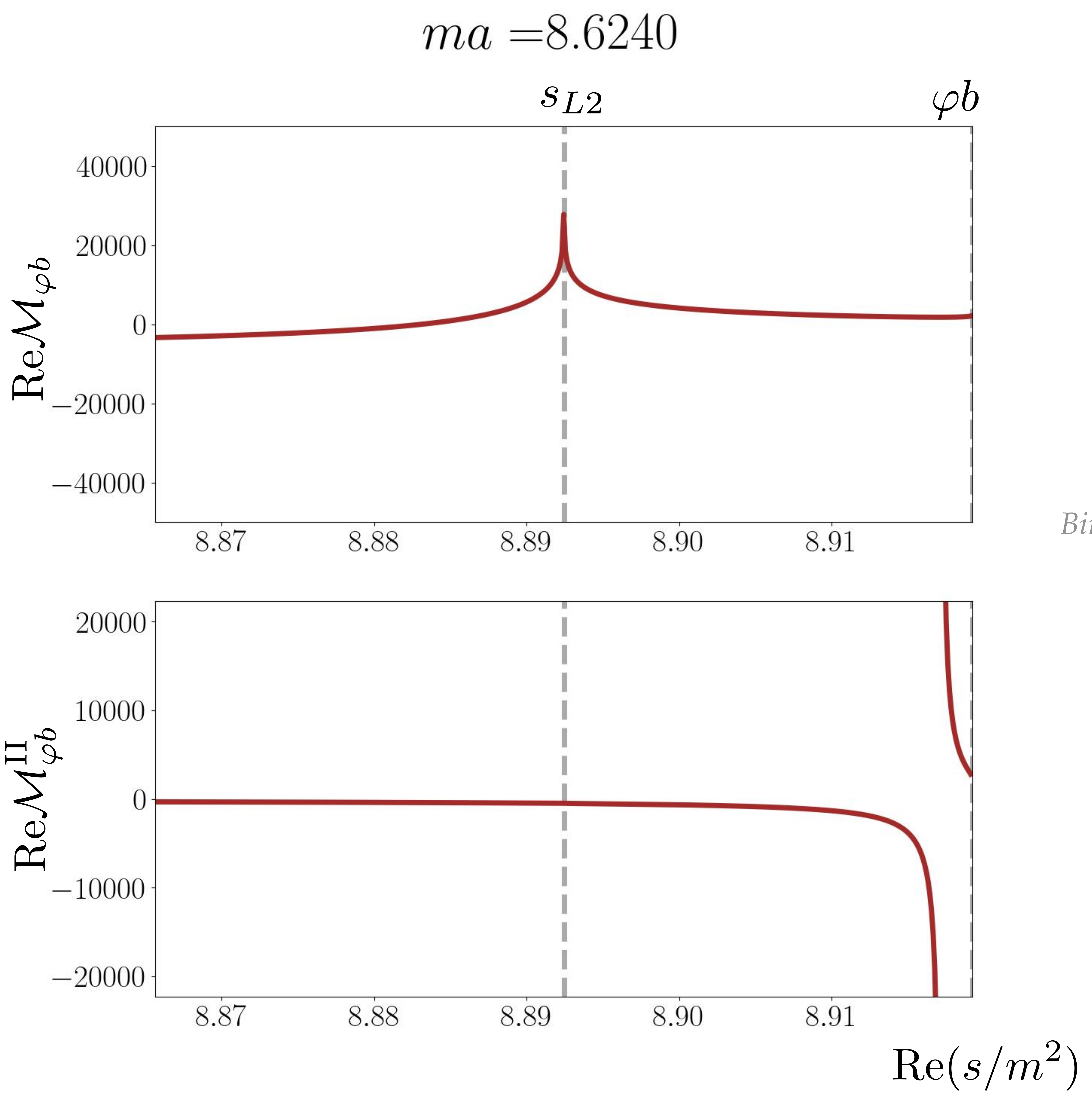

Amplitude on the Second Riemann Sheet

$$\mathcal{M}^{\mathrm{II}}_{\varphi b}(s) = \frac{\mathcal{M}_{\varphi b}(s)}{1 + 2i\rho_{\varphi b}(s)\mathcal{M}_{\varphi b}(s)}$$

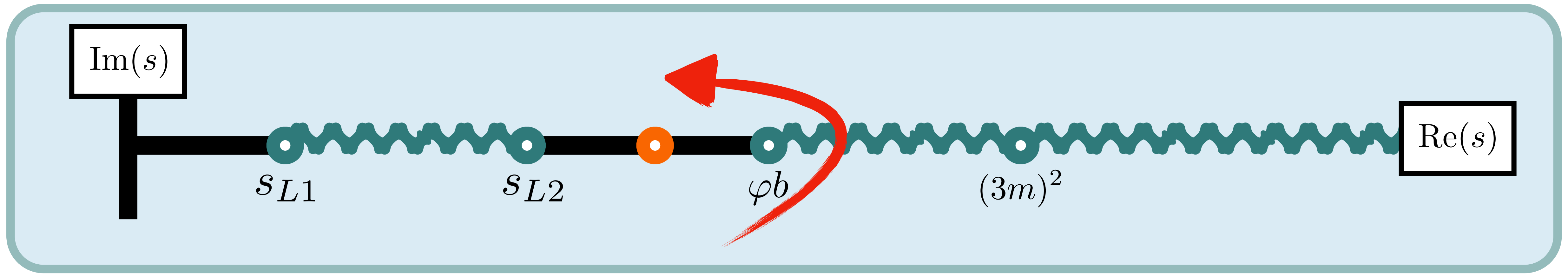

Binding energies E/m

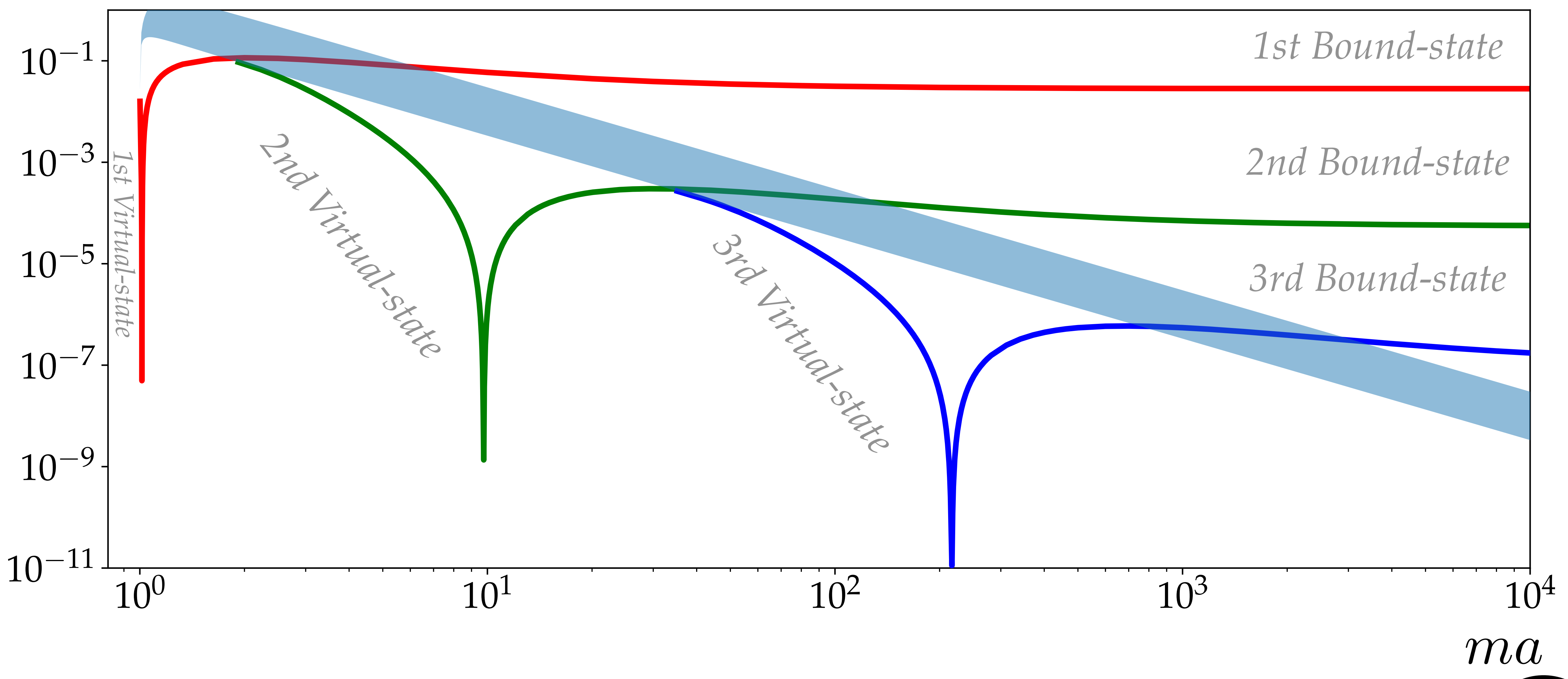

E11

Three-Body Bound-states and Virtual States

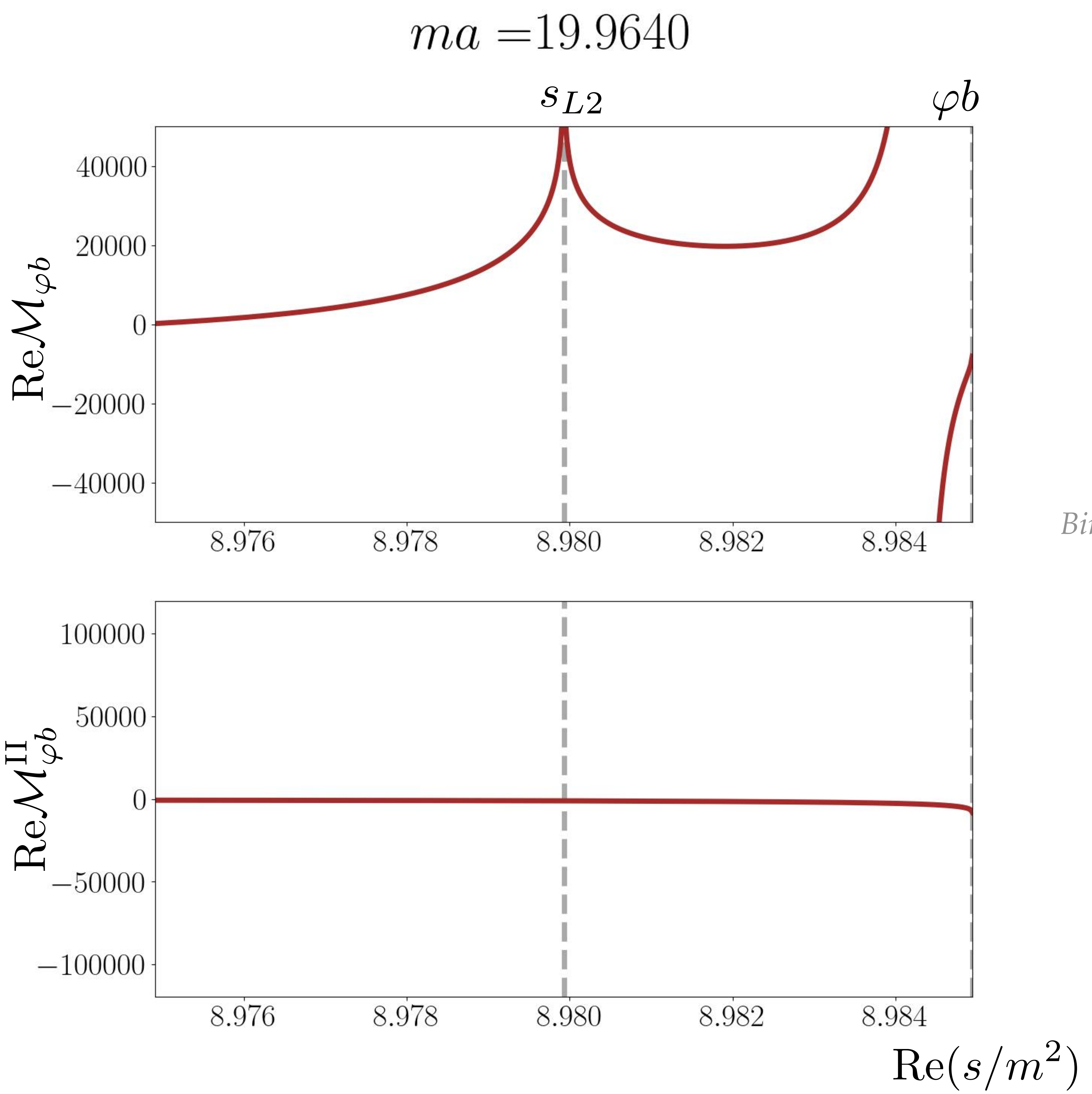

Amplitude on the Second Riemann Sheet

$$\mathcal{M}^{\mathrm{II}}_{\varphi b}(s) = \frac{\mathcal{M}_{\varphi b}(s)}{1 + 2i\rho_{\varphi b}(s)\mathcal{M}_{\varphi b}(s)}$$

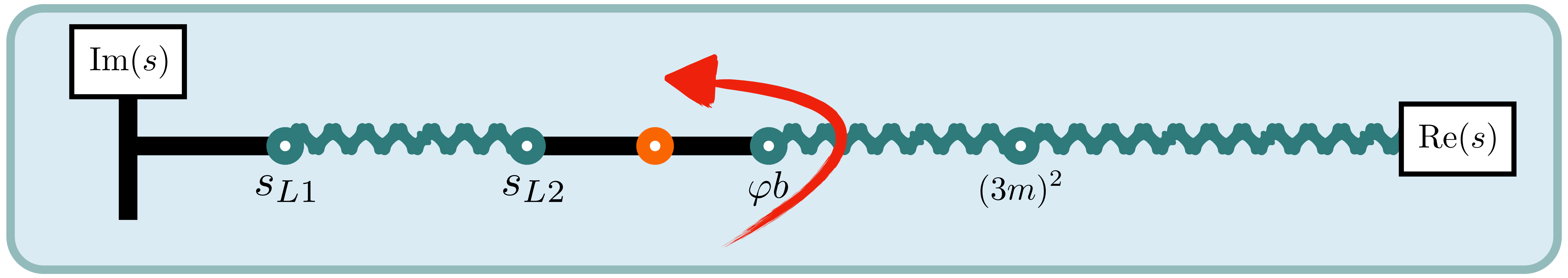

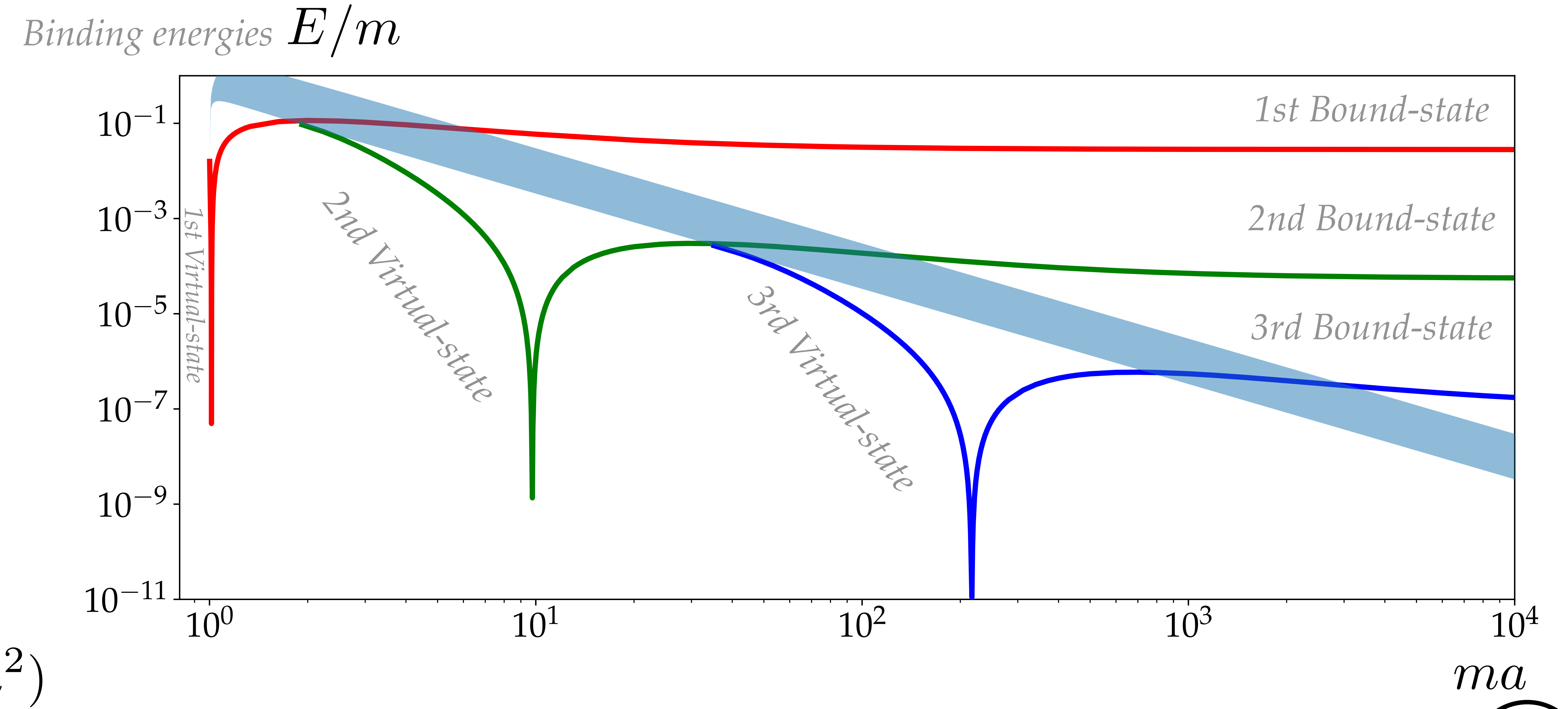

E12

Recovering Efimov Physics

Preliminary Results

For finite two body scattering length, ma, we have a finite number of three body bound-states

For a specific scattering length, we take the ratio of the binding energies of two consecutive three-body bound-states

For increasing scattering length, the ratio becomes close to Efimov's prediction

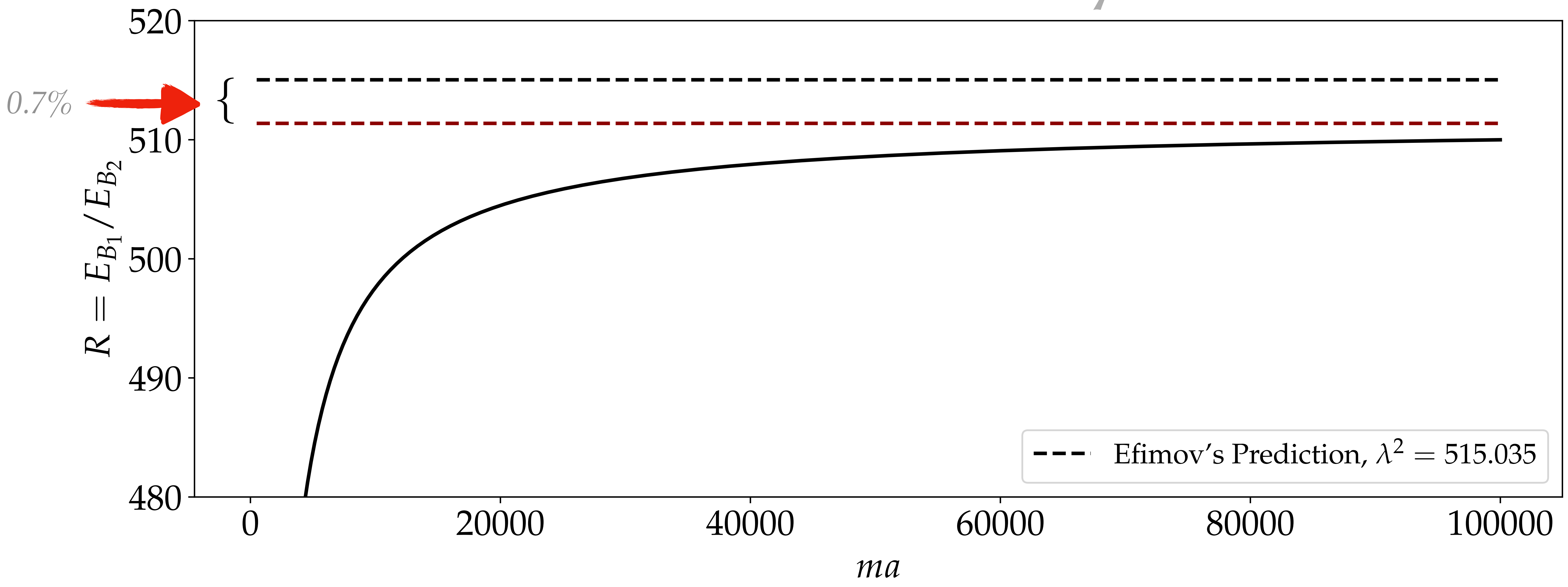

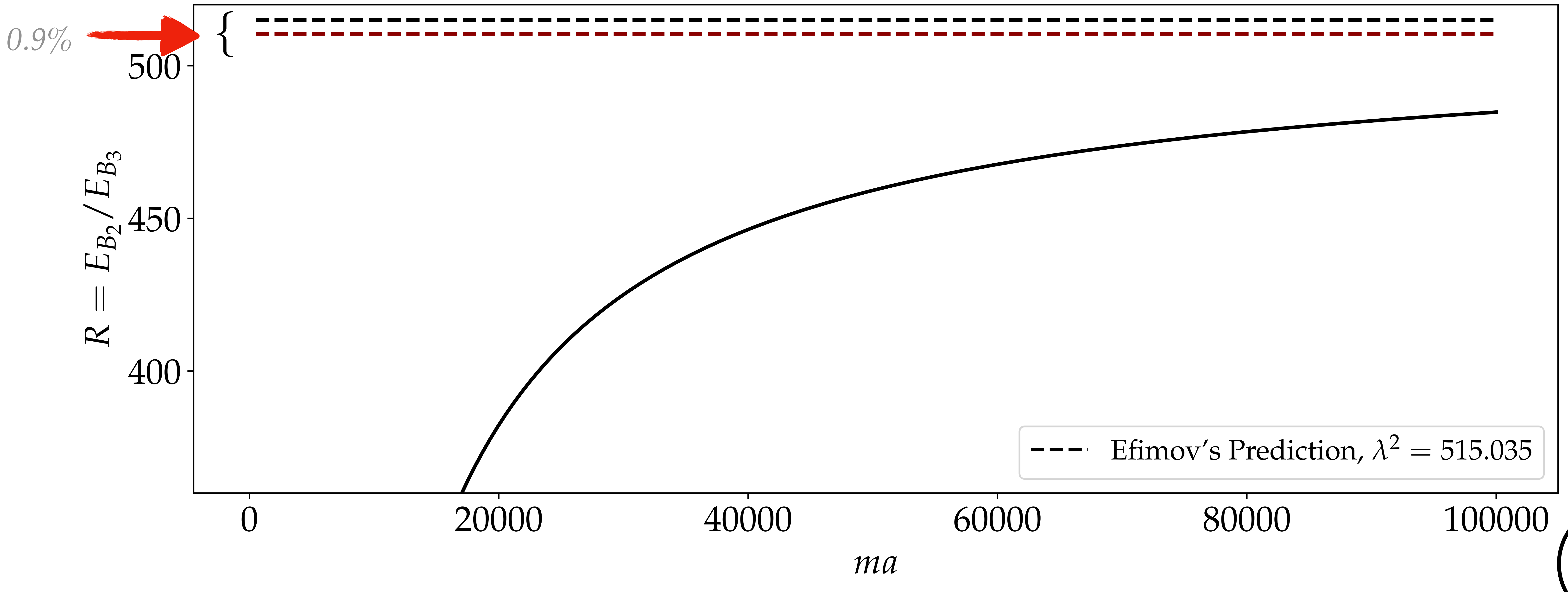

Trimer Trajectories

Preliminary Results

Binding momentum, $\kappa \sim \sqrt{E}$

☆ *Emergence of virtual state*

△ *Value at unitarity limit*

○ *End points of Trimer trajectory*

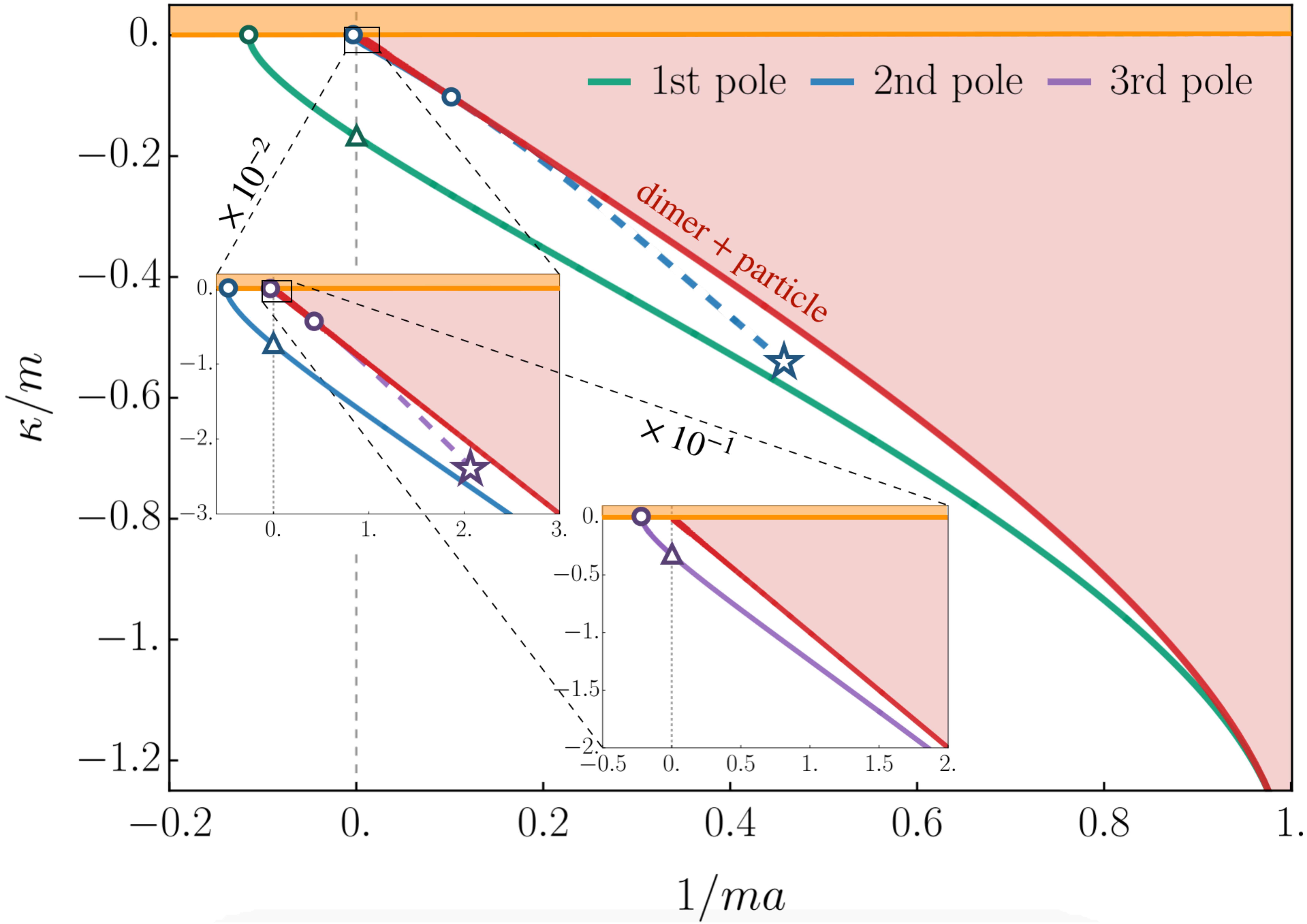

Resonances

Preliminary Results

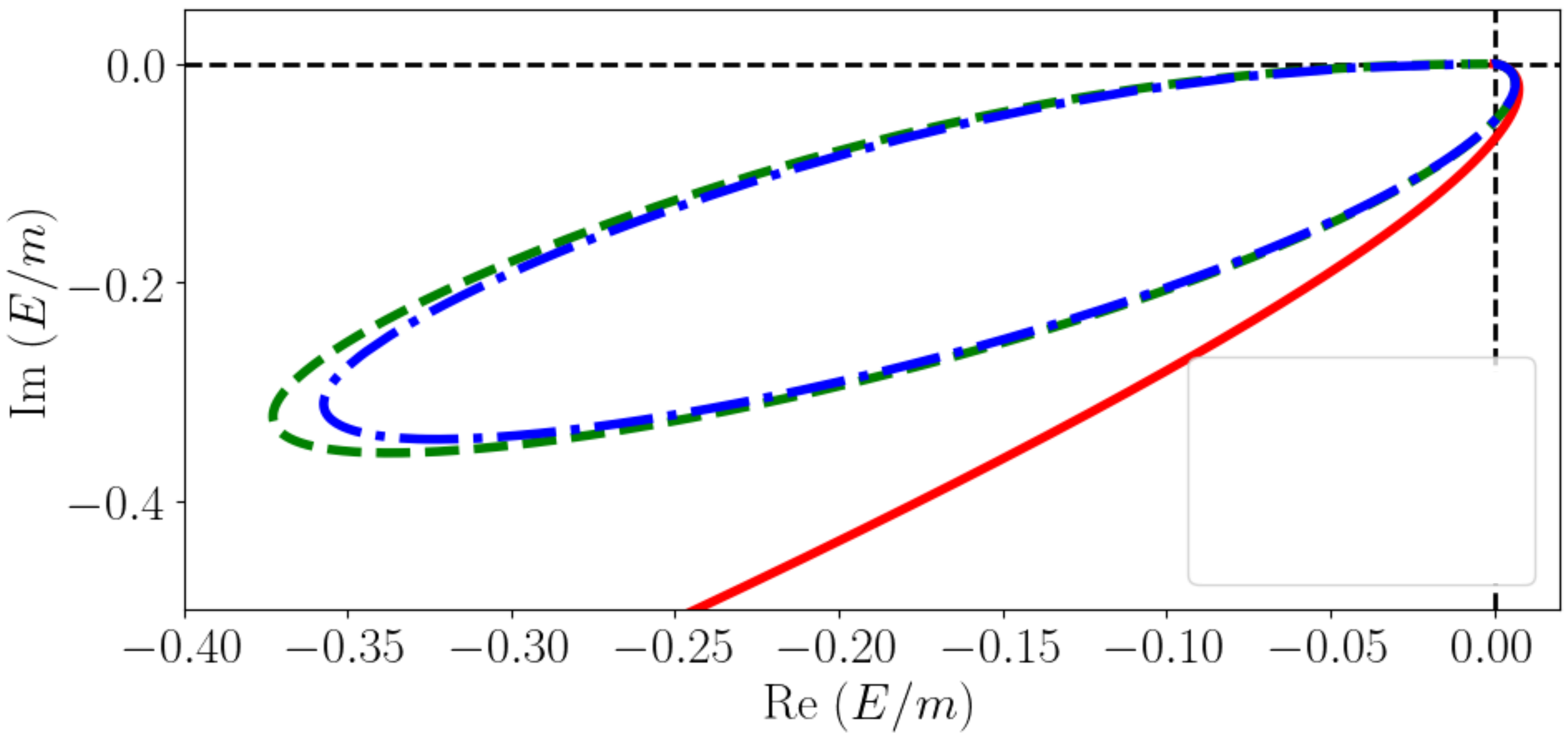

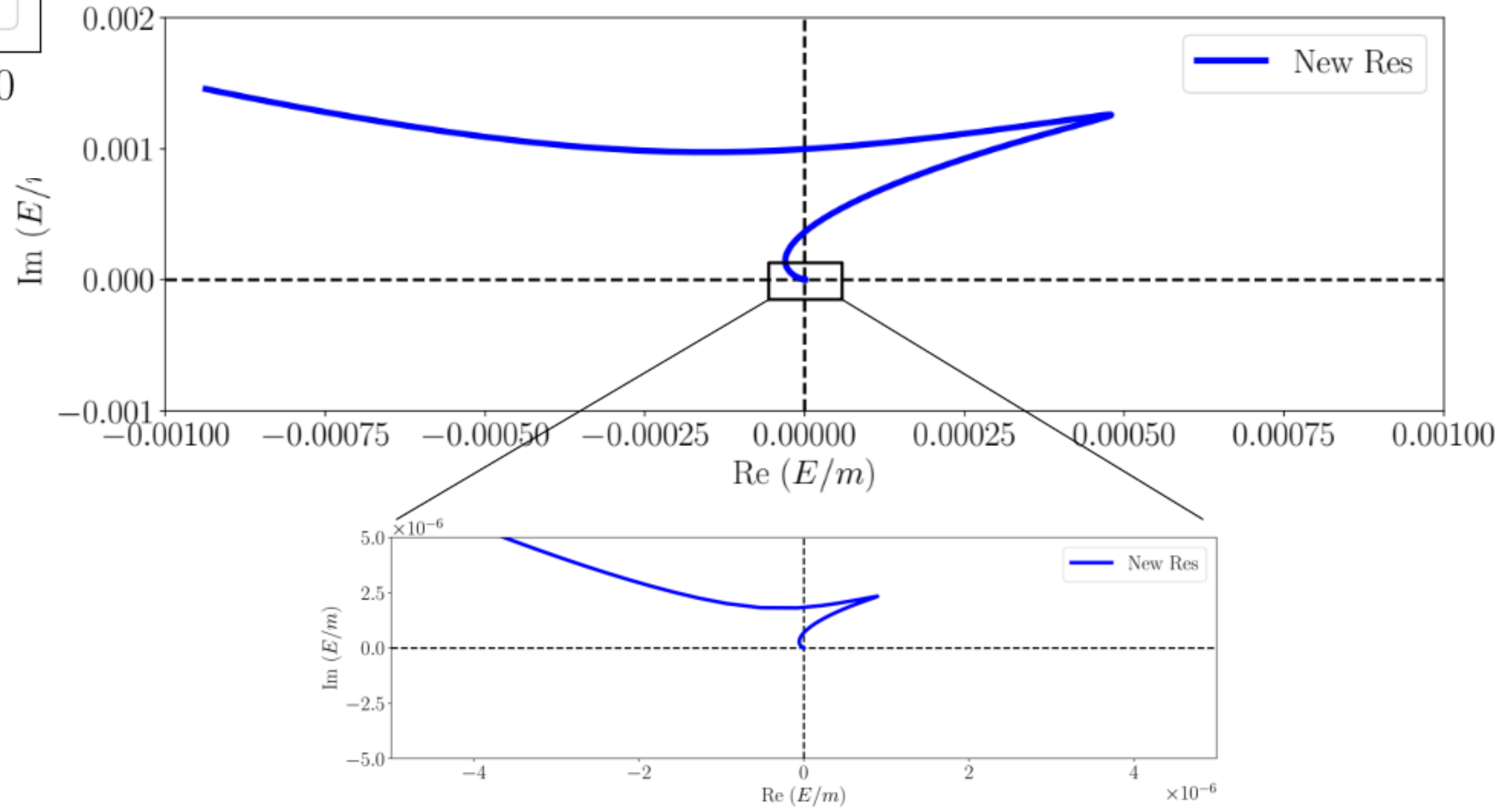

(E14

Mesons

$n^{2s+1}\ell_J$	J^{PC}	I $=1$ $u\bar{d}$, $\bar{u}d$, $\frac{1}{\sqrt{2}}(d\bar{d}-u\bar{u})$	I $=\frac{1}{2}$ $u\bar{s}$, $d\bar{s}$; $\bar{d}s$, $\bar{u}s$	I $=0$ f'	I $=0$ f
1^1S_0	0^{-+}	$\boldsymbol{\pi}$	$\boldsymbol{K}$	$\boldsymbol{\eta}$	$\boldsymbol{\eta'}(958)$
1^3S_1	1^{--}	$\boldsymbol{\rho(770)}$	$\boldsymbol{K^*(892)}$	$\boldsymbol{\phi(1020)}$	$\boldsymbol{\omega(782)}$
1^1P_1	1^{+-}	$\boldsymbol{b_1(1235)}$	$\boldsymbol{K_{1B}}$[a]	$\boldsymbol{h_1(1415)}$	$\boldsymbol{h_1(1170)}$
1^3P_0	0^{++}	$\boldsymbol{a_0(1450)}$	$\boldsymbol{K_0^*(1430)}$	$\boldsymbol{f_0(1710)}$	$\boldsymbol{f_0(1370)}$
1^3P_1	1^{++}	$\boldsymbol{a_1(1260)}$	$\boldsymbol{K_{1A}}$[a]	$\boldsymbol{f_1(1420)}$	$\boldsymbol{f_1(1285)}$
1^3P_2	2^{++}	$\boldsymbol{a_2(1320)}$	$\boldsymbol{K_2^*(1430)}$	$\boldsymbol{f_2'(1525)}$	$\boldsymbol{f_2(1270)}$
1^1D_2	2^{-+}	$\boldsymbol{\pi_2(1670)}$	$\boldsymbol{K_2(1770)}$[a]	$\boldsymbol{\eta_2(1870)}$	$\boldsymbol{\eta_2(1645)}$
1^3D_1	1^{--}	$\boldsymbol{\rho(1700)}$	$\boldsymbol{K^*(1680)}$[b]	$\phi(2170)$[d]	$\boldsymbol{\omega(1650)}$
1^3D_2	2^{--}		$\boldsymbol{K_2(1820)}$[a]		
1^3D_3	3^{--}	$\boldsymbol{\rho_3(1690)}$	$\boldsymbol{K_3^*(1780)}$	$\boldsymbol{\phi_3(1850)}$	$\boldsymbol{\omega_3(1670)}$
1^3F_4	4^{++}	$\boldsymbol{a_4(1970)}$	$\boldsymbol{K_4^*(2045)}$	$f_4(2300)$	$\boldsymbol{f_4(2050)}$
1^3G_5	5^{--}	$\rho_5(2350)$	$K_5^*(2380)$		
2^1S_0	0^{-+}	$\boldsymbol{\pi(1300)}$	$\boldsymbol{K(1460)}$	$\boldsymbol{\eta(1475)}$[c]	$\boldsymbol{\eta(1295)}$
2^3S_1	1^{--}	$\boldsymbol{\rho(1450)}$	$\boldsymbol{K^*(1410)}$[b]	$\boldsymbol{\phi(1680)}$	$\boldsymbol{\omega(1420)}$
2^3P_1	1^{++}	$\boldsymbol{a_1(1640)}$			
2^3P_2	2^{++}	$\boldsymbol{a_2(1700)}$	$\boldsymbol{K_2^*(1980)}$	$\boldsymbol{f_2(1950)}$	$f_2(1640)$

$n^{2s+1}\ell_J$	J^{PC}	I $=0$ $c\bar{c}$	I $=\frac{1}{2}$ $c\bar{u}$, $c\bar{d}$; $\bar{c}u$, $\bar{c}d$	I $=0$ $c\bar{s}$; $\bar{c}s$
$1\,^1S_0$	0^{-+}	$\boldsymbol{\eta_c(1S)}$	$\boldsymbol{D}$	$\boldsymbol{D_s^\pm}$
$1\,^3S_1$	1^{--}	$\boldsymbol{J/\psi(1S)}$	$\boldsymbol{D^*}$	$\boldsymbol{D_s^{*\pm}}$
$1\,^3P_0$	0^{++}	$\boldsymbol{\chi_{c0}(1P)}$	$\boldsymbol{D_0^*(2300)}$[a]	$\boldsymbol{D_{s0}^*(2317)^{\pm}}$[b]
$1\,^3P_1$	1^{++}	$\boldsymbol{\chi_{c1}(1P)}$	$D_1(2430)$	$\boldsymbol{D_{s1}(2460)^{\pm}}$[b]
$1\,^1P_1$	1^{+-}	$\boldsymbol{h_c(1P)}$	$\boldsymbol{D_1(2420)}$	$\boldsymbol{D_{s1}(2536)^\pm}$
$1\,^3P_2$	2^{++}	$\boldsymbol{\chi_{c2}(1P)}$	$\boldsymbol{D_2^*(2460)}$	$\boldsymbol{D_{s2}^*(2573)^\pm}$
$2\,^1S_0$	0^{-+}	$\boldsymbol{\eta_c(2S)}$	$D_0(2500)^0$	$D_{s0}(2590)^+$
$2\,^3S_1$	1^{--}	$\boldsymbol{\psi(2S)}$	$D_1^*(2760)^0$	$\boldsymbol{D_{s1}^*(2700)^{\pm}}$[c]
$1\,^3D_1$	1^{--}	$\boldsymbol{\psi(3770)}$		$D_{s1}^*(2860)^{\pm}$[c]
$1\,^3D_2$	2^{--}	$\boldsymbol{\psi_2(3823)}$	$D_2(2740)^0$	
$2\,^3P_J$	$0^{++}, 1^{++}$	$\chi_{c0}(3860)$		
	2^{++}	$\boldsymbol{\chi_{c2}(3930)}$		
$3\,^3S_1$	1^{--}	$\boldsymbol{\psi(4040)}$		
$2\,^3D_1$	1^{--}	$\boldsymbol{\psi(4160)}$		
$4\,^3S_1$	1^{--}	$\boldsymbol{\psi(4415)}$		
$1\,^3D_3$	3^{--}	$\boldsymbol{\psi_3(3842)}$	$D_3^*(2750)$	$D_{s3}^*(2860)^\pm$

Scalar and tensor resonances

	Mass (MeV)	Width (MeV)	$\mathcal{B}(f \to \pi\pi)$ (%)	$\mathcal{B}(f \to K\bar{K})$ (%)	$\mathcal{B}(f \to 4\pi)$ (%)
$f_0(1370)$	1200–1500	300–500	< 10 [11]	35 ± 13 [79]	> 72 [33]
$f_0(1500)$	1506 ± 6	112 ± 9	34.5 ± 2.2	8.5 ± 1.0	48.9 ± 3.3
$f_0(1710)$	1704 ± 12	123 ± 18	$3.9^{+3.0}_{-2.4}$ [80]	36 ± 12 [26]	–
$[f_0(2020)]$	1992 ± 16	442 ± 60	–	–	–
$[f_0(2200)]$	2187 ± 14	207 ± 40	–	–	–
$[f_0(2330)]$	2324 ± 35	195 ± 71	–	–	–
$f_2(1270)$	1275.5 ± 0.8	$186.7^{+2.2}_{-2.5}$	$84.2^{+2.9}_{-0.9}$	$4.6^{+0.5}_{-0.4}$	$10.4^{+1.6}_{-3.7}$ $^{(a)}$
$[f_2(1430)]$	≈ 1430	–	–	–	–
$f_2'(1525)$	1517.4 ± 2.5	86 ± 5	0.83 ± 0.16	87.6 ± 2.2	–
$[f_2(1565)]$	1542 ± 19	122 ± 13	–	–	–
$[f_2(1640)]$	1639 ± 6	99^{+60}_{-40}	–	–	–
$[f_2(1810)]$	1815 ± 12	197 ± 22	21^{+2}_{-3} [80]	$2 \times 0.3^{+1.9}_{-0.2}$ [80]	–
$[f_2(1910)]$	1900 ± 9 $^{(b)}$	167 ± 21 $^{(b)}$	–	–	–
$f_2(1950)$	1936 ± 12	464 ± 24	–	–	–
$f_2(2010)$	2011^{+62}_{-76}	202^{+67}_{-62}	–	–	–
$[f_2(2150)]$	2157 ± 12	152 ± 30	–	–	–
$[f_2(2300)]$	2297 ± 28	149 ± 41	–	–	–

Consistency checks using Toy Model:

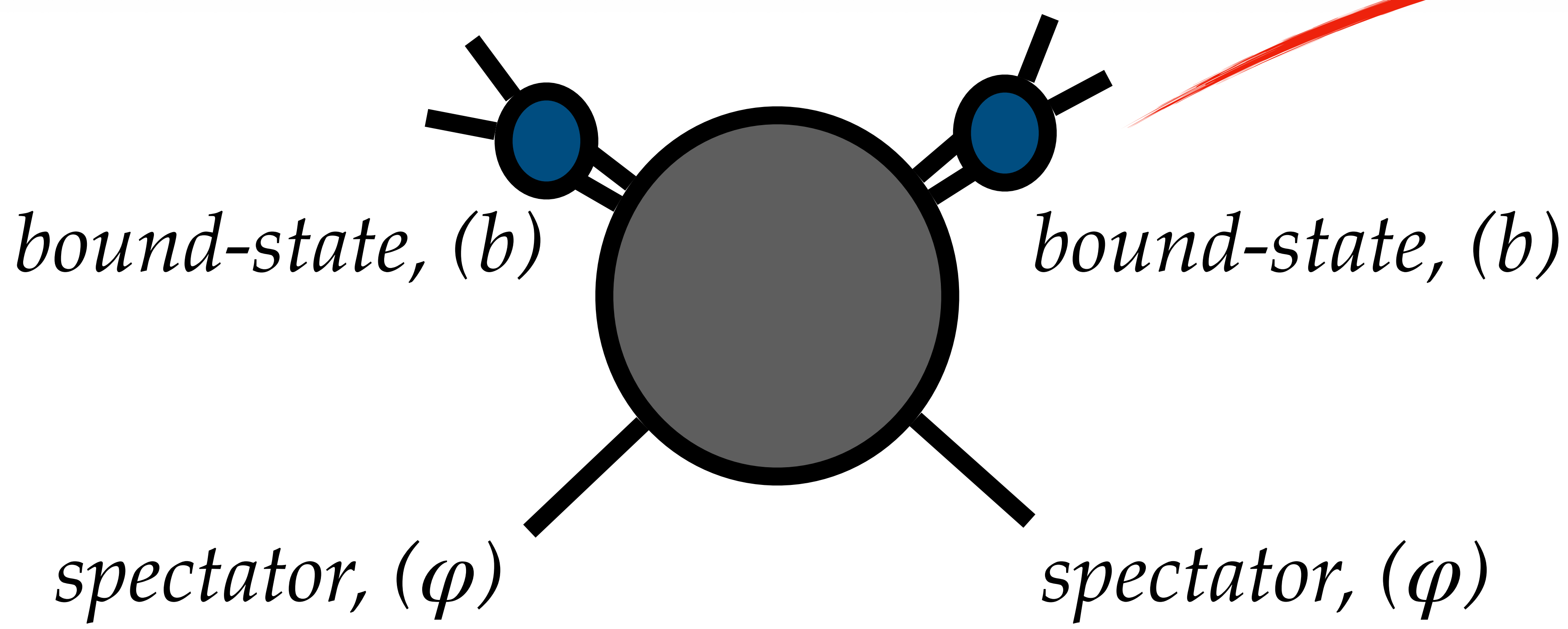

$$\mathcal{D} = \frac{-g}{\sigma_p - m_b^2}\mathcal{M}_{\varphi b}\frac{-g}{\sigma_k - m_b^2}$$

1. System dynamics fixed by two-body scattering length only.
2. Bound state pole in the integration interval, numerically most demanding scenario.
3. Finite volume results are available for comparison *(Romero-López, Sharpe, Blanton, Briceño and Hansen, 2019)*
4. Hints at **Efimov Physics**:

Unitarity Limit:

$$q \cot \delta_0 = -1/a = 0$$

Two body scattering amplitude has a pole at the threshold:

$$\mathcal{M}_2 = \frac{16\pi\sqrt{\sigma_q}}{-i\sqrt{\frac{\sigma_q}{4} - m^2}}$$

Geometrically separated, infinite tower of three-body bound-states:

$$E_{N+1} = E_N/\lambda^2$$

$$\lambda = 22.69438$$

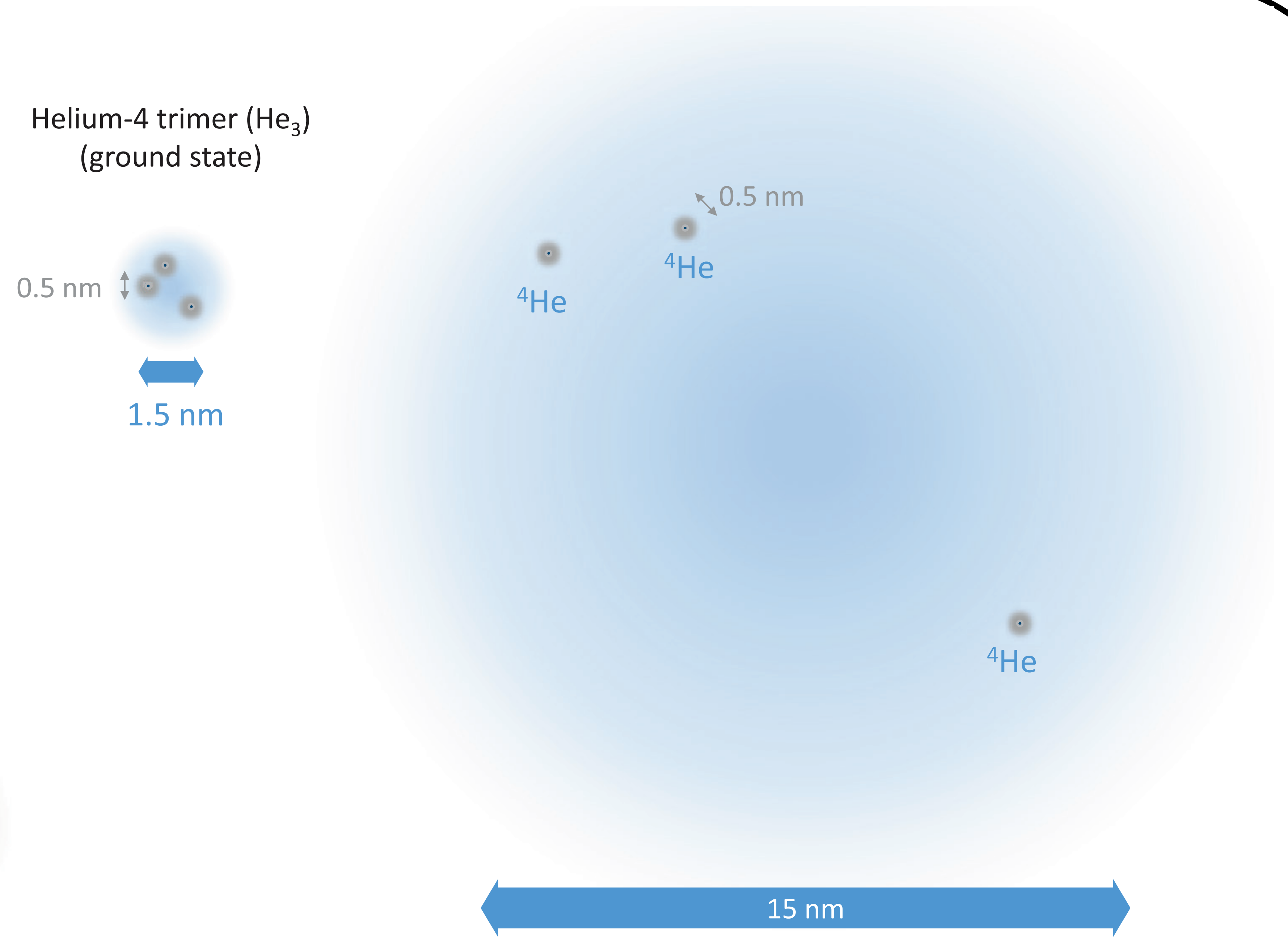

Vitaly Efimov, 1970
Naidon and Endo, 2016

Singularities in Region of Interest

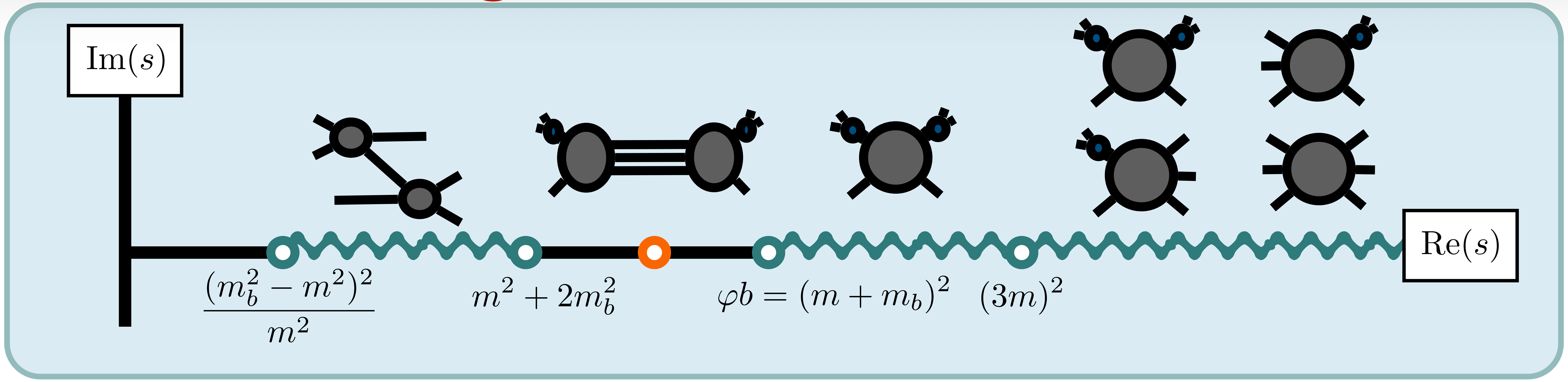

$$d_S(p,s,k) = -G_S(p,s,k) - \int_0^{q_{max}} dq \frac{q^2}{(2\pi)^2 \omega_q} G_S(p,s,q)\mathcal{M}_2(q,s) d_S(q,s,k)$$

$K(p,s,q)$

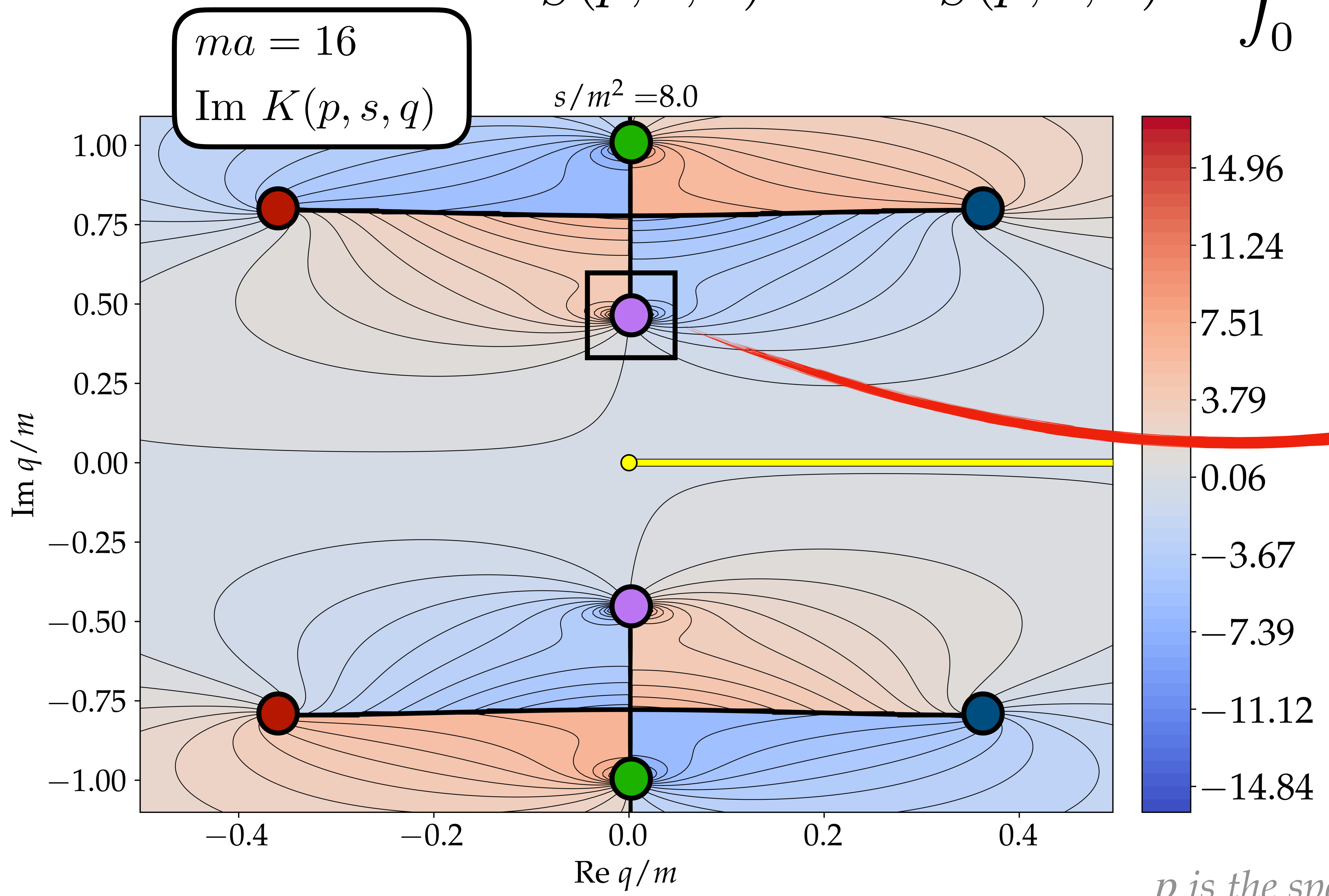

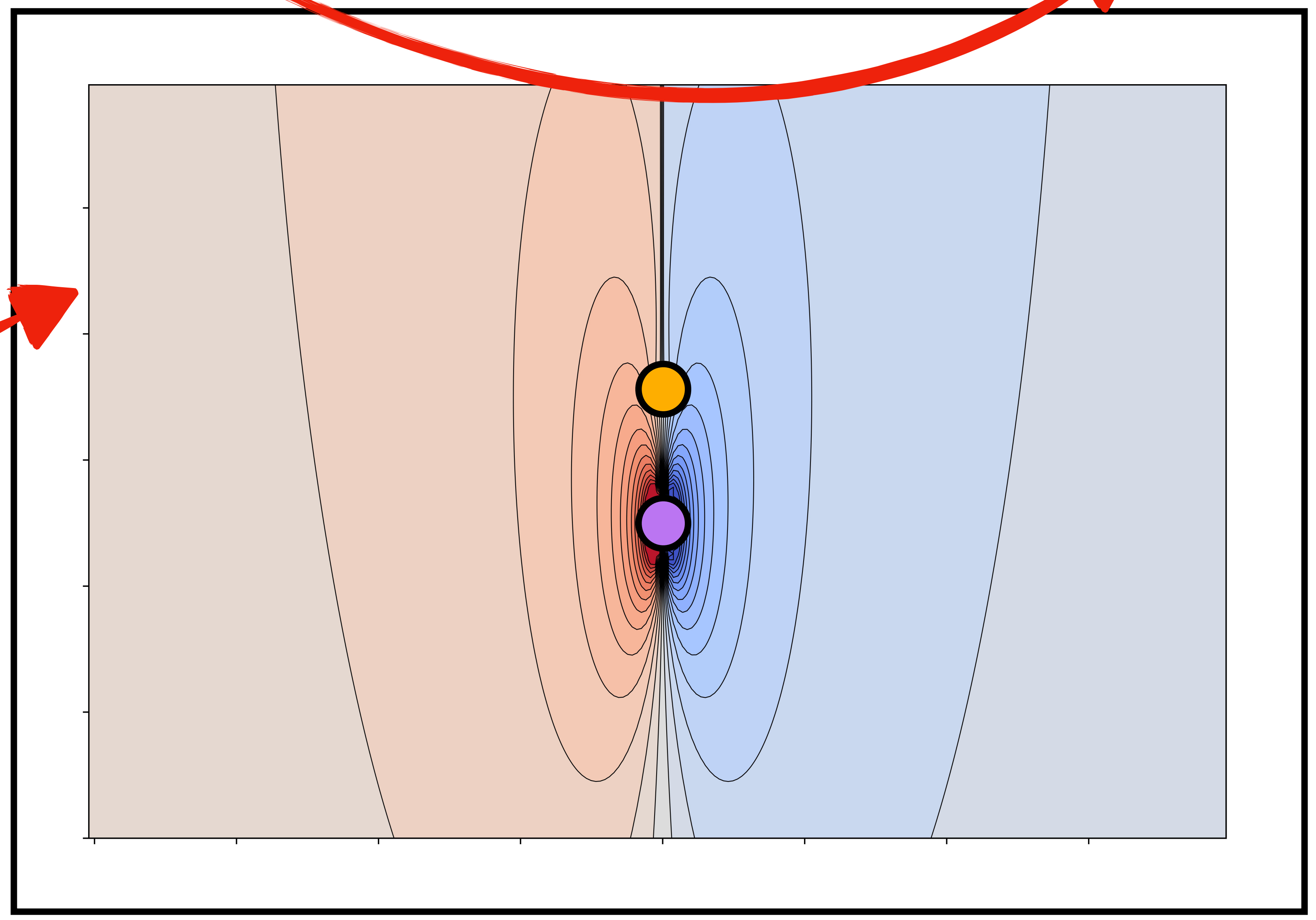

p is the spectator momenta corresponding to two-body subchannel energy, $\sigma_p = 2m^2$

Singularities in Region of Interest

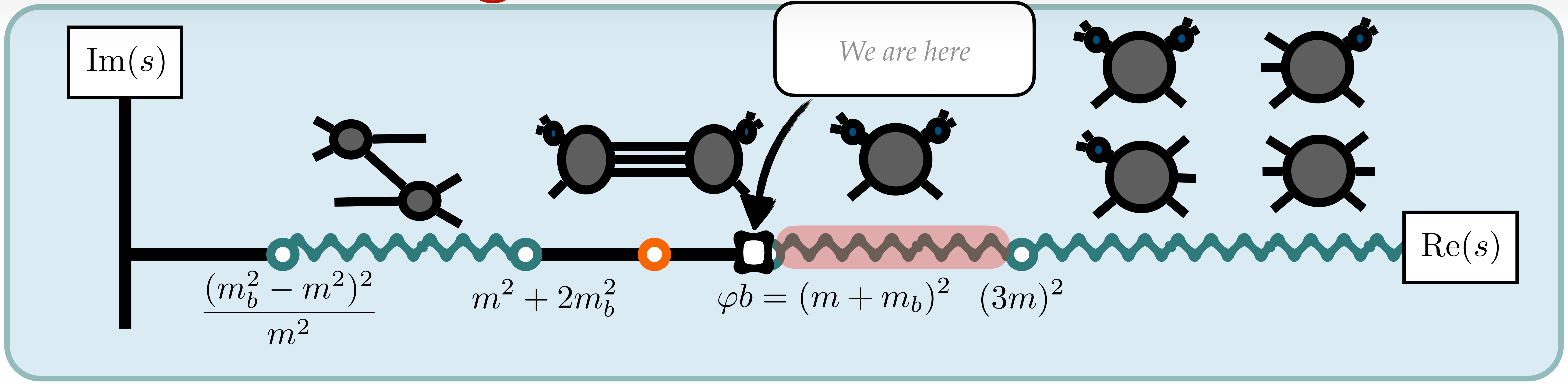

$$d_S(p, s, k) = -G_S(p, s, k) - \int_0^{q_{max}} dq \frac{q^2}{(2\pi)^2 \omega_q} G_S(p, s, q) \mathcal{M}_2(q, s) d_S(q, s, k)$$

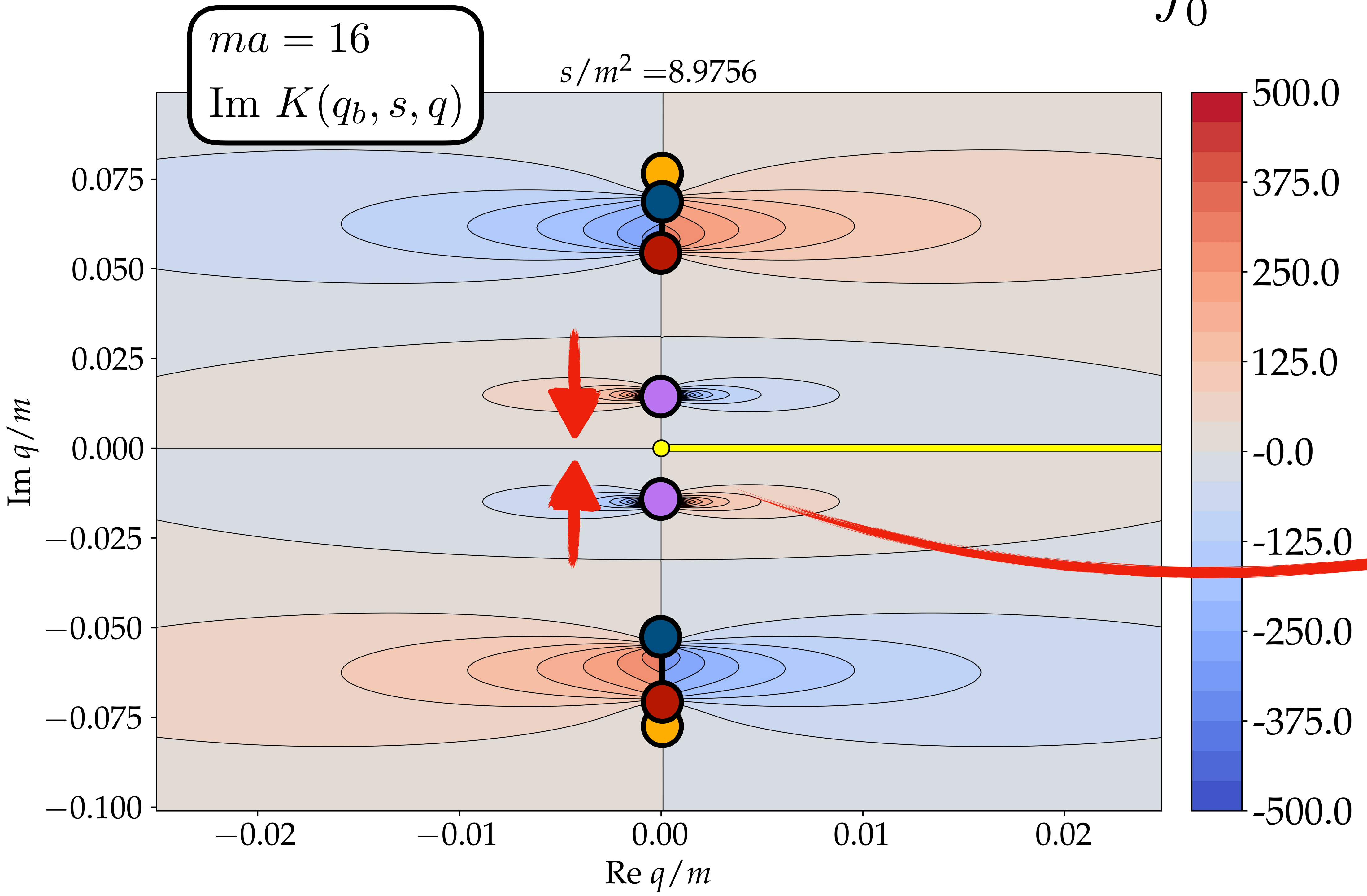

Two-body poles enclosing the end-point of integration

$$K(p, s, q) = \frac{q^2}{(2\pi)^2 \omega_q} G_S(p, s, q) \mathcal{M}_2(q, s)$$

q_b is the spectator momenta corresponding to two-body subchannel energy, $\sigma_q = m_b^2$

Singularities in Region of Interest

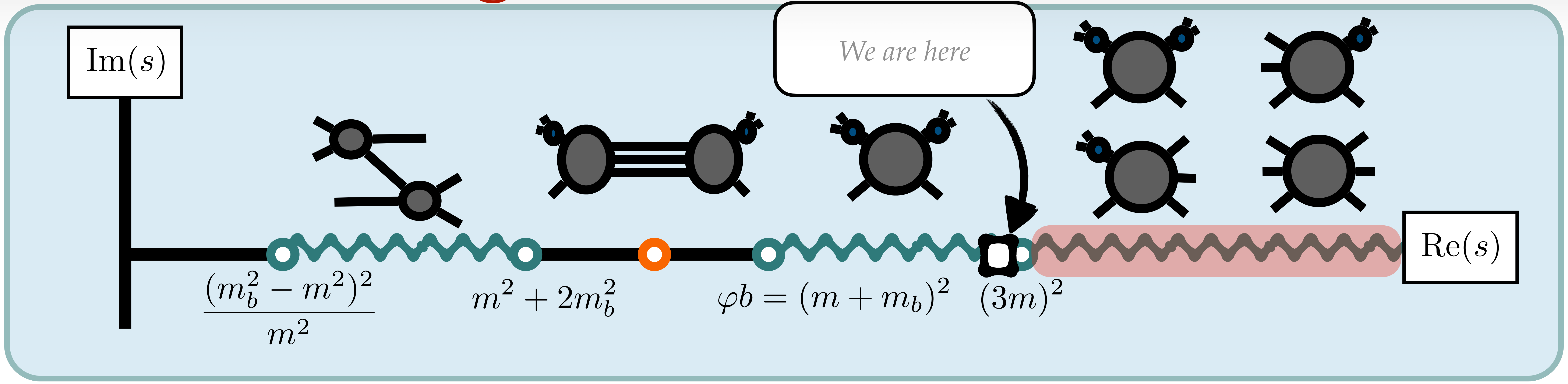

$$d_S(p,s,k) = -G_S(p,s,k) - \int_0^{q_{max}} dq \frac{q^2}{(2\pi)^2 \omega_q} G_S(p,s,q) \mathcal{M}_2(q,s) d_S(q,s,k)$$

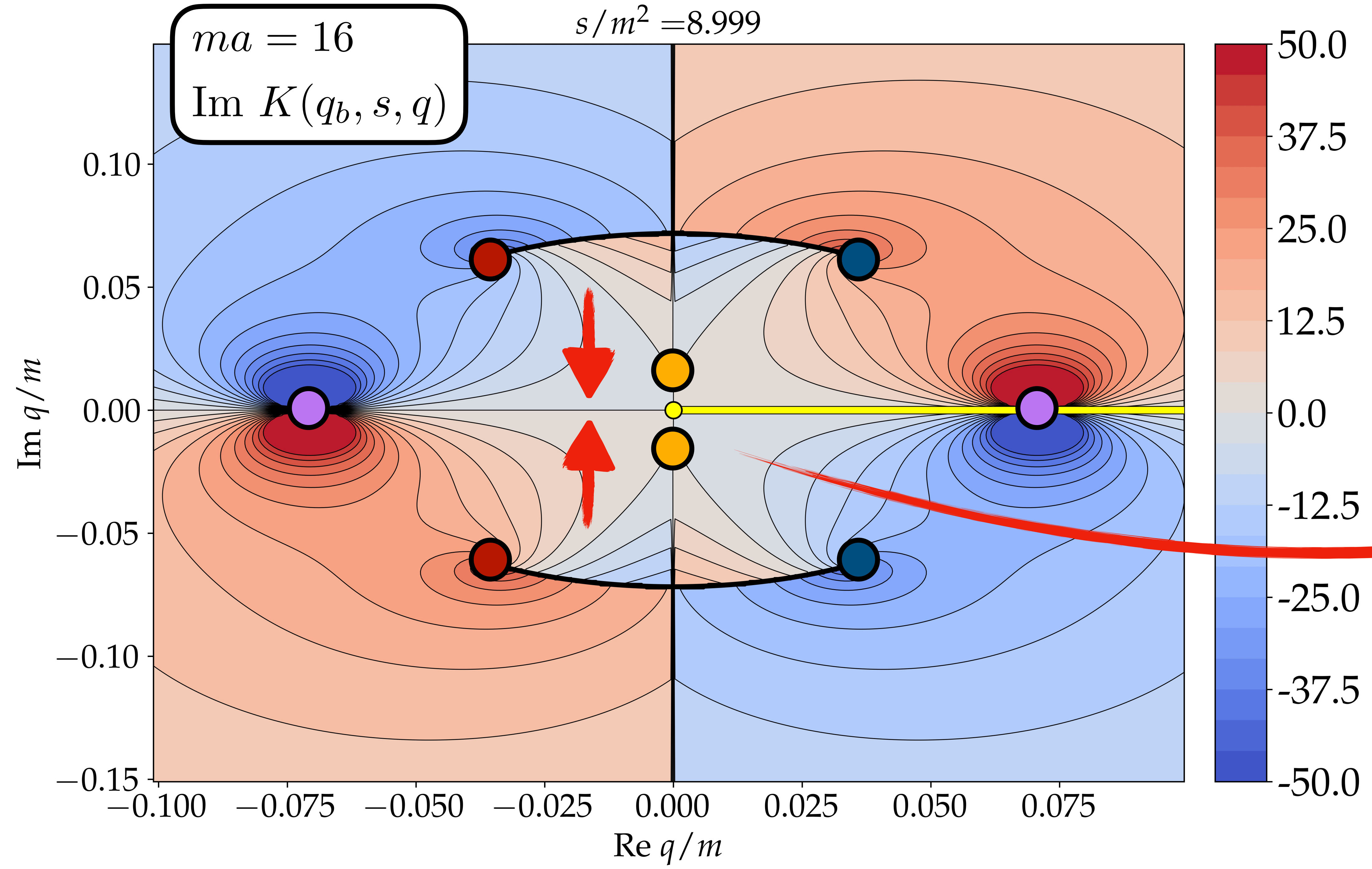

Two-body branch points enclosing one end-point of the integration interval

$$K(p,s,q) = \frac{q^2}{(2\pi)^2 \omega_q} G_S(p,s,q) \mathcal{M}_2(q,s)$$

q_b is the spectator momenta corresponding to two-body bound-state energy, $\sigma_q = m_b^2$

Complications in obtaining amplitude

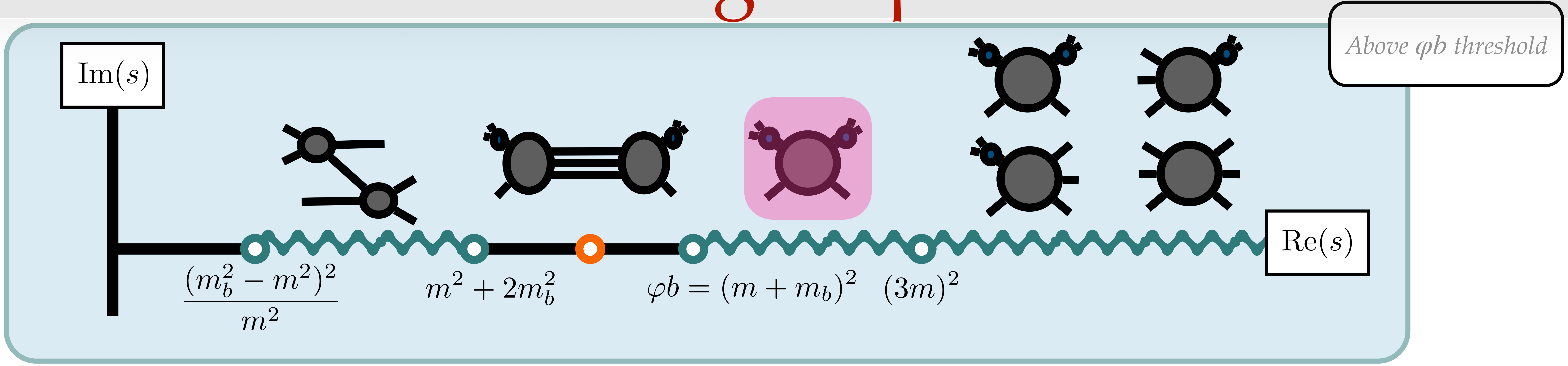

$$d_S(p,s,k) = -G_S(p,s,k) - \int_0^{q_{max}} dq \frac{q^2}{(2\pi)^2\omega_q} G_S(p,s,q)\mathcal{M}_2(q,s) d_S(q,s,k)$$

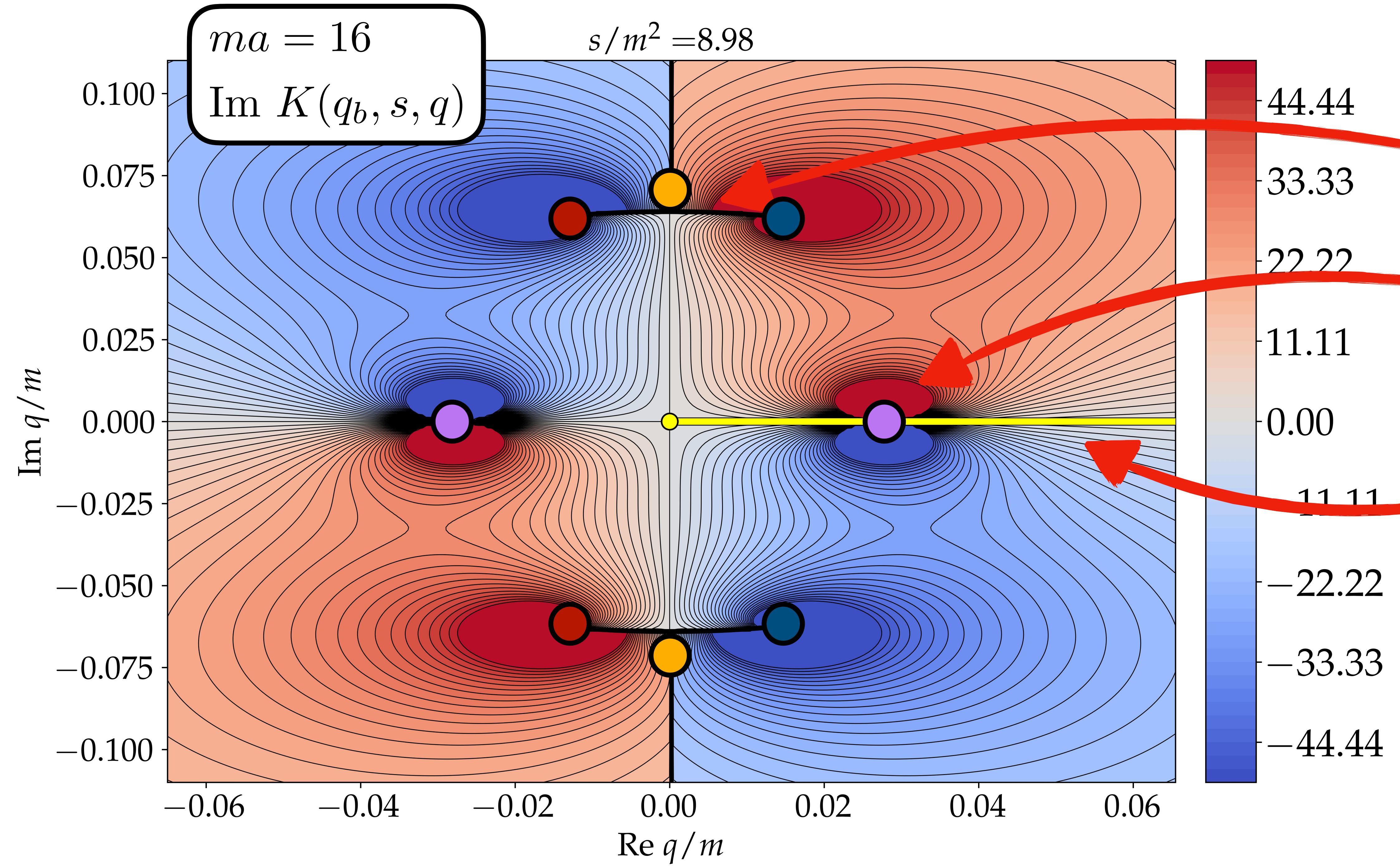

Set $p, k = q_b$ spectator momenta corresponding to two body bound state

Singularity cut from the one particle exchange function

Two body amplitude has a pole in the integration region

Momentum integration interval

$$K(p,s,q) = \frac{q^2}{(2\pi)^2\omega_q} G_S(p,s,q)\mathcal{M}_2(q,s)$$

$\mathcal{M}_{\varphi b}$ on the real s axis

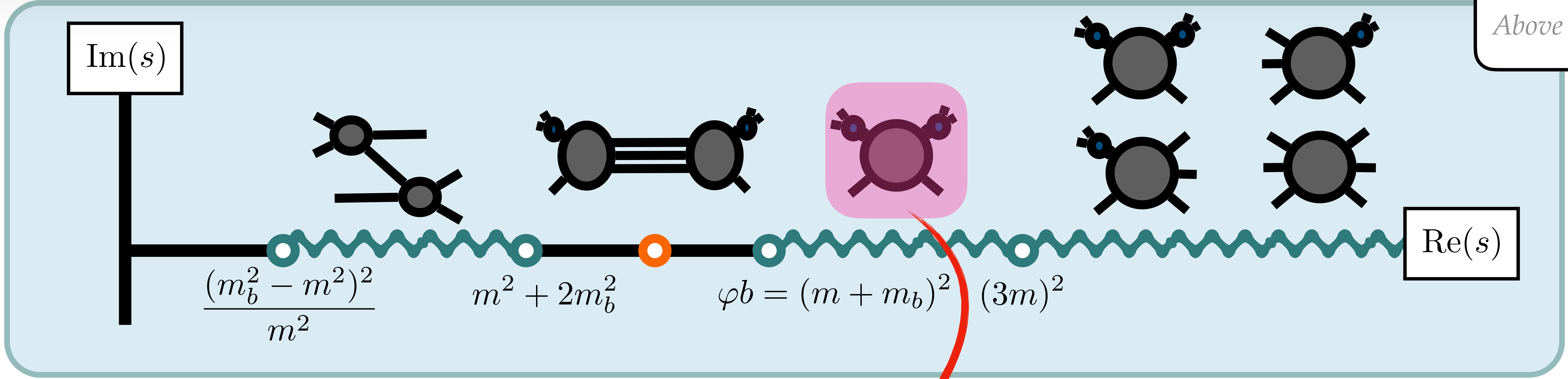

Above φb threshold

Follows two-body unitarity condition:

$|\rho_{\varphi b}\mathcal{M}_{\varphi b}| \leq 1$

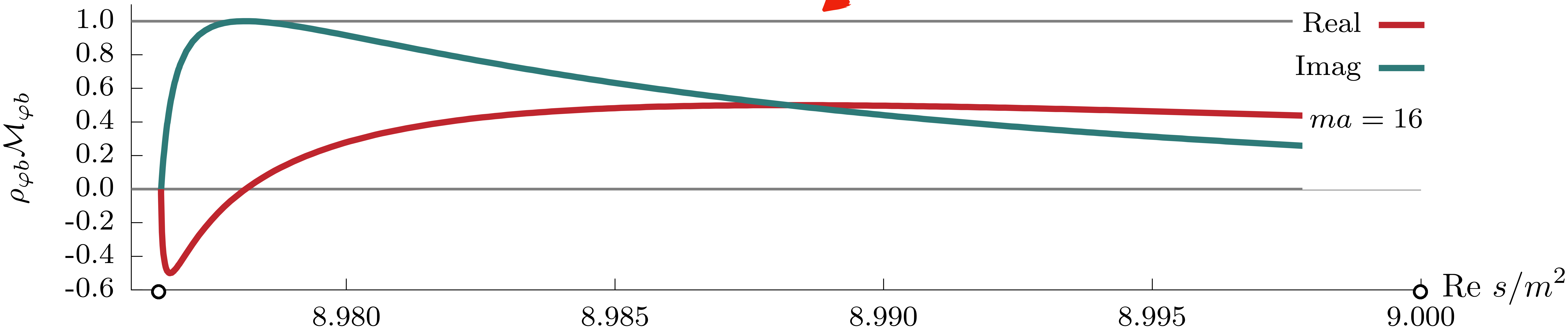

$\mathcal{M}_{\varphi b}$ on the real s axis

Above φb threshold

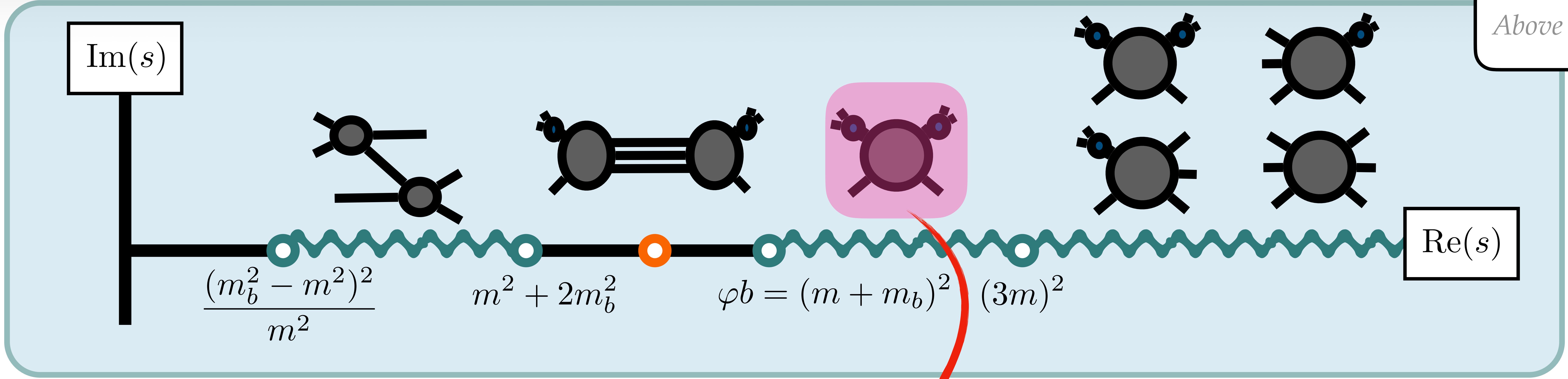

Follows two-body unitarity condition:

$$|\rho_{\varphi b}\mathcal{M}_{\varphi b}| \leq 1$$

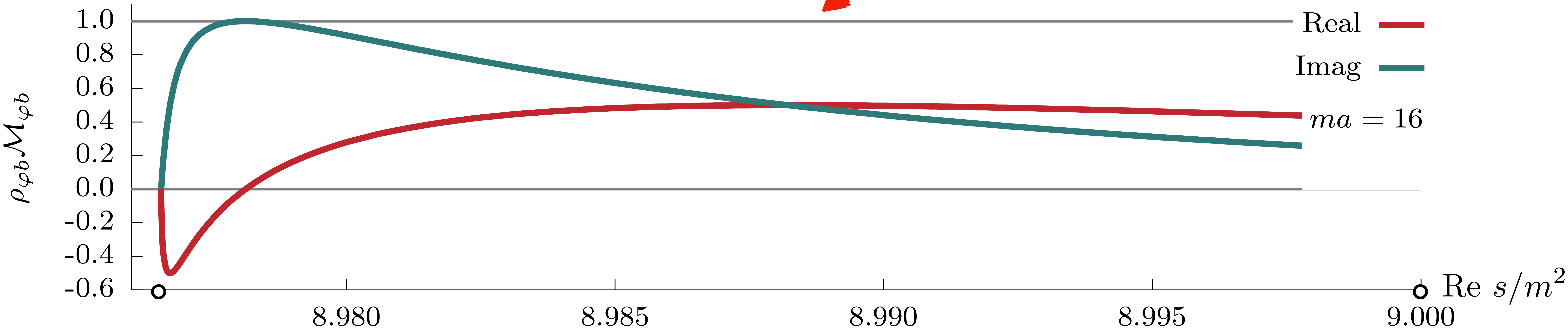

Singularities in Region of Interest

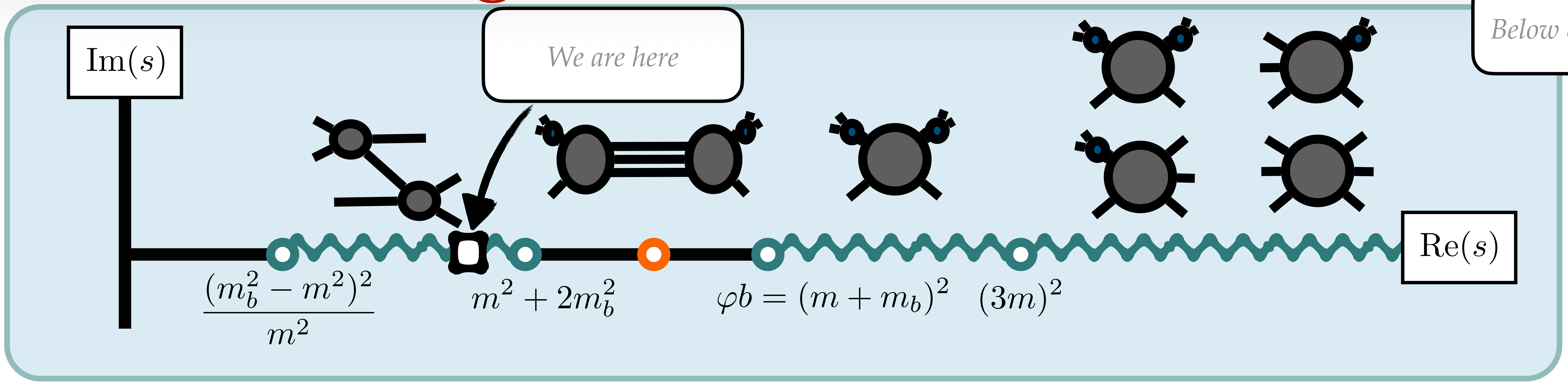

$$d_S(p,s,k) = -G_S(p,s,k) - \int_0^{q_{max}} dq \frac{q^2}{(2\pi)^2 \omega_q} G_S(p,s,q) \mathcal{M}_2(q,s) d_S(q,s,k)$$

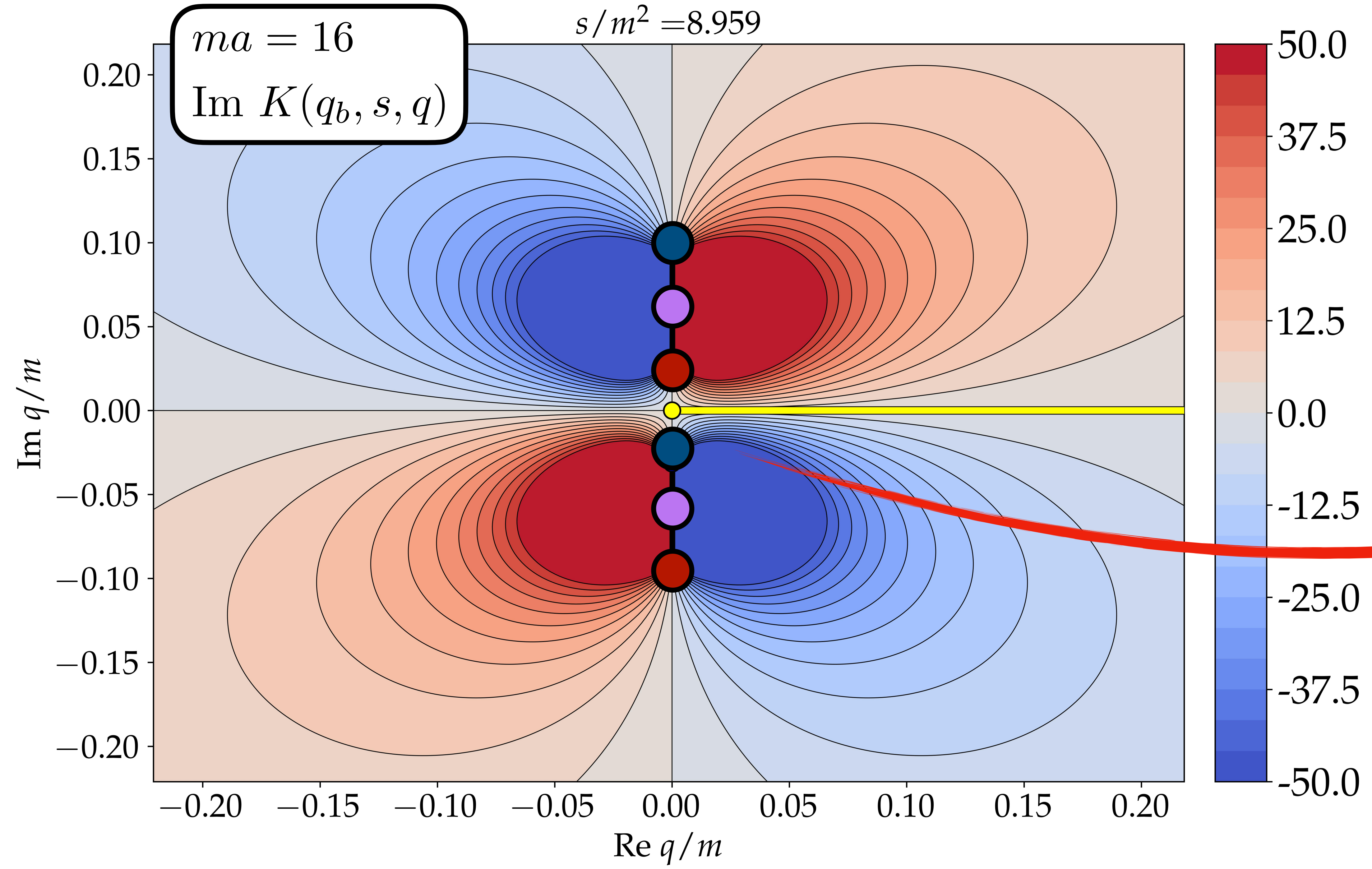

Two-body pole lies on top of the logarithmic cut

$$K(p,s,q) = \frac{q^2}{(2\pi)^2 \omega_q} G_S(p,s,q) \mathcal{M}_2(q,s)$$

q_b is the spectator momenta corresponding to two-body bound-state energy, $\sigma_q = m_b^2$

Singularities in Region of Interest

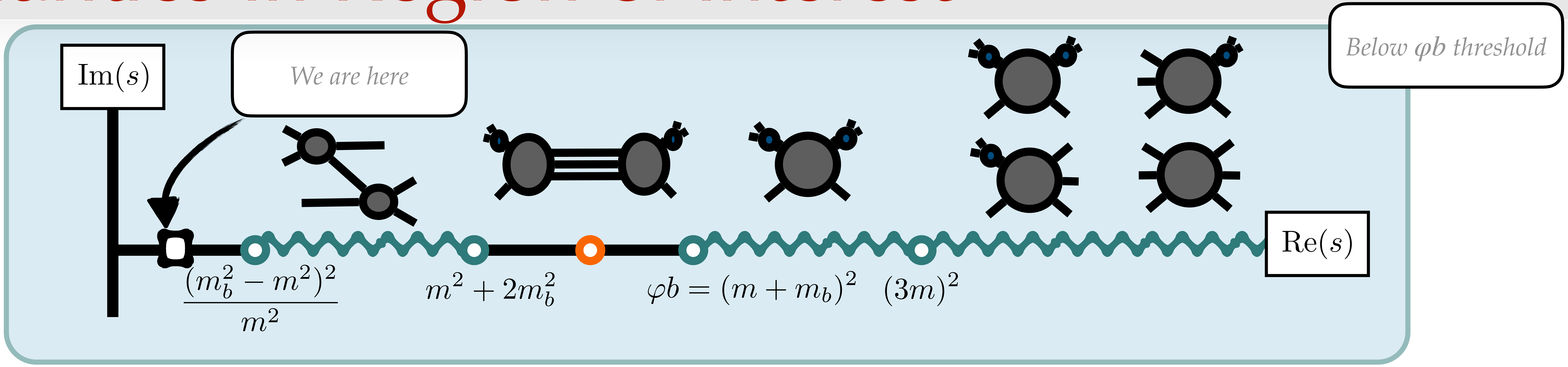

$$d_S(p,s,k) = -G_S(p,s,k) - \int_0^{q_{max}} dq \frac{q^2}{(2\pi)^2 \omega_q} G_S(p,s,q) \mathcal{M}_2(q,s) d_S(q,s,k)$$

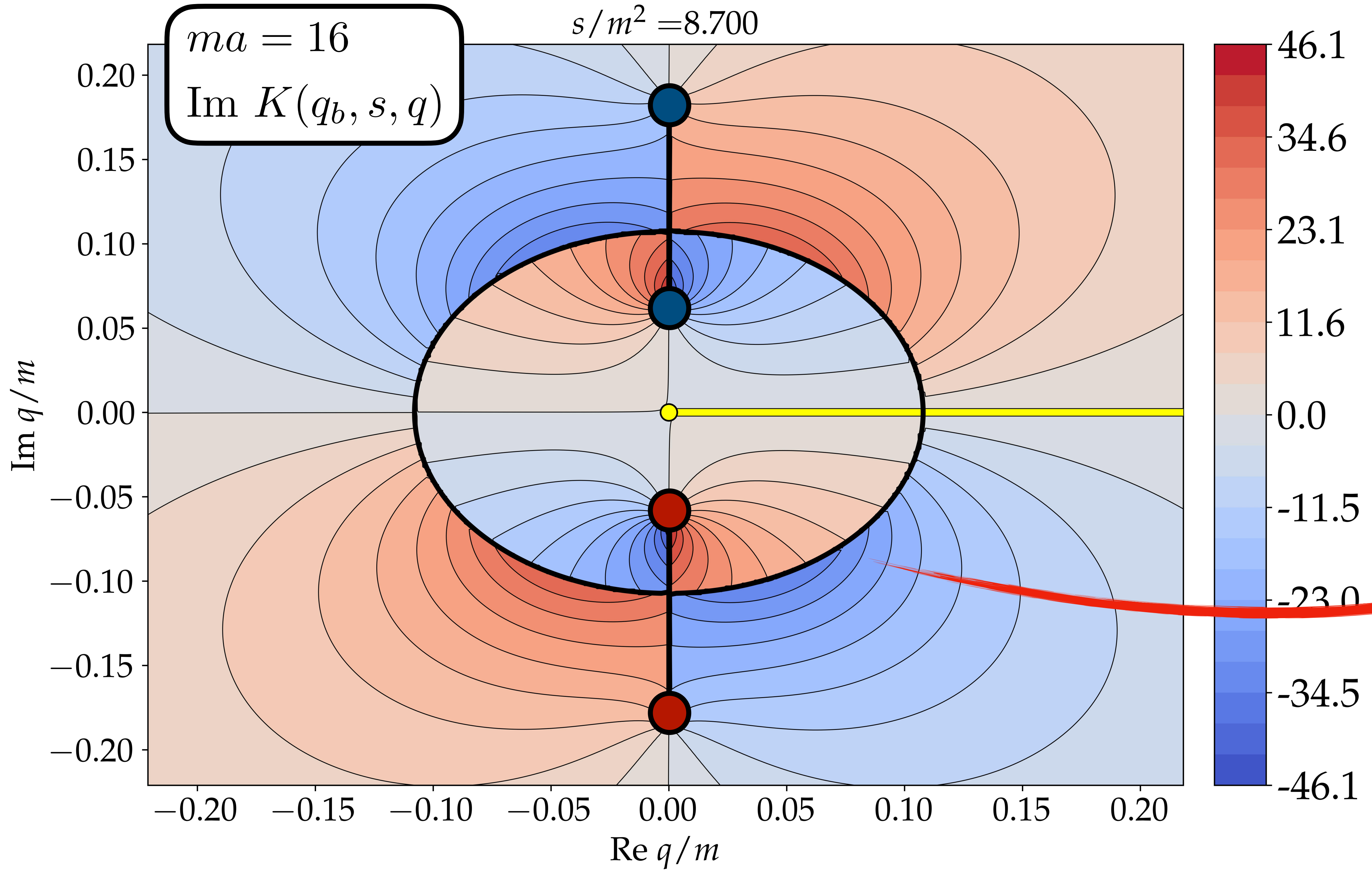

Logarithmic cut forms a circle around the end point of integration

$$K(p,s,q) = \frac{q^2}{(2\pi)^2 \omega_q} G_S(p,s,q) \mathcal{M}_2(q,s)$$

q_b is the spectator momenta corresponding to two-body bound-state energy, $\sigma_q = m_b^2$

Contour Deformation

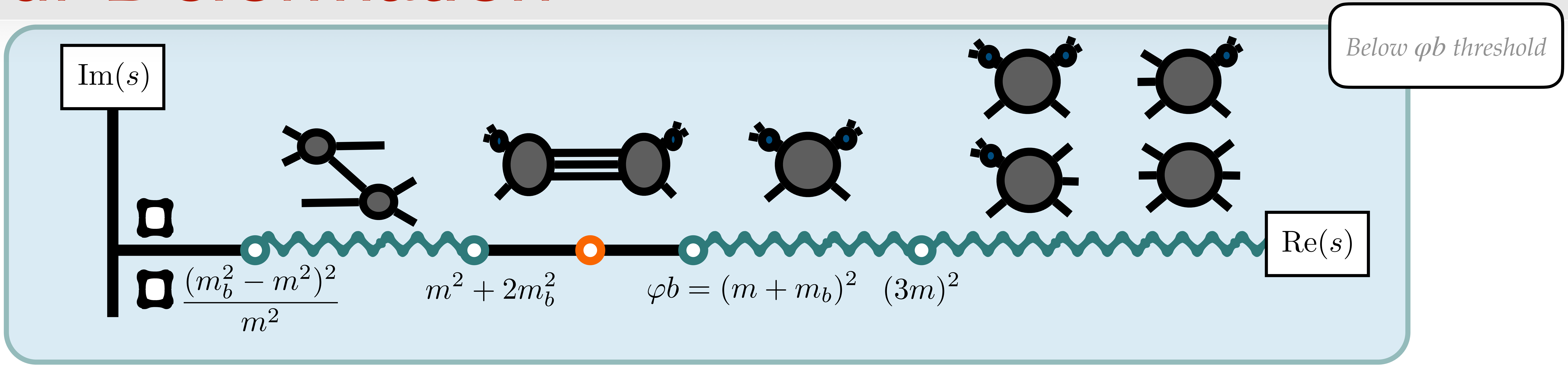

$$d_S(p, s, k) = -G_S(p, s, k) - \int_0^{q_{max}} dq \frac{q^2}{(2\pi)^2 \omega_q} G_S(p, s, q) \mathcal{M}_2(q, s) d_S(q, s, k)$$

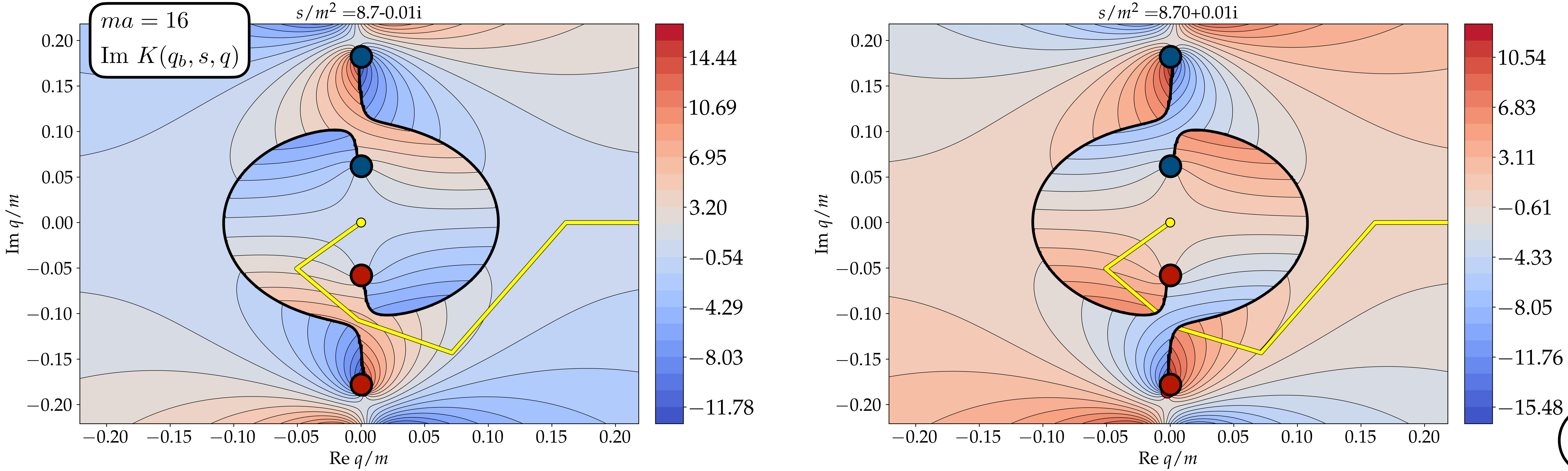

$\mathcal{M}_{\varphi b}$ on the real s axis

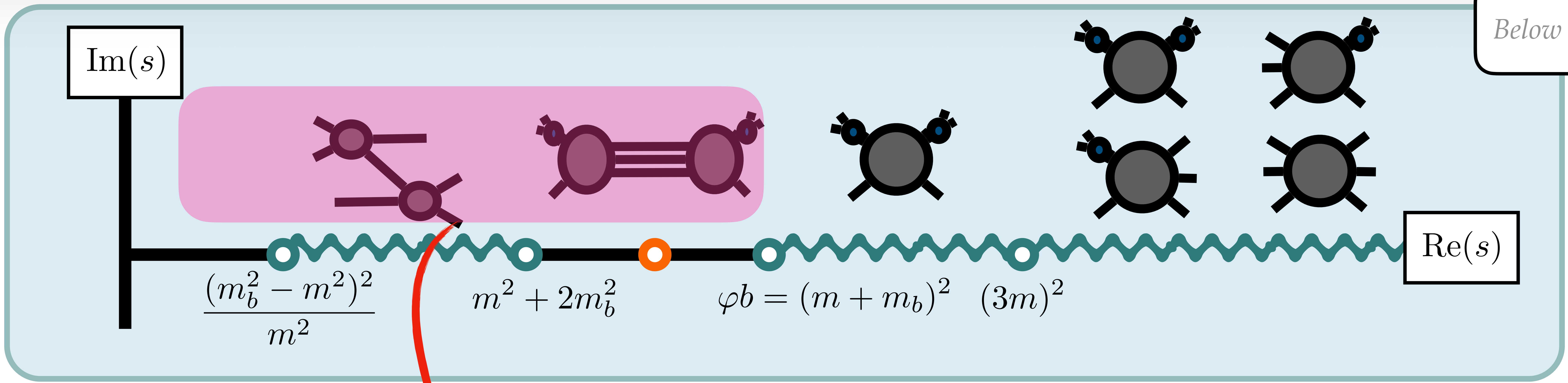

Below φb threshold

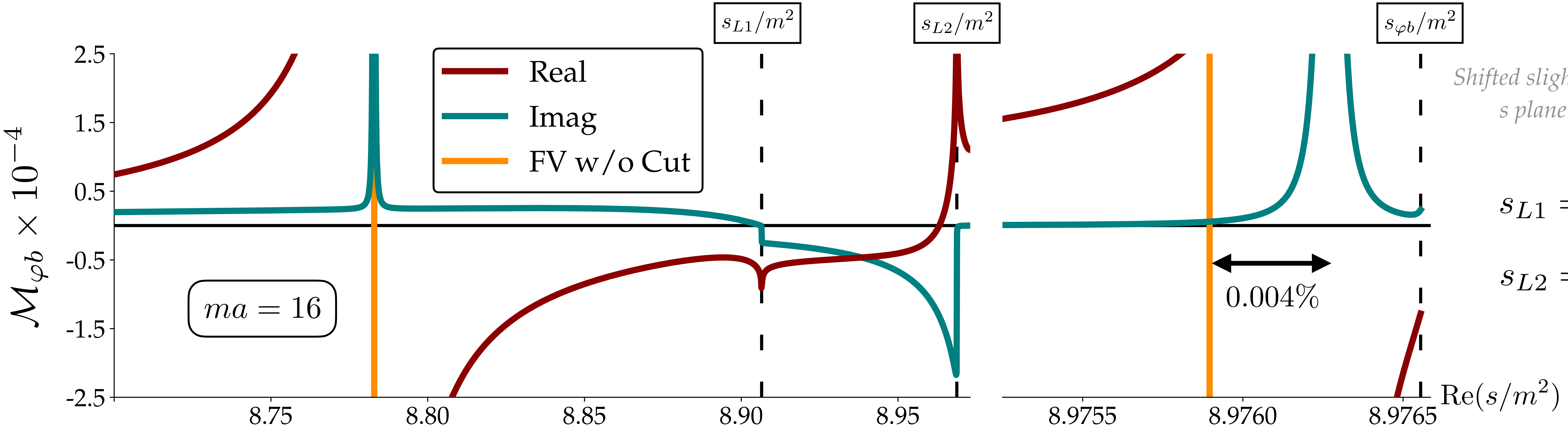

Shifted slightly into the complex s plane by Im(s)=10^{-5}

$$s_{L1} = \frac{(m_b^2 - m^2)^2}{m^2}$$

$$s_{L2} = m^2 + 2m_b^2$$